Max-Planck-Institut für Astronomie Heidelberg
Centro Astronomico Hispano Aleman Almeria

Max-Planck-Institut für Astronomie

Heidelberg-Königstuhl

Annual Report 1999

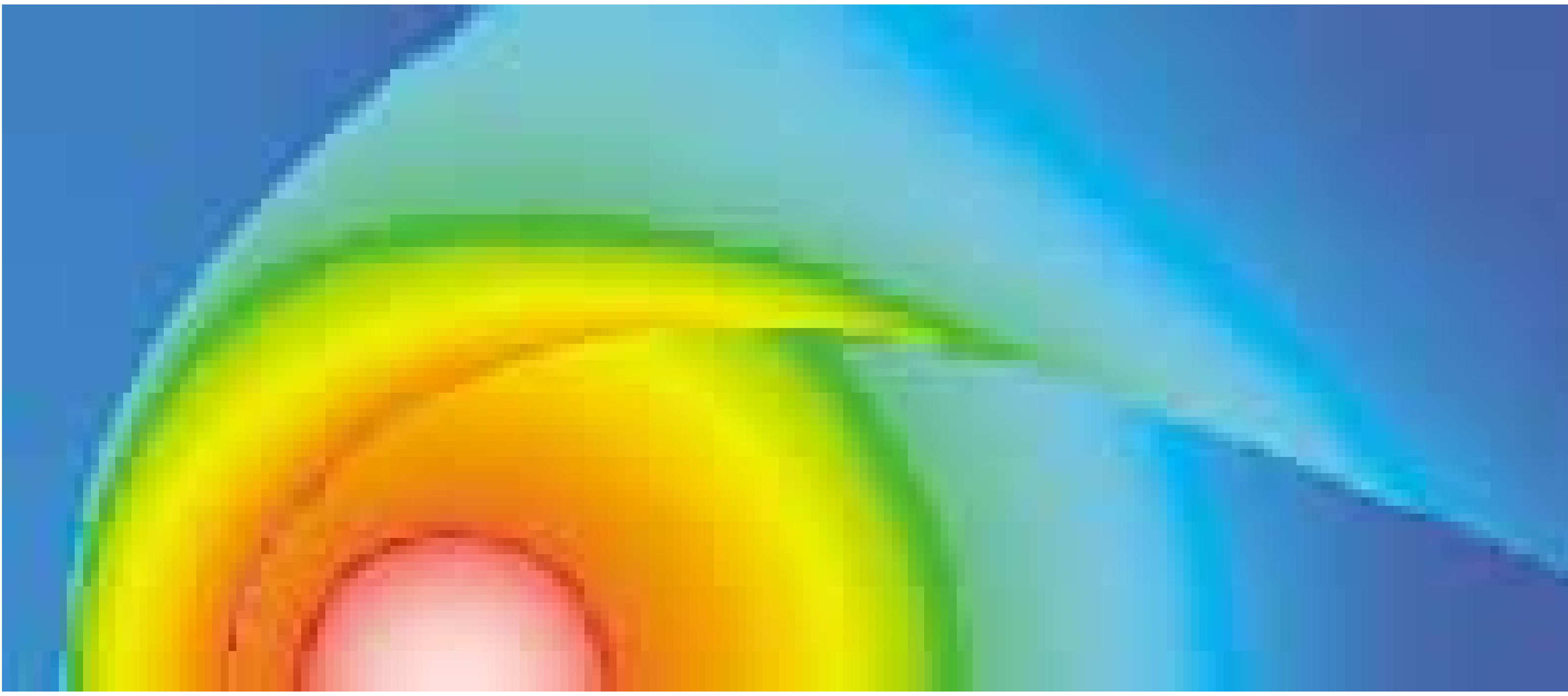

MAX-PLANCK-GESELLSCHAFT

Cover Picture:
In the hot intergalactic particle wind, dwarf galaxies loose their interstellar gas within few billion years. Theoretical studies of this process are described on p. 64–67.

Max-Planck-Institut für Astronomie

Heidelberg-Königstuhl

Annual Report 1999

Max-Planck-Institute of Astronomy

Managing Director:
Prof. Immo Appenzeller

Scientific Members, Governing Body, Directors:
Prof. Immo Appenzeller (until 31. 7. 2000, temporary)
Prof. Steven Beckwith (on leave to STScI)
Prof. Hans-Walter Rix

Emeritus Scientific Members:
Prof. Hans Elsässer, Prof. Guido Münch

External Scientific Members:
Prof. Immo Appenzeller, Heidelberg
Prof. Karl-Heinz Böhm, Seattle
Prof. George H. Herbig, Honolulu

Scientific Oversight Committee:
Prof. R. Bender, Munich; Prof. R.-J. Dettmar, Bochum; Prof. G. Hasinger, Potsdam; Prof. P. Léna, Meudon; Prof. M. Moles Villamante, Madrid; Prof. F. Pacini, Florence; Prof. K.-H. Schmidt, Potsdam; Prof. P.A. Strittmatter, Tucson; Prof. S.D.M White, Garching; Prof. L. Woltjer, St. Michel l'Observatoire.

The MPIA currently employs a staff of approximately 186 (including externally funded positions). There are 34 scientists and 30 junior and visiting scientists. Students of the Faculty of Physics and Astronomy of the University of Heidelberg work on dissertations at the degree and doctorate level in the Institute. Apprentices are constantly undergoing training in the Institute's workshops.

Address: MPI für Astronomie, Königstuhl 17, D-69117 Heidelberg.
Tleelphone: 0049-6221-5280, Fax: 0049-6221-528246.
E-mail: Name@mpia-hd.mpg.de
Anonymous ftp: //ftp.mpia-hd.mpg.de
Internet: http://www.mpia-hd.mpg.de

Calar Alto Observatory

Address: Centro Astronomico Hispano Aleman
Calle Jesus Durbán Remón 2/2, E-04004 Almería, Spanien
Telefon: 0034-50-230988, -632500, Fax: 0034-50-632504
E-mail: name@caha.es

Publication Information

Editors: Dr. Jakob Staude, Prof. Hans-Walter Rix
Text: Dr. Thomas Bührke
Illustrations: MPIA and others
Graphics and picture editing: Dipl. Phys. Axel Quetz
Layout: Josef Hegele
Printing and Production: Colordruck Leimen
ISSN: 1437-2932 – Internet: ISSN 1617-0504

Contents

I General

I.1 History and Research Goals of the MPIA

The Calar Alto Observatory

In 1967, the Senate of the Max Planck Society decided to establish the Max Planck Institute of Astronomy in Heidelberg with the aim of restoring astronomical research in Germany to a leading global position after the major setbacks it had suffered due to two World Wars. Two years later, the Institute commenced its work in temporary accommodation on the Königstuhl, under the direction of Hans Elsässer. The Institute moved into its new building in 1975 (Fig. I.1). A long-term goal for the newly established MPIA was to build up and operate two cutting-edge observatories, one in the northern hemisphere and one in the southern hemisphere. In 1970, after an intensive search for a site, the choice for the northern hemisphere was made in favour of Calar Alto mountain (height: 2168 metres) in the province of Almería, southern Spain. This European location offers good climatic and meteorological conditions for astronomical observations. 1972 saw the establishment of the German-Spanish Astronomical Centre (DSAZ), known in short as the Calar Alto Observatory.

The complex technological problems associated with the planning and construction of the telescopes were solved in cooperation with Carl Zeiss of Oberkochen and other companies. In this way, a large number of firms have acquired know-how which has helped them to secure leading positions on the world market.

Between 1975 and 1984, the 1.2 metre reflector financed by the German Research Society (DFG) as well as the 2.2 metre and 3.5 metre telescopes started opera-

Fig. I.1: The Max Planck Institute of Astronomy in Heidelberg.

Fig. I.2: The dome of the 3.5 metre telescope on Calar Alto.

Fig. I.3: ALFA on the Cassegrain flange of the 3.5 metre telescope, together with the shimmering golden OMEGA camera.

tion on Calar Alto (Fig. I.2). The 80 centimetre Schmidt reflector was transferred from the Hamburg Observatory. The site also hosts a Spanish 1.5 metre telescope operated by the Observatorio Nacional de Madrid is in charge of this instrument. The original plans to construct a southern observatory on the Gamsberg in Namibia could not be implemented for political reasons. The 2.2 metre telescope which was intended for this purpose has been loaned to the European Southern Observatory (ESO) for 25 years. Since 1984, it has been in operation on La Silla Mountain in Chile, where 25 % of its observation time is available to the astronomers at the MPIA.

One aspect of the MPIA's present mission is the operation of the Calar Alto Observatory. This includes the constant optimization of the telescopes and instrumentation capabilities: now that the ALFA adaptive optical system has been commissioned (Fig. I.3) the 3.5 metre telescope is once again at the forefront of technological development (Chapter III). Other aspects include the development and building of new instruments in Heidelberg, the preparation of observation programs and the evaluation of the data obtained from the telescopes. A substantial part of the Institute's work is devoted to building new instruments for the telescopes (Chapter III). The MPIA is equipped with ultra-modern precision mechanics and electronics workshops for this purpose. The Calar Alto Observatory provides the MPIA with one of the two European observatories with the highest performance. Research concentrates on the »classical« visible region of the spectrum and on the infrared range.

International Cooperation in Ground-based Astronomy

Participation in international ground-based observatories and projects is also of central importance. For example, on one of the largest telescopes in the northern hemisphere – UKIRT (United Kingdom Infrared Telescope), the British 3.9 metre telescope in Hawaii – MPIA has built the infrared camera MAX (Mid-Infrared Array eXpandable), has been operational for some years. In 1996, the same telescope was equipped with a light-weight tip-tilt secondary mirror built under the coordinating leadership of the MPIA. In the reporting year, a new mirror was supplied with even higher surface accuracy. This makes it possible to achieve diffraction-limited photographs with a resolution of 0.″3 in the near infrared (Fig. I.4) (see Chapter III). In return for these ac-

Fig. I.4: The new secondary mirror unit of the UKIRT with a dummy mirror in the workshop at the MPIA.

Fig. I.5: The four telescopes of the Very Large Telescope and the scientific instruments that are already operating or under construction.

tivities, the Heidelberg astronomers receive a fixed fraction of the observing time at this telescope.

The MPIA is leading the development and construction of the high-resolution CONICA infrared camera for the Very Large Telescope (VLT). Built by ESO on the Mount Paranal in Chile, the VLT will become the world's largest telescope. Work has already started on the development and construction of MIDI, an interferometry instrument for the VLT (Fig. I.5) (see Chapter III). From 2002, this ground-breaking instrument will make it possible to combine for the first time ever the light from two large telescopes interferometrically at infrared wavelengths.

Above and beyond this, the MPIA is playing a decisive part in the Large Binocular Telescope (LBT, Fig. I.6). As ist name implies, the LBT contains two mirrors with diameters of 8.4 meters each in a shared mount. Together, the two mirrors have a light-gathering power which is equal to that of a single 11.8 metre mirror. This will make the LBT the world's most powerful single telescope after its foreseen commissioning date of 2004. It is also planned to use the two mirrors of the LBT for interferometric observations. In this case, its spatial resolution will correspond to that of a mirror with a diameter of 22.8 metres. The LBT is currently being built by an American-Italian-German consortium on Mount Graham in Arizona, USA. Under the auspices of the »LBT Participation Group« together with the MPI for Extra-Terrestrial Physics in Garching, the MPI for Radio Astronomy in Bonn, the Potsdam Astrophysical Institute and the Heidelberg State Observatory, the MPIA will have a 25 % share in the costs and use of the LBT.

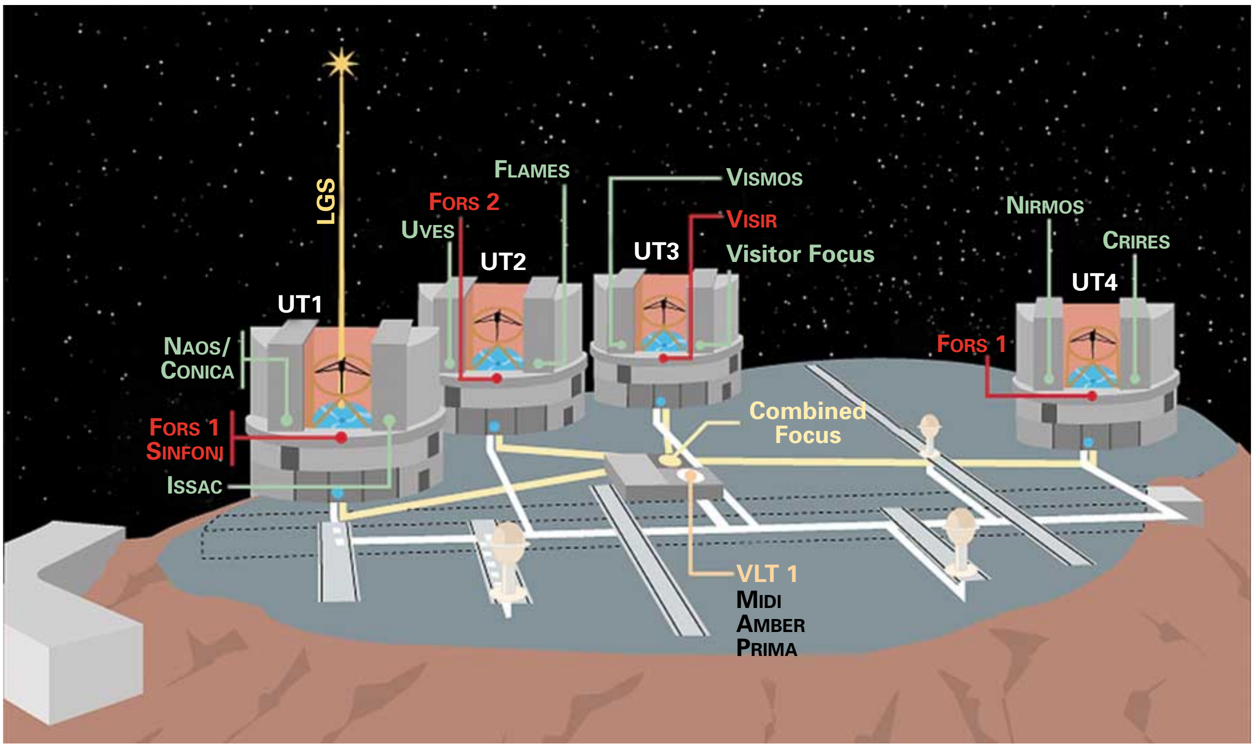

Fig. I.6: The Large Binocular Telescope on Mount Graham will be among the world's most powerful telescopes in a few years' time.

Space Research

Ever since it was established, the MPIA has been engaged in space research ever since it was established. These activities were associated with an early start on infrared astronomy, which has played a growing role in the Institute's later development as a whole. In the 1970's, two photometers were developed and built at the MPIA, which flew on board the two solar probes HELIOS 1 and HELIOS 2, where they worked faultlessly. A more or less parallel development for the Helios mission involved the THISBE balloon gondola (Telescope of Heidelberg for Infrared Studies by Balloon-borne Experiments). This altitude research balloon was designed to carry telescopes and equipment weighing as much as 400 kilograms up to a height of 40 kilometres, where infrared observations are possible. Four telescopes with apertures of 6 to 20 centimetres were built in the workshops of the MPIA and were deployed on THISBE. Niteworthy scientific achievements include the first observation of the central region of the Milky Way at a wavelength of 2.4 µm, and the measurement of the airglow, a luminescence of the OH radical in the atmosphere.

Nowadays, the MPIA has a substantial involvement in the ISO project of the European Space Agency ESA. ISOPHOT, one of four measuring instruments on ISO, was developed under the coordinating leadership of the Institute. For over two years, ISO supplied brilliant data until it was switched off on 8 April 1998, after its supply of coolant had been exhausted. In the meantime, numerous publications concerning all areas of astronomy have appeared, attesting to the scope of this space telescope's achievements.

Summer 1998 saw the start of the post-operative phase which is due to last three years. During this phase, the data must be carefully calibrated and archived. In this instance, particular importance is attached to a clearly arranged archive classified by objective criteria. To accomplish this task, ESA set up a central archive at its station in Villafranca, Spain, in 1998, and in addition the four institutes responsible for the measuring instruments each built up a data centre.

Under an agreement with ESA, the ISOPHOT Data Centre at the MPIA is one of the nodes in this international network totalling six ISO data centres (Fig. I.7) (See1998 Annual Report, p. 6). In cooperation with the ISO Science Operations Center, Madrid, the standard »PHT Interactive Analysis« software (PIA) has been developed at the MPIA to evaluate the raw data supplied by the satellite.

In the second year of the post-operative phase, the work on programme development and calibration analysis for a new version of the automatic data analysis software was completed. At the same time, it was possible to increase the accuracy for so-called »chopped point source measurements«. In this observation mode, the science target itself is measured in alternation with a background reference field. The main goal of the new software development was to improve chopped photometry, which accounts for about 20 % of all ISOPHOT measurements, totalling some 3000 observations.

As well as pure archiving and recalibration, the Heidelberg Data Centre acts as a service facility for astronomers. Assistance was provided for about 50 visitors in 1999.

On the scientific side, the this years mile-stone was the publication of the first point source catalogue based on random sampling at a wavelength of 170 µm (Chapter IV.2). Important research articles also appeared on circumstellar dust clouds around young stars (Chapter IV.1), on polycyclical aromatic hydrocarbon molecules in the interstellar medium (Chapter IV.1.) and on dust in quasars (Chapter IV.2.).

Fig. I.7: The Astrolaboratory on the Königstuhl, where the ISOPHOT data centre is now housed.

The experience gained with ISOPHOT was a decisive factor in the MPIA's major involvement in the construction of the PACS Infrared Camera. This instrument will operate on board the Far-Infrared and Submillimeter Telescope (FIRST) of the ESA (Chapter III). The launch of this 3.5 metre space telescope is planned for the year 2007.

The Institute is participating in a satellite experiment proposed to NASA by Johns Hopkins University, Baltimore. The telescope known as PRIME (Primordial Explorer) is intended to chart a large part of the sky, down to a magnitude of 24.5, in the wavelength range from 0.9 to 3.4 µm. PRIME would be a predecessor of the New Generation Space Telescope, the planned successor to the Hubble telescope. It would comprise a 75-cm telescope which would move around the Earth in a circular polar orbit at an altitude of 650 km. The focal plane of the telescope is split up over three mirrors into four wavelength channels, equipped with newly-developed infrared arrays containing 2000 × 2000 Pixels.

Individual exposures each lasting 150 seconds would allow a quarter of the entire sky to be scanned within three years. Compared to the currently most sensitive survey of the sky in the near infrared, named the American 2 Micron Astronomical Sky Survey (2MASS), PRIME would provide a sensitivity increase by a factor of 1000. PRIME would supply a vastly improved data base for virtually every field of modern astronomy. For example, in the redshift range of $1< z < 5$, the telescope could find at least 1000 supernovae of type Ia and measure their light curves, as well as finding hundreds of brown dwarfs at distances of up to 1000 parsecs, extrasolar planets of the size of Jupiter at distances of up to 50 parsecs, quasars at redshifts of up to $z = 25$ or protogalaxies at redshifts of up to $z = 20$.

If this proposal is incorporated into the NASA program, a start can be made on Phase A of its development in the summer of 2000, and the satellite can be launched in the spring of 2004.

* * *

Aided by this wide and varied range of instruments, the MPIA will be able to go on making a major contribution towards astronomical research in the future.

Thanks to its location in Heidelberg, the MPIA has the opportunity to work in a particularly active astronomical environment. There has constantly been a rich variety of cooperation with the Landessternwarte, the Astronomisches Rechen-Institut, the University's Institute of Theoretical Astrophysics or the Cosmophysics Department of the MPI of Nuclear Physics. One particularly striking and effective aspect of this cooperation comprises the Special Research Area (SFB) no. 1700 (»Galaxies in the Young Universe«), a project lasting many years in which all the Heidelberg Institutes mentioned above are involved, with major portions of their resources.

Teaching and Public Relations Work

Several members of the Institute's scientific staff also work as lecturers at the University of Heidelberg in addition to their research work at the MPIA. The Institute's tasks also include informing an extensive public audience about events in astronomical research. Members of the Institute give lectures in schools, adult education centres and planetariums, and they appear at press conferences or on radio and television programs, especially when there are astronomical events which attract major attention from the public. Numerous groups of visitors come to the MPIA on the Königstuhl and to the Calar Alto Observatory. Since 1976, the premises of the MPIA have been the setting for a regular one-week teacher training course held in the autumn, which is very popular among teachers of physics and mathematics in Baden-Württemberg.

Finally, the monthly journal *Sterne und Weltraum* (*Stars and Space*), co-founded by Hans Elsässer in 1962, is published at the MPIA. This journal is aimed at the general public and it offers a lively forum both for specialist astronomers and for the large body of amateurs in this field.

I.2 Scientific Questions

The central question of all cosmological and astronomical research deals with the creation and the evolution both of the universe as a whole, and of the stars, the galaxies, the sun and its planets. The MPIA's research programme is oriented around this question. In the field of galactic research, the Institute concentrates on the formation of stars from large interstellar gas and dust clouds. In the field of extra-galactic astronomy, the focus is on the search for protogalaxies and their subsequent evolution, the dynamical structure of galaxies, and on understanding active galaxies and quasars. The latter are remote stellar systems with an enormous radiation power. The observational research is supported asnd complemented by the MPIA theory group, which uses computer simulations to recreate processes in the universe extending over millions or billions of years. In this way, the MPIA achieves a fruitful synthesis of observation and theory.

Galactic Research

One focus of galactic research at the MPIA concerns questions about the formation of stars. The first phases of this process unfold in the interior of dense dust clouds, and hence remain hidden from our view in visible light. However, the infrared radiation emitted by these proto-stars and their warm surroundings is capable of penetrating the dust, making this wavelength range preferable for studying the early stages of the birth of stars.

The new-born star is surrounded by a dense equatorial dust disc in which the material can condense either to form other stars or to form planets. After a few million years, the disc finally disintegrates. This is also how astronomers envision the birth of our solar system, 4.5 billion years ago. Empirical evidence for the actual existence of the protoplanetary discs emerged during the 1980's, thanks in part to a great deal of work carried out at the MPIA. At present, MPIA researchers try to answer the following questions: Are all young stars surrounded by a gas and dust disc when they are born, and how long does this disk last? Which factors decide whether one or more stars or whether planets will form in a dust disc of this sort? Do discs also surround stars of much greater mass than our Sun (Chapter IV.1)?

Nowadays the idea that planets can form in the dust discs of solar-like stars is undisputed. For some years, it has been possible to prove that so-called exoplanets exist with the help of an indirect method. In a computer simulation, theoreticians explored how the new-born planets behave in the disc. In the process of this work, they established that under certain circumstances, the planets migrate from the outer region of the disc towards the central star within a relatively short period of time. This could explain why so many extrasolar planets similar to Jupiter have been observed on very close orbits around their respective central stars (Chapter IV.1).

The dynamics and evolution of our own galaxy, the Milky Way, have also been central features of research at the Institute for a long time now. Last year, it has been possible to use data from the HIPPARCOS astrometry satellite to establish that the Milky Way system is a barred spiral galaxy (Chapter IV.1). And the abundant data records supplied by the Calar Alto Deep Imaging Survey (CADIS, see below) – really intended for the search for the first galaxies in the universe - has providedimportant clarification about an essential component of the Milky Way system: it has been possible to arrive at a clear identification of the much debated »thick« disc which is the ancient precursor of the Milky Ways dominant »thin« disk (Chapter IV.1).

Extragalactic Research

It is a cosmologist's dream to be able to look back into the era of the universe when the first galaxies were forming. However, these protogalaxies are so remote, and the light from them is consequently so faint, that it has so far been impossible to discover them. In order to attain this goal, astronomers must use sensitive detectors working at the limits of the most powerful telescopes, and they also need to develop ingenious search strategies. Since the mid-1990's, the CADIS (Calar Alto Deep Imaging Survey) observing programme has been running on the 3.5 metre telescope at Calar Alto, with the aim of searching for the earliest populations of galaxies in the universe (Chapter IV.2). This programme is intended to run for at least five years and it is currently one of the MPIA's key projects (see 1997 Annual Report, p. 18). While the search for the protogalaxies is still in progress, it has already been possible to use the CADIS data to determine the evolution of the galaxies up to redshift $z = 1$ (Chapter II.1).

Another important topic concerns the quasars, the most luminous objects in the universe, which are suspected to have black holes at their centres. New data obtained with ISOPHOT indicate that some quasars are surrounded by large masses of dust. In many cases, however, the activity of the black hole at the centre of these quasars is not sufficient to explain the far infrared emission that has been measured. Extremely active star forming regions must also be present, of the sort also found in colliding ultra-luminous galaxy systems (Chapter IV.2).

Less spectacular, but equally as important for our understanding of galactic evolution, are the dwarf galaxies. These show certain features which it has not yet been possible to explain unambiguously. For example, it is not clear why dwarf systems in dense galaxy clusters contain less gas on average than those in less dense clusters. A theoretical study has now proven that the hot intergalactic medium blows the interstellar gas out of most dwarf galaxies within a few billion years (Chapter IV.2).

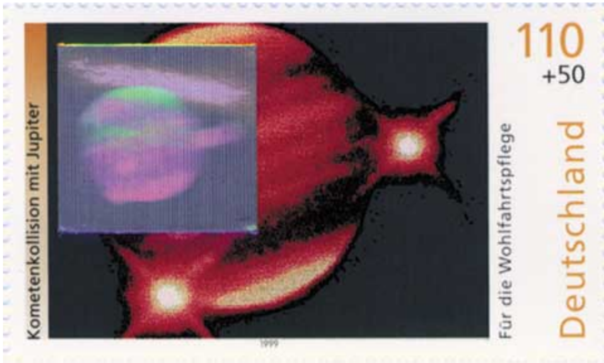

Fig. I.8: The first series of holographic stamps in Germany shows the crash of the comet Shoemaker-Levy 9 onto Jupiter in july 1994. The images used were taken at Calar Alto.

The Solar System

On several occasions,, when important events take place within the solar system, the telescopes on Calar Alto have been able to demonstrate their capabilities time and time again. In 1994, images from the Calar Alto Observatory went around the world, showing the impact of debris from comet Shoemaker-Levy 9 on Jupiter (Fig. I.8). In 1997, Comet Hale-Bopp was the focus of a great deal of attention on the part of the public.

In the reporting year, the theory group devoted its attention to the bodies in the Kuiper belt. Beyond 42 astronomical units (AU), the paths of these objects show unusually high eccentricities, and they are inclined sharply with respect to the ecliptic. Computer simulations now indicate a possible explanation for this: a star at a distance of only about 160 AU disturbed these celestial bodies in the outer protoplanetary disc. As a result, they went into sharply eccentric and inclined paths, which they have retained until the present (Chapter IV.3).

II Highlights

II.1 CADIS and the Evolution of Galaxies

Galaxies such as our Milky Way system form the basic building-blocks of the universe. They contain as many as several hundred billion stars, and they extend up to several hundred thousand light years. Modern cosmology has found some surprising answers to the burning questions about the birth and evolution of these »island universes«, but a great deal remains unclear. As part of the CADIS research project, astronomers at the Institute have been able to investigate the evolution of different types of galaxies over the last ten billion years. This study was the first in which a statistically significant number of galaxies could be used.

In the first models of cosmic evolution, it was assumed that individual gas clouds with the masses of today's galaxies were drawn together by gravity in the first billion years after the Big Bang, and that they then developed as largely isolated systems into the present-day galaxies. However, more recent observations have shown that this simple picture requires major revision. For example, it is impossible to ignore the interaction of the young galaxies which were considerably closer together in the earlier (and denser) universe than they are now.

In the so-called Hubble Deep Field, a selected area of the sky which was photographed using a ten-day exposure with several filters in 1995, a number of blue, irregular galaxies were discovered which increased sharply with redshift. They were only about ten thousand light years in diameter. In the present-day universe, they account for a substantially lower fraction of all galaxies. One possible explanation for this is that these small systems fused together to form larger galaxies later on.

Apart from morphological studies, the so-called luminosity function of the galaxies is suitable as a suitable means to describe the characteristics of galaxy distributions. It indicates the frequency of galaxies with differing absolute luminosity in a given volume. Accordingly, the luminosity function for different redshifts (distances) describes the evolution of galaxy populations with the age of the universe.

3000 Galaxies to Determine Luminosity Functions

Regarding the technical observation requirements, some major difficulties arise with determining the luminosity function. The objective is to record as many galaxies as possible, down to the lowest possible luminosities, and to determine their redshifts. In the 1990's, there were some attempts based on direct images followed by spectroscopy of the objects. However, selection effects occurred here which could only be corrected with difficulty. Moreover, it is not possible to reach such faint objects with spectroscopic observations, although this can be done with direct images.

Astronomers at the MPIA now embarked on a different path. They used the unique data record of the Calar Alto Deep Imaging Survey, CADIS. This is a long-term programme designed to search for the proto-galaxies in the universe (see Chapter IV.1). In connection with this project, several fields of the sky with areas of 100 to 150 square arcminutes (corresponding to a quarter of the area of the full moon) were imaged through a large number of colour filters. The 2.2 metre and the 3.5 metre telescopes at the Calar Alto observatory are available for this purpose.

In addition to the large image field, the CADIS images also have two other decisive advantages: first of all, photometric images are obtained with a large number of filters, so that the spectral energy distribution can already be determined from them very accurately. Second, objects emitting very faint light, up to magnitude 23, are visible due to the long exposure times of several hours.

The fields around 1^h, 9^h and 16^h right ascension were used to determine the luminosity functions of galaxies. The exposure times were typically 5.5 hours for the narrow band filters. Since the fields of the sky were located at high galactic latitudes, extinction due to interstellar dust is negligible.

Special software was written to separate the galaxies from the stars and quasars. The separation is not based on the morphology, but solely on the colours. A spectral atlas was used for this purpose, containing the spectral energy distributions of stars, quasars and hundreds of different galaxy types, ranging from old elliptical galaxies to young populations with high star formation rates (starburst galaxies). These energy distributions were gradually red-shifted towards higher wavelengths on the computer, and then it was determined which colours these objects would have in the filters used for CADIS. In this way, 132 spectral energy distributions were obtained for stars, 45,000 for quasars and 20,000 for galaxies up to a maximum redshift of $z = 1$. In the three fields up to magnitude 23, this classification procedure made it possible to identify 939 stars, 71 quasars and 2779 galaxies. It was possible to use Monte Carlo simulations to show that the accuracy of the redshift values is 0.04, resulting in an adequate accuracy of 0.2 mag for the absolute luminosity.

This method makes it possible to find more galaxies and reach weaker objects than with spectroscopic observations. The result is the most extensive group of galaxies obtained to date, with apparent luminosities of up to 22 mag, which is free of selection effects. For the first time ever, this enables us to make statistically confirmed statements about the luminosity function for different redshift values. Because the CADIS image field contains too few near galaxies, only luminosity functions for the near galaxies ($z < 0.2$) could not be obtained. The CADIS data are therefore suitable for the luminosity function of galaxies for redshift values in the range between $z = 0.2$ and $z = 1$.

The model of the universe that is assumed plays a major part here. Since the universe is expanding, a given volume element at a specified redshift will also expand. If we intend to compare the spatial densities of galaxies in the universe at earlier and later times, this increase in volume has to be taken into account. However, it depends on the chosen cosmological model. In the MPIA study, a universe was adopted with critical density ($\Omega = 1$) and a Hubble constant $H_0 = 100$ km s^{-1}/Mpc.

Has the Luminosity Function Developed over Time?

In the mid-1970's, the American astronomer Paul Schechter found a function which can be used to describe the luminosity distribution of nearby galaxies. According to his work, the density of galaxies generally decreases as the luminosity increases, that is to say that there are more faint galaxies than bright ones. A Schechter function of this sort can be divided into two sections: above a characteristic luminosity L^*, the distribution falls exponentially, and below it ($L < L^*$), the distribution falls according to a power law. For nearby galaxies, the characteristic absolute luminosity is somewhat above $L^* = 10^{10}$ solar luminosities, which corresponds fairly accurately to the value for the Milky Way. The luminosities of the galaxies are often converted into their absolute magnitudes. In this case, the characteristic absolute magnitude in the blue for nearby galaxies is about $B^* = -20$ mag.

Investigations have so far failed to produce a clear answer to the question as to whether the luminosity function has changed over time. The CADIS data contained so many galaxies that it was possible to obtain the distribution for the four redshift ranges from 0.1 to 0.3, 0.3 to 0.5, 0.5 to 0.75 and 0.75 to 1. A distinction was also drawn between so-called »early type« galaxies (elliptical and spiral galaxies with Hubble types prior to Sb) and the late type, which are dominated by starburst galaxies.

To start with, the luminosity function is not dependent on the redshift for early type galaxies (Fig. II.1). This means that the early universe contained just as many elliptical and spiral galaxies as it does today. The characteristic absolute magnitude in the blue is about – 19.9 mag, and it remains unchanged, as does the shape of the luminosity function.

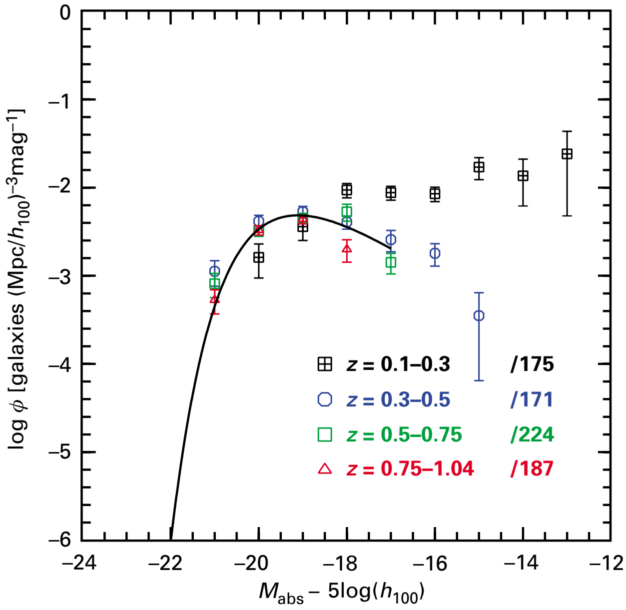

Fig. II.1: The luminosity function for early type galaxies shows no significant evolution in the four redshift ranges indicated.

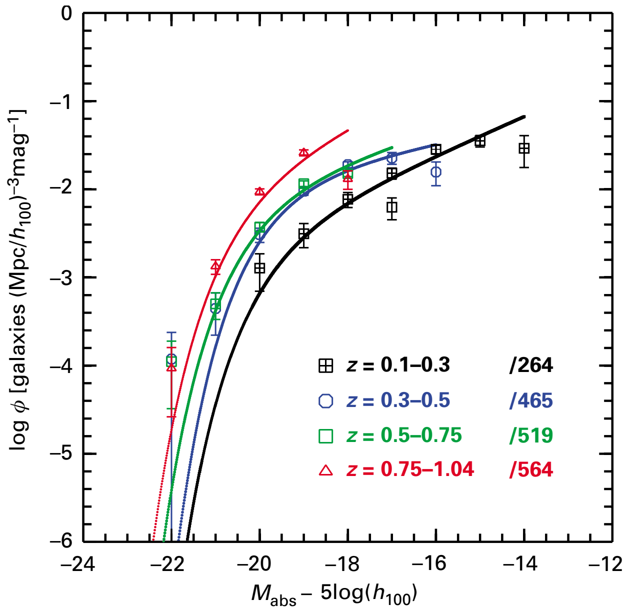

Fig. II.2: The luminosity function for late type galaxies changes with redshift.

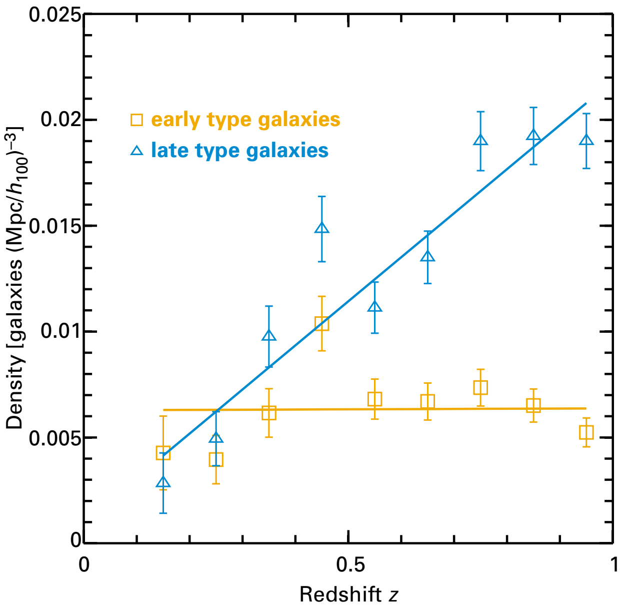

Fig. II.3: The spatial density of the early and late type galaxies in relation to the redshift. As the age of the universe increased, the density of the late type galaxies decreases, while that of the early types has remained constant.

The situation is different for late type galaxies (starburst galaxies) (Fig. II.2). The curves here show different gradients, the characteristic luminosity rises with increasing redshift, and the curves shift to higher values. This means that there were about five times more starburst galaxies in the universe approximately ten billion years ago, and that the galaxies were typically more luminous than they are today.

Fig. II.3 shows how the spatial densities of the different galaxy types have developed as the age of the universe has increased. One can clearly see that the spatial density (given as the number per million cubic megaparsec) has remained more or less constant for the early types, while the density of the late types has decreased as the age of the universe has increased. The expansion of the universe has been taken into account here.

The interpretation of the new data is not entirely without ambiguity, but when results from other work are included, an interesting scenario of cosmic evolution begins to emerge. For example, it has long been clear that the starburst galaxies were largely systems where two galaxies merged together. This procedure stirs up the interstellar gas and extensive star formation sets in. Most of the starburst systems from the CADIS data would very probably appear as irregular systems for this reason. More recent studies now suggest that the early universe contained more merging irregular galaxies than it does today. The CADIS study has confirmed this on the basis of a statistically significant group for the first time. Above and beyond this, it supplies absolute figures which can be used as the basis for cosmological evolution models.

II.2 Astrophysics with Gravitational Lenses

In modern astrophysics, gravitational lenses are becoming more and more important. Although they were predicted as long ago as the 1930's, the first gravitational lenses were only discovered in 1979. Since then, this initially exotic area of astronomical research has developed at a breathtaking pace. In collaboration with groups at the Center for Astrophysics in Boston and the University of Arizona in Tucson, researchers at the Institute are currently taking part in a wide-ranging programme dubbed CASTLES, in which the Hubble Space Telescope is being used to observe a large number of gravitational lenses. In many systems, as part of this CASTLES project, it has been possible to use multiple images of the same background source to prove the presence of previously undetectable galaxies which act as lenses. Furthermore, this unique dataset allows an independent determination of the Hubble constant.

The gravitational lens effect is based on the effect predicted by the General Theory of Relativity, according to which matter bends the space-time which surrounds it (Fig. II.4). If light from a remote object passes through a space-time volume which has been bent in this way en route to the Earth, it will be deflected from the straight line along its direction of propagation. The angle of deflection is proportional to the mass acting on it.

Bent space-time regions of this sort act like lenses. Depending on their geometry, the more remote object appears to the observer either as a multiple image or a ring because of this effect. The latter case applies if the background and foreground objects are precisely on the same line of sight for the observer. The term »Einstein Ring« is used to describe this phenomenon. The gravitational lens effect also increases the intensity of one of the images generated. A »lensed« object will then appear brighter than it would without this effect.

The gravitational lens effect was already proven for the first time during the solar eclipse on 29 March 1919. Two expeditions led by Sir Arthur Eddington set out for South America at the time, in order to observe this phenomenon. In fact, Einstein had calculated the light deflection in the Sun's field of gravity beforehand, predicting a value twice as high as the one obtained with Newton's theory. Accordingly, the positions of stars directly at the edge of the Sun should be shifted by almost two arcseconds in relation to their normal positions. In actual fact, the astronomers were able to confirm Einstein's prediction, which meant the breakthrough for the General Theory of Relativity.

Then in 1937, Fritz Zwicky, the Swiss astronomer who had emigrated to the USA, predicted that galaxies should cause more remote stellar systems to appear as multiple images, or to be distorted into rings. Even then, Zwicky pointed out some cosmological applications of the gravitational lens effect. However, four decades still had to pass before the discovery of the first gravitational lens.

In 1979, two quasars separated from one another by only six arcseconds were discovered, with almost identical spectra: suspicions were immediately aroused that these must actually be two images of one single quasar. When a nearby galaxy was subsequently found between the two quasar images, astronomers were convinced that this must

Fig. II.4: Principle of the gravitational lens effect. The gravitational field of a galaxy cluster or even of one single galaxy bends the light from a remote quasar, creating two or more images. If the lens and the source are directly behind one another, the source is distorted into an Einstein ring.

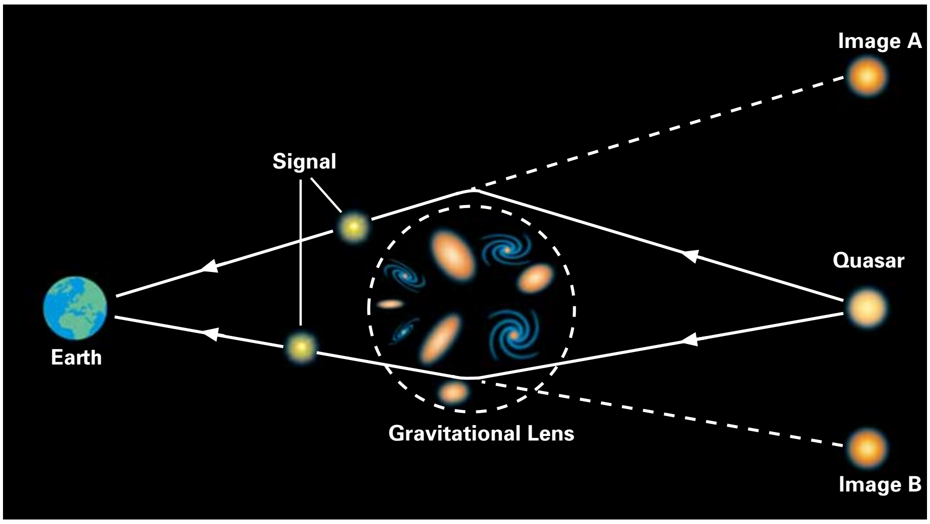

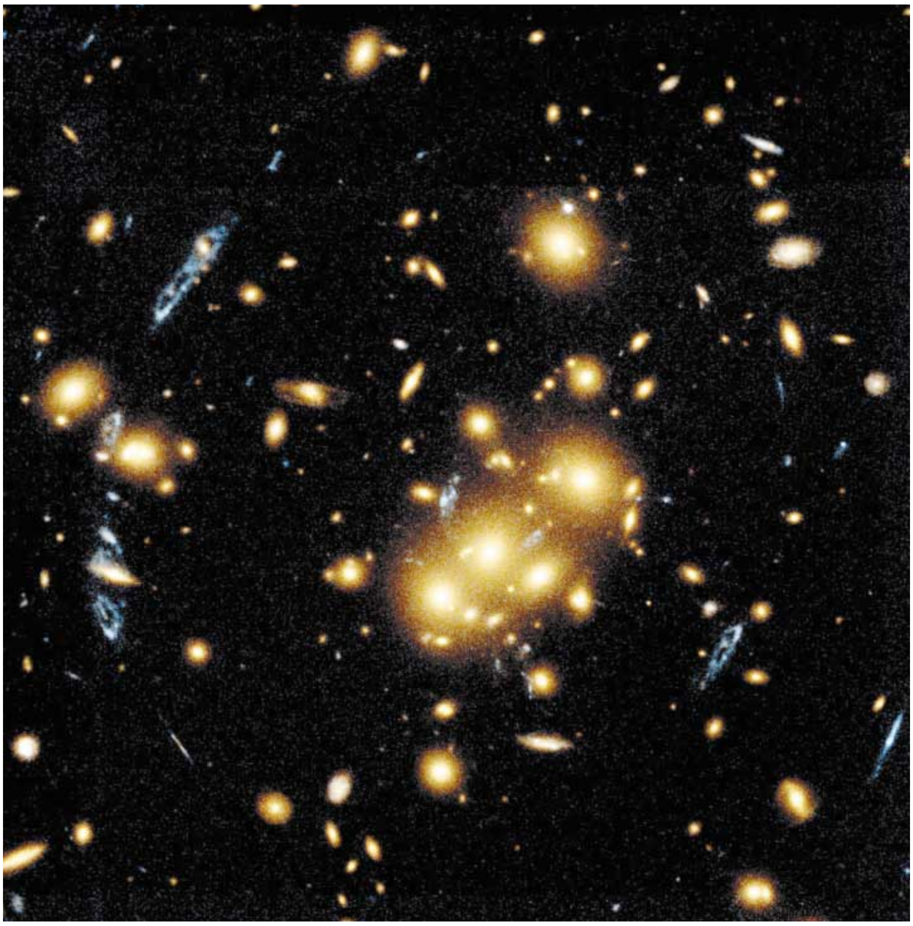

Fig. II.5: In the galaxy cluster CL0024+1654, one background galaxy is imaged seven times (blue) (Photo: NASA/ ESA)

be the lens. In the 1980's, images of very remote galaxies were also found to show curved distortions. In this case, the gravitational potential of a whole galaxy cluster was acting as a lens (Fig. II.5).

The CASTLES Project

By the end of 1999, more than 50 gravitational lens systems were known in which one single galaxy acts as a lens creating multiple images of quasars and radio sources located behind it. Almost all lenses are massive elliptical galaxies. They represent a special group inasmuch as they are selected on the basis of their masses, rather than in the usual way according to their luminosities. The astronomers are pursuing the following goals with CASTLES (CfA-Arizona-Space-Telescope-Lens-Survey, `cfa-www.harvard.edu/castles`):

- to find as yet undiscovered lens galaxies,
- to measure the exact positions of the images and the lens,
- to determine the redshift of the lens by photometry,
- to prove the existence of lensed galaxies (host galaxies) around active galactic cores,
- to determine the structure and evolution of the galaxies which act as lenses,
- to measure the extinction in the galaxies acting as lenses,
- to detect dark matter and
- to determine the Hubble constant.

This list underscores the far-reaching possibilities offered by the gravitational lens effect.

Observational data already exist for many of the systems examined with CASTLES, but the material available is of differing quality, and the images were obtained in numerous different filter ranges, so that comparative studies are virtually impossible. Since 1997, the 54 known systems have been observed with the HST. Use is made of the Wide Field Planetary Camera 2 in the visual (V, at a wavelength of 555 nm), in the red (R, 675 nm) and in the near infrared (I, 814 nm); and the NICMOS camera is used in the infrared (H, 1600 nm). By the end of 1999, 60 % of all planned photographs had been taken in V, 70 % in I and 80 % in H.

Critical Point: the Models

The discovery and characterisation of lenses in all systems is certainly the primary goal of CASTLES, but this work must be followed by an intensive examination and theoretical interpretation of the data. The basic requirement for this is a theoretical model which reproduces the gravitational field for the lens. The following points must be taken into particular account here: first of all, the relative central position of the lens galaxy must be determined as accurately as possible. On the HST photographs, this is possible to within a few hundredths of an arcsecond. Then, a mass profile of the lens galaxy must be generated, describing the mass within the Einstein ring radius and the ellipticity and orientation of the galaxy. Three models have proven to be the most realistic for this purpose, depending on the type of galaxy: the isothermal ellipsoid sphere, the de Vaucouleurs model and a disc with an exponential density profile.

In addition to this, the light deflection due to neighbouring galaxies must be taken into account. Finally, there may be effects due to gravitational fields generated by large-scale structures, located at random redshifts on the line of sight to the lensed object. The latter are not directly recognizable on the photographs, so it can be especially difficult to take them into consideration.

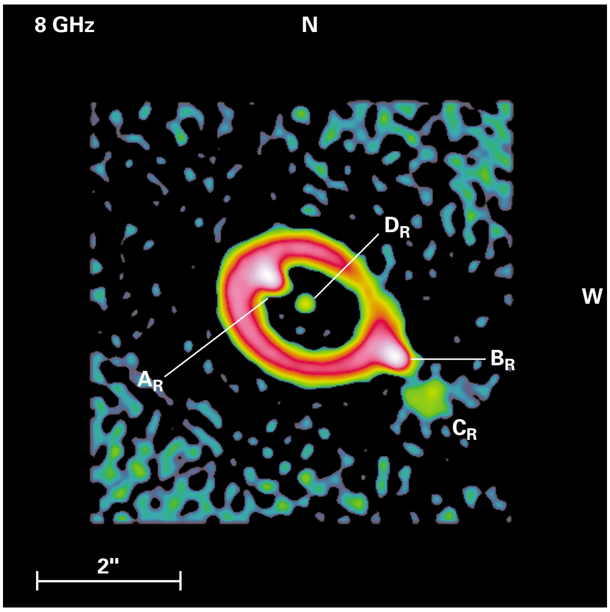

Fig. II.6: In the radio range, the Einstein ring of MG 1131+0456 is apparent with the two bright nodes and the central lens galaxy (DR). The images of the active galactic core are identified as AR and BR.

Fig. II.7: The images of MG 1131+0456 obtained in the CASTLES ▶ project in filter ranges H, I and R using the HST. The images of the galactic core are marked as A and B, and the lens galaxy is marked as G.

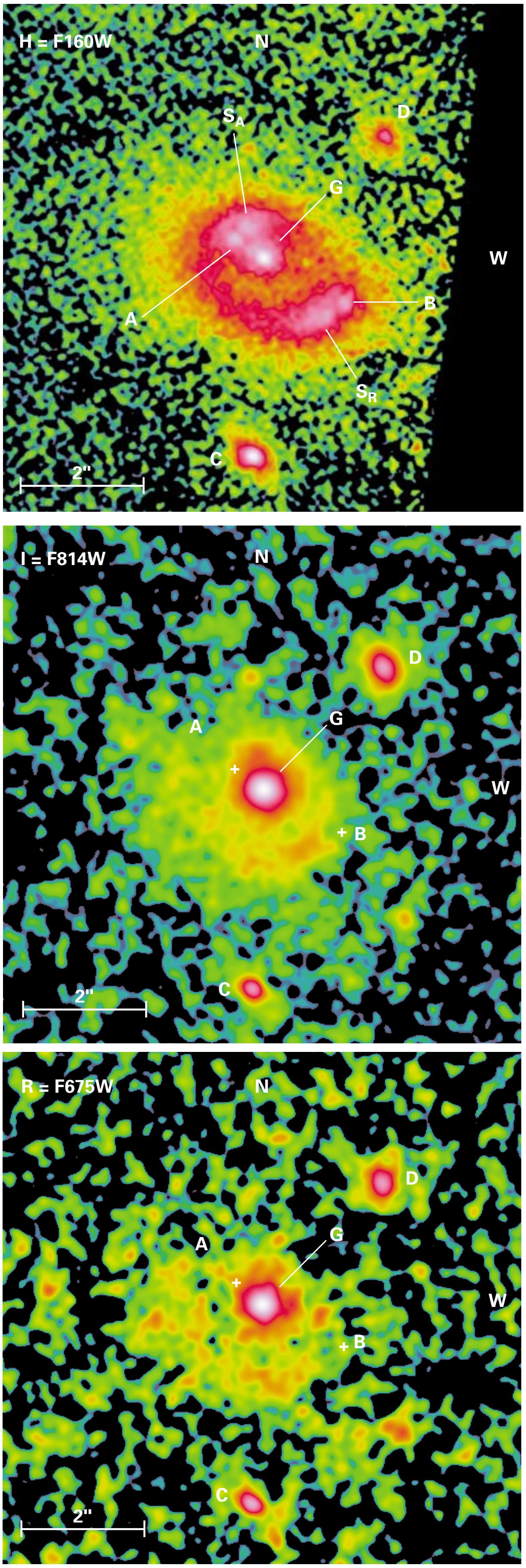

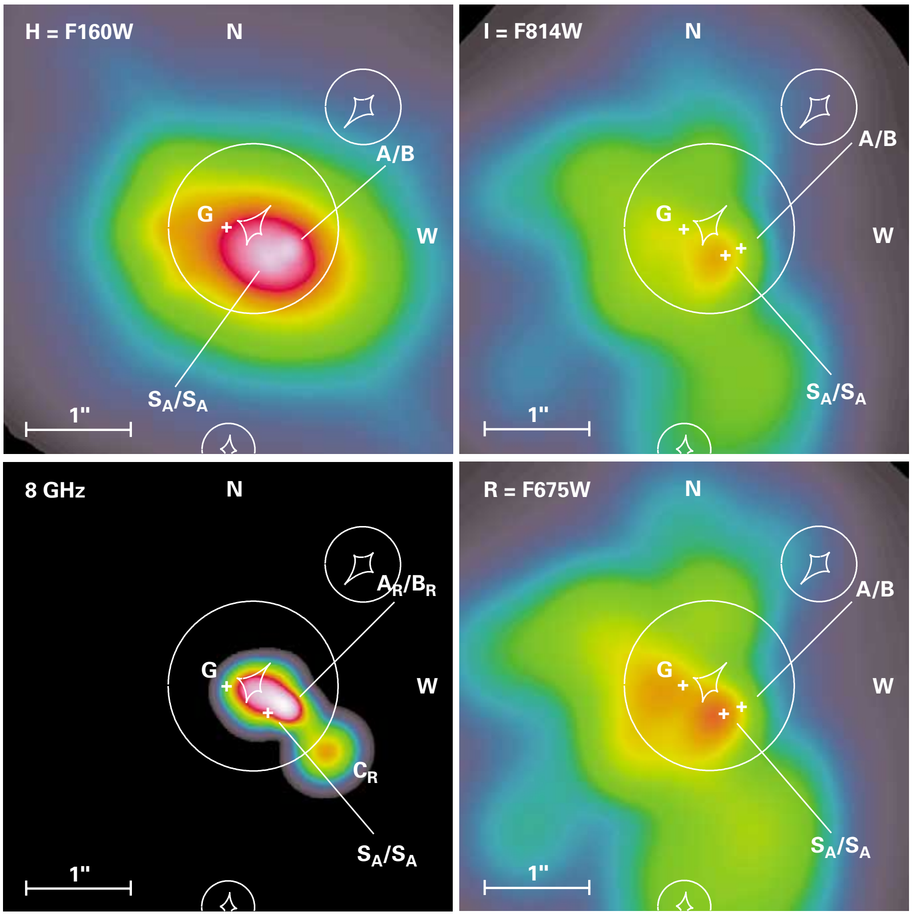

Fig. II.8: Reconstruction of the lensed source in the three filter ranges of the HST and in the radio range (8 GHz). The radio image clearly shows the jet and the other images show the optical emission which appears to be partially associated with the jet. The suspected active core cannot be recognised, probably because it is covered by dust.

The Einstein Ring MG 1131+0456

MG 1131+0456 was the first Einstein ring to be discovered. It was found in 1988 during radio observations. At a frequency of 8 GHz, an elliptical ring is apparent with a diameter of about two arcseconds; two bright nodes are located on it at opposite points (marked in Fig. II.6 as A_R and B_R). During subsequent observations, it was determined that the radiation from these cores varies in intensity. Moreover, a weak point source appears in the centre of the ring (D_R).

The nature of these different components in the gravitational lens image remained in dispute for years. Nowadays, we are certain that the central object is the lens galaxy, whereas the lensed background source is an active galaxy from whose central region a jet shoots out. The Einstein ring is the image of the jet, and the two nodes A_R and B_R are two images of the point-shaped active core of the galaxy. A faintly luminous small cloud close to radio node B_R is interpreted as an unlensed part of the jet. The modelling of the system proved to be very difficult.

As part of the CASTLES project, it was possible to obtain high-quality photographs of MG 1131+0456 in the optical and near infrared (Fig. II.7). The lens galaxy appears on all the images. In the near infrared (H image), in addition to the lens, we can see the light from the stars in the remote galaxy distorted into a spectacular Einstein ring. The distribution of intensity in the lens galaxy can be described very well by a de Vaucouleurs profile with an effective radius of 0.68″, and the colours match an elliptical or S0 galaxy in a redshift range between z = 0.8 and z =1.0. Estimates by other astronomers had led to redshifts of 0.85 or 0.89. This boosts confidence in the determination of the redshift by multicolour photometry which was used here.

Other galaxies are located at the same distance as the lens, and they very probably all belong to one cluster. They contribute towards the distortion of the image, and they must therefore be taken into account in the model.

It was possible to use these data to compile a mass model for the entire galaxy cluster, including the lens galaxy. This now made it possible to remove the distortion from the distorted image of MG1131+0456 and to reconstruct the image of the source (Fig. II.8).

The radio image then clearly shows the elongated jet structure. The distorted emission in the near infrared now appears as an elliptical distribution with a bright centre: so we are suddenly confronted with a »normal« galaxy image. At even shorter wavelengths around 600 nm (V-image), half of the reconstructed source appears to be much fainter. This asymmetrical structure and the colour of the source suggest larger quantities of dust.

Moreover, part of the optical emission comes from a region along the jet – a phenomenon which has only been found on a very few extragalactic jets in the past. As other work has also shown, the background source is at a redshift of about $z = 2$, so that the jet galaxy has emitted the observed radiation in the UV. This could be scattered light from the core region, but it could also have originated in the interstellar medium of the galaxy in which the jet triggers shocks. It is also conceivable that dust is shadowing the active core. This would explain why it can only be detected in the radio and near infrared ranges.

MG 1131+0456 is a good example of how a high-quality dataset can be used to obtain an abundance of information about the lensed celestial bodies at high redshifts.

The Hubble Constant

Even before the first gravitational lens was discovered, theoreticians were studying how this effect could be used to determine the Hubble constant. In the 1960's, Sjur Refsdal, of the Hamburg-Bergedorf Observatory, found the following principles leading to a solution to this problem. If a galaxy generates two images of a quasar, the two collimated light beams travel from the source to the observer along different paths (Fig. II.4). These two light paths will generally have different lengths, and the light from the source will take different times to travel along them. The light will also undergo a relativistic delay, since it passes through different regions of the gravitational field. This means that a signal emitted by a quasar reaches the observer at different times via the two paths. To be precise, the light of the image which appears closest to the centre of the lens will have a longer travelling time.

The goal is now to design a computer model in which the mass distribution of the lens galaxy is varied until the observed astronomical variables – such as angular distances and brightness ratios between the images, and the brightness of the lens galaxy – are reproduced correctly. If the redshifts of the lens galaxy and the quasar are known, the total travelling time for the signals can be calculated on the basis of the difference in travelling times. This will then yield the actual distance at a specified redshift, and hence the Hubble constant which is the proportionality constant between redshift and distance.

This procedure to determine the Hubble constant is very simple in principle, and it is the only one of a purely geometrical nature. Ultimately, the value still has a 5 to 10 % dependency on the cosmological model which is chosen. In practice, however, the gravitational lens method proves to be very difficult. First of all, it is difficult to measure the differences in travelling time, which are so far known for only four systems. Second, the mass models must be very precise if the Hubble constant is to be determine to within less than 10 %.

Especially in cases where only two or more images of a quasar can be recognised, the problem of ambiguity occurs. This means that there are several mass models which reproduce the observed lens image equally well. Additional Einstein rings or distorted images of the »Parent Galaxy« which contains the quasar can be of further help here. It has so far only been possible to arrive at an approximate determination of the Hubble constant in real detail (but not really unambiguously) in two cases: for PG 1115+080 and Q 0957+561.

PG 1115+080 is the second known »lensed« object. It consists of four quasar images (Fig. II.9). The source is a quasar at redshift $z = 1.722$, and the lens is an elliptical galaxy at $z = 0.31$. Between images B and C, it was possible to measure a time delay of 25 days. The ratio of the time delays between A and C, and between A and B, is also known. Earlier investigations had led to a Hubble constant of 53 km s^{-1}/Mpc.

New images obtained in connection with CASTLES, especially in the near infrared (H filter), have now supplied stricter boundary conditions for the mass model of the lens galaxy. For the first time, spatial resolution of the lens galaxy has been possible, so that better models can be produced for it. It was represented by a de Vaucouleurs brightness profile, yielding an effective radius of 0.6″. The virtually circular form led the astronomers to conclude that this is a normal elliptical galaxy containing no significant dust components. This is also an important piece of information as regards interpreting the brightness ratios of the images, because two collimated light beams which have passed through different regions of a dust-rich galaxy may be attenuated to different degrees by the dust.

After the images of the lens galaxy and the quasar had been fitted with intensity functions, it was possible to remove them from the near infrared image. An Einstein ring then emerged clearly. This is the distorted image of the mother galaxy of the quasar. This ring supplies a second marginal condition for the mass model of the lens galaxy. Moreover, the gravitational fields of nine more galaxies located in the image field had to be taken into account. They create the tidal forces on the gravitational field of the lens galaxy, as mentioned above. Despite the substantial improvement in the data, it was impossible to determine the Hubble constant without ambiguity. The main reason for this is the ambiguity of the mass model of

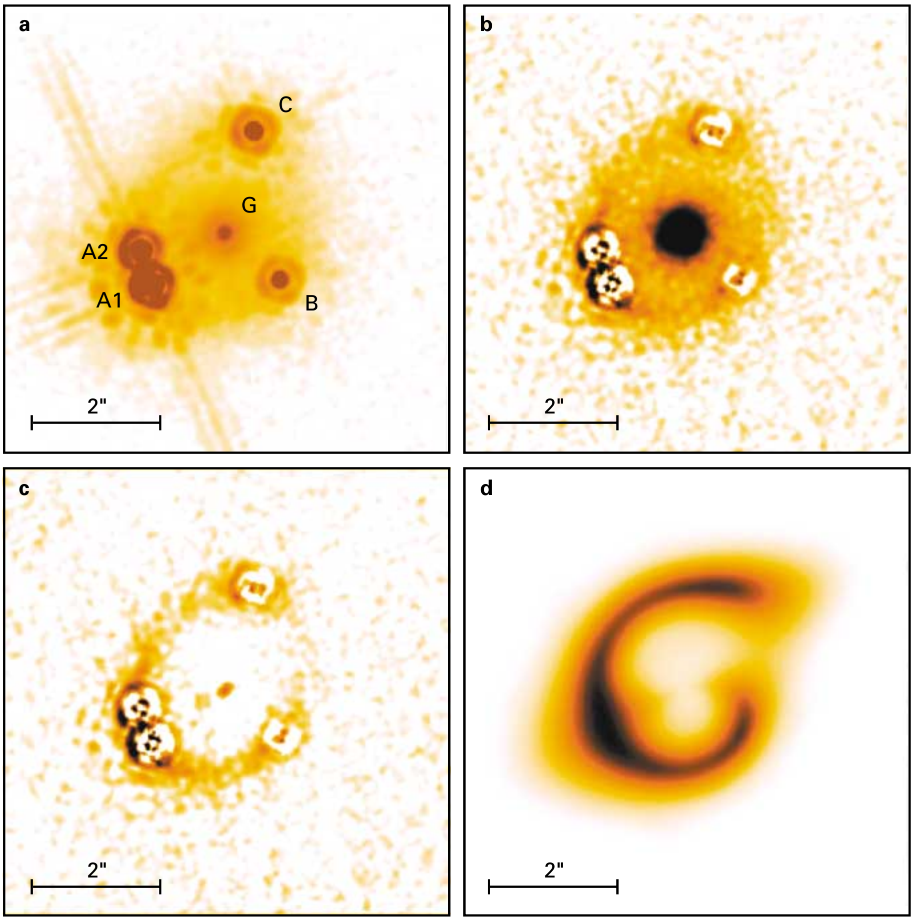

Fig. II.9: HST image of PG 1115+080 in the near infrared. **(a)** original H photograph. After subtraction of the quasar images **(b)** and the lens galaxy **(c)**, the Einstein ring can be recognized; **(d)** shows the ring that was calculated with the mass model.

the lens galaxy. If we use an isothermal ellipsoid to describe it, we obtain a value of H_0 = 44 km s^{-1} Mpc^{-1}. But if we select a model with a constant mass-to-light ratio, we obtain H_0 = 65 km s^{-1}/Mpc. Both these values are applicable to a universal model with critical density of $\Omega = 1$). They increase by about 10 %, if we assume an open universe with $\Omega = 0.1$. In the future, the uncertainty can be reduced still further if we measure the difference in travelling times more accurately and if deeper images are obtained, so that the Einstein ring is better defined. Even now, however, the second value represents a good, independent confirmation of the best estimate at present, on the basis of near galaxies. This value is 67 km s^{-1}/Mpc.

This method's difficulty in determining the Hubble constant is also shown by the case of system Q 0957+561. This is the first known lens system, which was discovered in 1979. It consists of a lens galaxy at $z = 0.36$ in a cluster, creating two images of a quasar at $z = 1.41$. It has been possible to determine the travelling time delay in the two images as 417 days (Fig. II.10). After the image of the lens

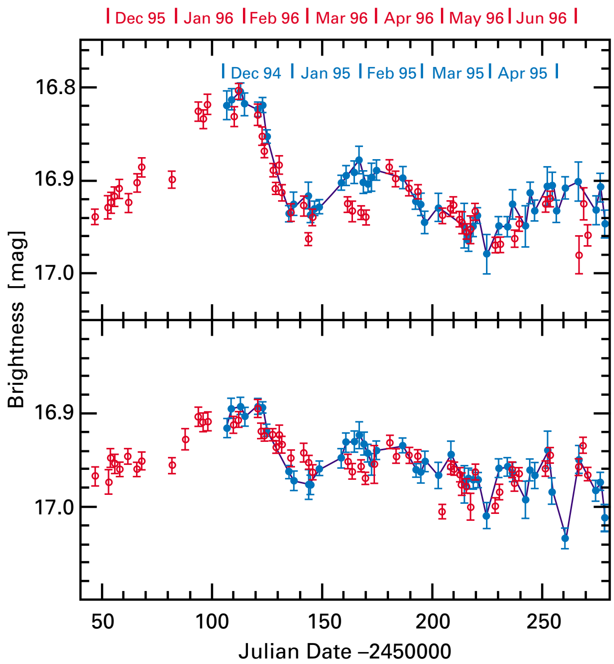

Fig. II.10: Brightness variation of the two images in the double quasar Q0957+561, in blue light above and in red light below. The light curves in both graphs are shifted against one another by the time delay of 417 days, so that they are now superimposed.

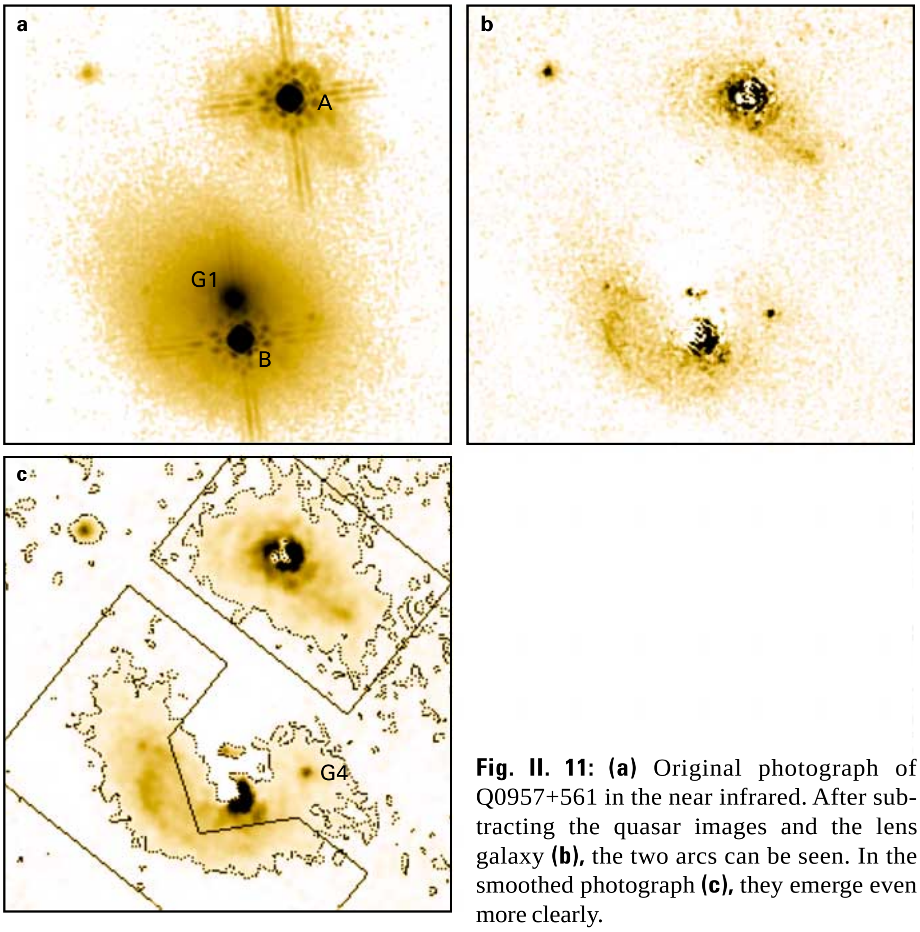

Fig. II. 11: (a) Original photograph of Q0957+561 in the near infrared. After subtracting the quasar images and the lens galaxy **(b)**, the two arcs can be seen. In the smoothed photograph **(c)**, they emerge even more clearly.

galaxy had been modelled with a de Vaucouleurs profile and the two quasar images had been modelled as single point functions, it was possible to subtract them from the image. This revealed two faint arcs adjoining the two images A and B (Fig. II.11). Both cases involve images of the mother galaxy of the quasar which are lensed and almost distorted into an Einstein ring. These two arcs were discovered in the CASTLES photographs, and now they are a very major restriction for the mass model of the lens galaxy.

Previous mass models described the lens galaxy with circular or elliptical symmetry. For the first time, the new work by the CASTLES team made it possible to derive an inner structure of the galaxy from the observations. What is more, the contribution from the surrounding galaxies was taken into account: this must be smaller than had been assumed until now. In general, it became clear that the existing models and the values derived from them for the Hubble constant were incorrect. Ultimately, it was possible to determine the mass model more accurately thanks to the discovery of the two arcs. Nevertheless, some ambiguity was still left here, leading to an inaccuracy of 25 % in the Hubble constant. As the most probable value remained an upper limit of 80 km s^{-1} Mpc^{-1}. This is again valid for $\Omega = 1$. For an open universe with $\Omega = 0.3$, the limit shifts to $H_0 = 84$ km s^{-1} Mpc^{-1}.

Even though this attempt at establishing the value of the Hubble constant was still unable to supply the desired accuracy, the procedure gives grounds for hope. It will certainly be possible to improve the result substantially if those parts of the Einstein rings which are only faintly discernible at present can be brought out more clearly on photographs with longer exposures. In addition, it should be possible to use the new Chandra (USA) and Newton (Europe) X-ray telescopes to observe the hot gas of the galaxy cluster in which the lens galaxy is located. This should then allow us to derive an improved mass model of the cluster.

The Evolution of Elliptical Galaxies

The formation and evolution of galaxies is one of the central problems in modern astrophysics. Previous observations suggest that the stars in most elliptical and S0 galaxies, located in rich clusters, came into being in an earlier epoch. Thereafter, the systems only continued to evolve passively. This means that once the star population had been formed, it aged constantly, without the subsequent formation of new stars. As a result, it became redder and fainter as time went on. This early phase of formation is expected in an era when the universe had about 10 to 20 %

of its present age, i.e. when it was about 1.4 to 2.8 billion years old. This corresponds to a redshift range of $2 < z < 3$.

One argument in favour of this scenario is the observation that the elliptical and S0 galaxies in clusters have very similar colours up to a redshift of about $z = 1$, both inside a cluster and also from one cluster to the next. This could hardly be explained if new stars had been formed in the galaxies over billions of years, independently of one another and to differing extents. There is a particularly striking correlation which was discovered at the end of the 1980's: as the effective radius increases, the velocity dispersion rises, while the average surface brightness decreases. If these variables are plotted against one another in a three-dimensional diagram, the galaxies are located very close to one plane, the so-called fundamental plane. This can quite easily be explained in physical terms if the galaxies are regarded as multiple particle systems which are in virial equilibrium.

So far, it has only been possible to verify this correlation for elliptical and S0 galaxies in rich clusters, which only account for a very small fraction of the total galaxy population at earlier epochs (at redshifts between 0.5 and 1). Whether it also applies to galaxies of this type in less dense clusters is a question which still remains largely unclear. There are theoretical models according to which the field galaxies formed later than those in rich clusters or, in other words, the stellar population of the field galaxies is younger than that of the cluster galaxies. This idea can now be tested: for example, since the luminosity of a galaxy changes as its age increases, the field galaxies should not lie on the fundamental plane of the cluster galaxies.

The group of galaxies which act as gravitational lenses is suitable as a way of finding evolution effects in field galaxies: these are primarily massive elliptical and S0 galaxies in a redshift range of between 0 and 1 which are not located at the centre of rich clusters. This is because the probability that a galaxy will function as a lens is dependent on its surroundings only to a minor extent.

In the cases which have been examined to date, the fundamental plane has always been determined for galaxies of one single cluster, whose members all essentially have the same redshift. But the analysis of the lens galaxies involves single systems at different redshifts, and therefore at different stages of evolution.

The background to the new analysis is the fact that the surface brightness varies sharply with the redshift, and this depends on the colour. If we now measure the effective radius and the velocity dispersion of a galaxy (provided that it lies on the fundamental plane), it is possible to calculate the surface brightness. This is extrapolated to the value which the galaxy would have had today (for $z = 0$) so that it can be compared with the values for nearby galaxies which have been measured adequately.

This transformation to $z = 0$ depends on the cosmological model and the epoch when the stars were formed. At present, the most probable cosmological models are a flat universe with $\Omega_0 = 0.3$ and $\Lambda = 0.7$, or an open universe with $\Omega_0 = 0.3$.

Since spectra are only available for a few lens galaxies, the relevant variables for the fundamental plane must be obtained from the angular distance of the lens images and the photometric data. For example, using the mass model of an isothermal sphere, the geometry supplies the total mass of the lens galaxy, and hence also the velocity dispersion. The effective radii and apparent magnitudes have been determined for all filters. A value of $H_0 = 65$ km s^{-1}/Mpc was assumed for the Hubble constant.

Unter diesen Voraussetzungen ließen sich die Galaxien aus dem CASTLES-Datensatz am besten mit dem kosmologischen Modell des offenen Universums und einer Sternentstehung in den Galaxien bei $z > 2$ erklären. Nur für diese Lösung gibt es im nahen Universum Galaxien, die man als weiterentwickelte Versionen der beobachteten Linsengalaxien betrachten kann.

This result contradicts a model which was produced only recently, according to which the field galaxies (i.e. the lens galaxies in this case) only formed at redshifts of between $z = 0.5$ and $z = 1.5$. It proves that elliptical and S0-galaxies have developed identically, regardless of their surroundings

II.3. Hydrocarbons – Puzzling Actors in Dust

Almost 30 years ago, it was discovered that the near infrared range contains emission bands which at first could not be assigned to any known type of molecule. Since then, they have been found almost everywhere in the interstellar medium, in planetary nebulae, HII regions and reflection nebulae. In the mid-1980's, the suspicion arose that large organic molecules – so-called polycyclical aromatic hydrocarbons (PAHs) – might be the cause of the infrared emission bands. Now for the first time, ISOPHOT has also made it possible to prove the presence of this spectroscopic signature in the interstellar cirrus and in the diffuse background IR radiation of the Milky Way, and to chart it in another spiral galaxy. The observations argue in favour of the omnipresent existence of PAHs, underlining their unusual stability and their great importance as highly effective interstellar »coolants«: the PAHs absorb the UV radiation and re-emit the energy they have absorbed in the form of the observed IR radiation. The new data obtained with ISO have heated up considerably the discussion about this class of complex molecules, and hypotheses about conceivable organic chemical processes in the interstellar medium have now come to fill whole volumes of congress proceedings.

The emission bands appear most clearly at wavelengths 3.3, 6.2, 7.7, 8.6 and 11.3 m. The origin of these »unidentified infrared bands« was unclear at the outset. The possibilities under discussion included dust granules of amorphous hydrocarbons, composite carbon compounds, coal or PAHs (Fig. II.12). The matter could only be finally clarified by a comparison with laboratory spectra of the relevant substances, which spoke increasingly in favour of PAHs.

Interstellar Cirrus

When the IRAS infrared satellite carried out the first sampling of the skies in the 1980's, astronomers established that a large fraction of the sky is covered by clouds which emit intensively at 100 m in particular. These clouds are known as interstellar cirrus, and some of these cirrus

Fig. II.12: The emission bands of different PAHs in the infrared (left) and conceivable possibilities as to how soot particles (bottom right) could be created starting from a ring molecule (top right) by further coagulation.

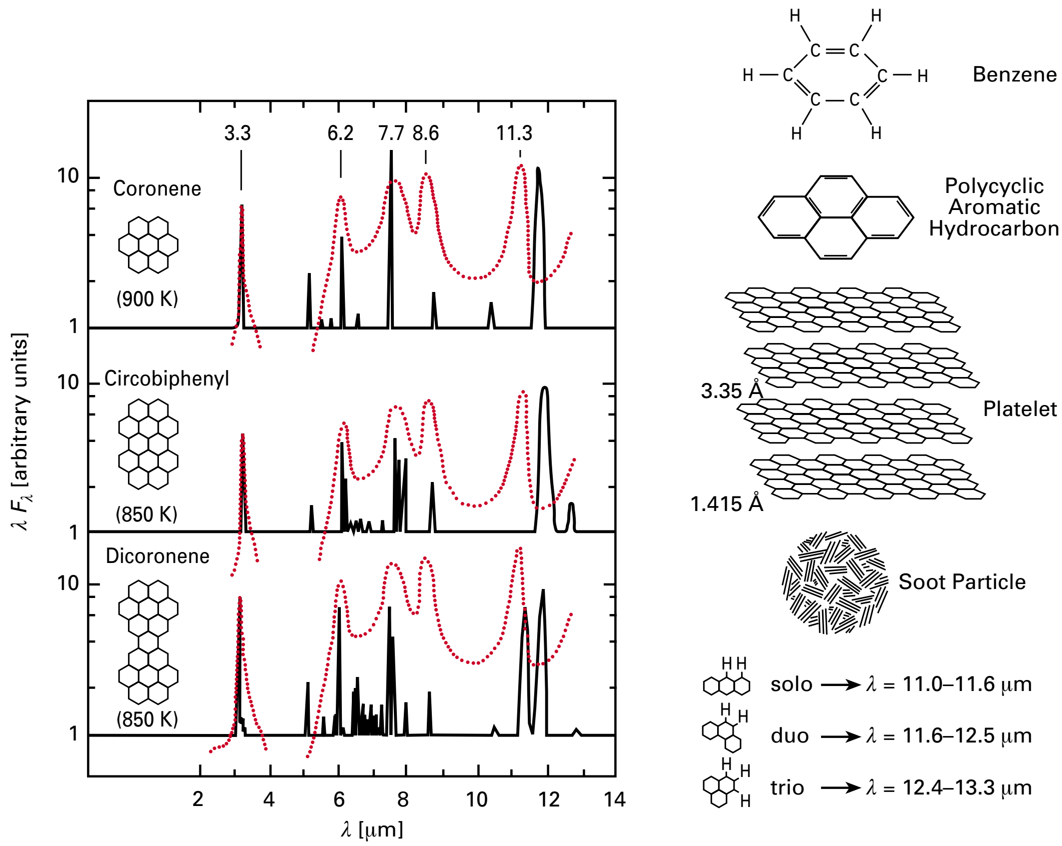

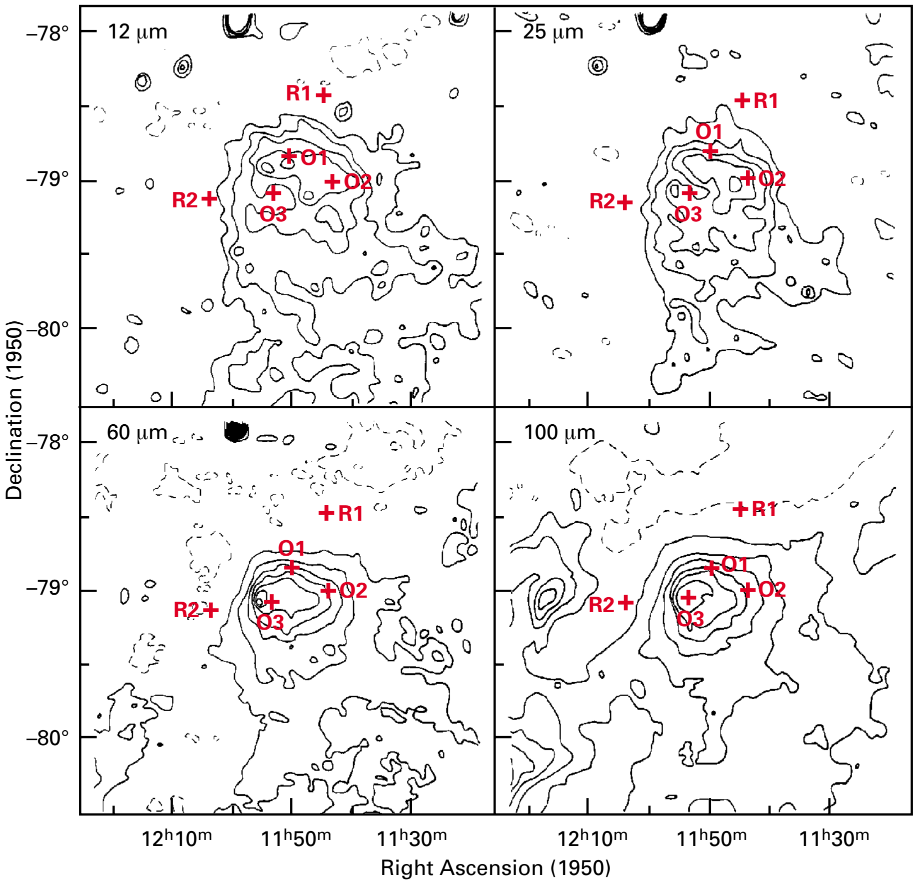

Fig. II.13: IRAS maps of the cirrus cloud G 300.2-16.8 which was observed with ISO. The observation positions inside (O) and outside (R) the cloud are marked.

clouds also radiated intensively in a wavelength range between 12 µm and 25 µm. Up to 30 % of the whole IR radiation came from this range alone – a larger fraction than could be explained solely by thermally radiating dust grains. For this reason, suspicions began to arise even then that the »unidentified infrared bands« also played a large part here. No decision could be reached on the basis of IRAS.

However, doubts about this interpretation remained. In other regions where these IR line bands were observed, there were intensive UV radiation fields from hot stars which excited the presumed PAHs to radiate. But in the cirrus clouds, the UV intensity was lower by two to three magnitudes, so that it was possibly incapable of exciting the particles sufficiently.

Using ISOPHOT, astronomers from the MPIA, together with colleagues from the Universities of Helsinki and Paris, observed a cirrus cloud which belongs to the large dark cloud complex in the constellation Chamaeleon. Its distance is estimated at about 550 light years. The IR flows were measured at three positions at an angular distance of about 20 arc minutes, in a wavelength range from 3.3 m to 16 m (Fig. II.13). Nine filters were available for this purpose, and the brightness at two positions outside of the cloud was also measured as a reference. In this way, it was possible to subtract the general foreground of the infrared zodiacal light. This emission originates from dust in our solar system, not from the cirrus cloud.

In the remaining IR signal, it was ultimately possible to discern the signatures of the unidentified infrared bands. As expected, the absolute radiation flow of the infrared bands is about one thousand times less than (for example) in HII regions. However, an accurate analysis showed that they account for 40 % to 50 % of the total emission in the wavelength range between 6.5 µm and 16 µm. At the same time, it was possible to determine a continuum emission which could originate from PAH clusters or very small silicate particles.

This highlights the importance which these particles have in the interstellar medium: they convert a large part of the UV radiation into IR radiation. The UV radiation heats up the interstellar medium because it is already absorbed at short distances from dust and molecules. In contrast, the IR radiation can penetrate the interstellar matter relatively unimpeded at wavelengths in excess of the diameter of the dust particles, thereby dissipating the energy contained in the hot UV radiation from the area of origin.

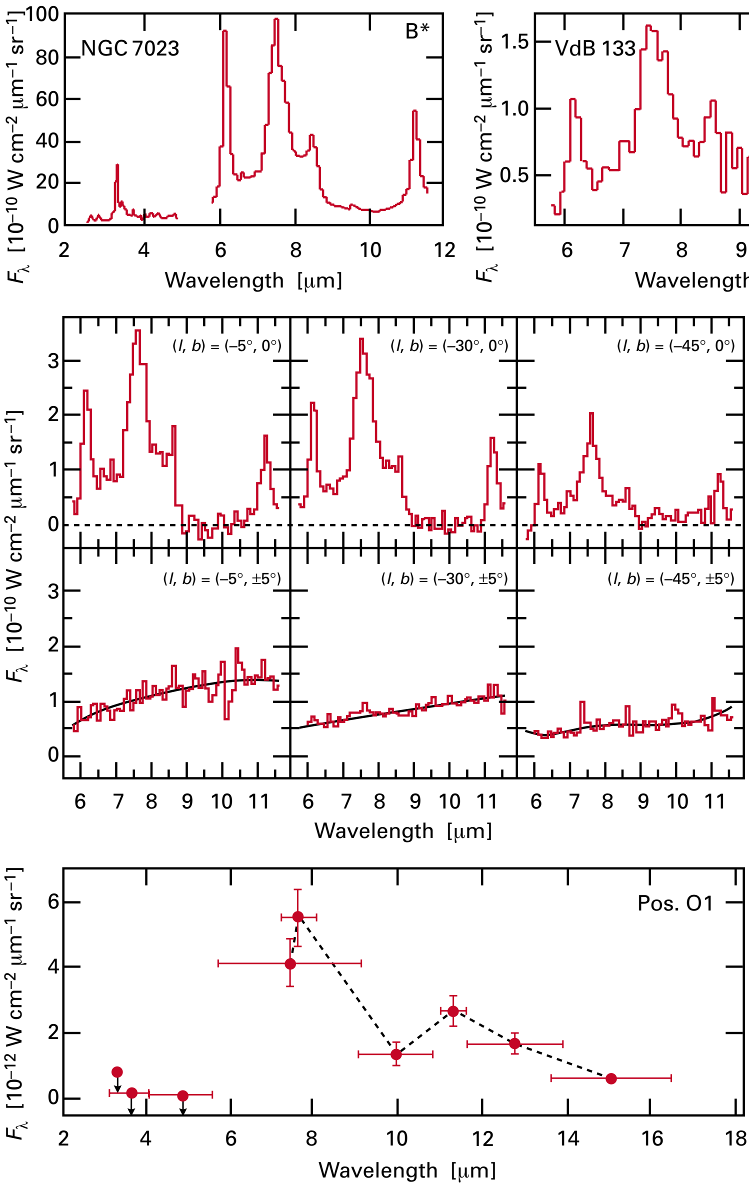

Fig. II.14: Left: spectra of various objects in the Milky Way obtained with ISOPHOT in the near infrared. Top, in reflection nebulae; middle, in the diffuse galactic medium, and bottom, in the cirrus.
Right: the spiral galaxy NGC 891 seen edge-on in an optical photograph, and the spectra obtained along its major axis. ▶

Diffuse Dust in the Milky Way

As part of an observaing programme with ISOPHOT within the guarantee time, an attempt was made to detect line bands in diffuse interstellar dust as well. For this purpose, several fields along the galactic plane were observed with the ISOPHOT spectrometer. The positions were selected so that there were no nearby bright objects in the infrared or optical. Here too, it was necessary to first subtract the IR emission of the zodiacal light. It was determined from fields above and below the galactic equator, where the radiation of the diffuse galactic medium is negligible. After this, it was possible to clearly discern the main lines at 6.2, 7.7, 8.6 and 11.3 m in all the positions (Fig. II.14).

In this case as well, a quantitative estimate suggested that the bands of the presumed PAHs account for at least 50 % to 60 % of the IR emission measured with IRAS. Although the UV radiation fields in the region of the diffuse clouds are less intensive than the typical values for reflection nebulae or HII regions by factors of 100 to 1000, the relative intensities of the lines are very similar.

The Spiral Galaxy NGC 891

Thanks to ISO, it has been possible to detect the infrared bands in many galaxies with active cores or intensive star formation. But it was not until last year that it became possible to map this emission in the interstellar dust of a quite normal galaxy for the first time too. At a distance of 30 million light years, the spiral galaxy NGC 891 was especially suited to the search for infrared emission, because the system is viewed directly edge-on, and the dust density in the line of sight

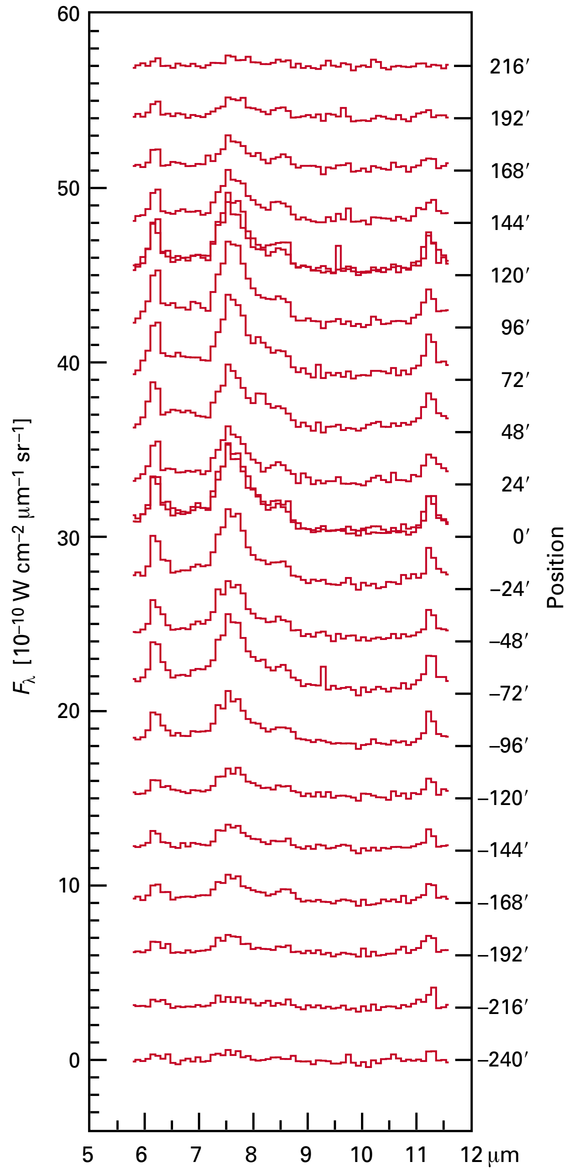

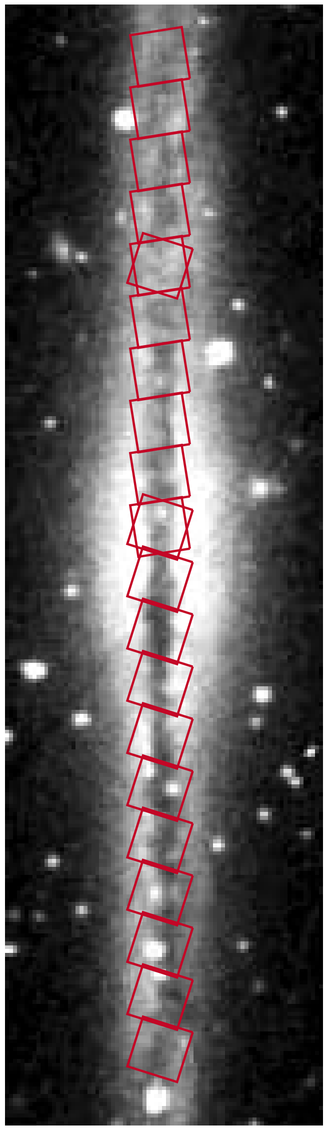

(column density) is therefore very high. NGC 891 is a spiral galaxy of type Sb, meaning th26t strongly resembles the Milky Way system. High-resolution photographs (Fig. II.14) indicate a branched network of dust clouds with average sizes of 150 to 300 light years and estimated masses of between 2×10^5 and 4×10^6 solar masses at distances of approximately 5000 light years from the central plane. Since this stellar system had already been examined in detail in other wavelength ranges, this created the opportunity to compare the spatial distribution of different constituents of the interstellar medium.

Along the central axis of NGC 891, the infrared fluxes were determined spectrophotometrically at 20 positions (Fig. II.14). The aperture with an extent of 24 arc seconds corresponded to a region with an extent of 3500 light years. The emission bands in the near IR are clearly discernible at distances of up to 30,000 light years to the north and south of the galactic core. The spectra are very similar to those from the Milky Way, and the intensity of approximately 7.7 m is only insignificantly higher than that of the diffuse emission in our Milky Way.

The emission regions are arranged almost symmetrically in relation to the centre of the galaxy. A marked maximum is apparent at the centre. From there, the intensity decreases towards both sides, until it increases again in a region between 70 and 120 arc seconds (10,000 and 17,000 light years) to the south and north of the centre. This is probably a ring-shaped area which surrounds the core of NGC 891 (Fig. II.15). This distribution coincides remarkably accurately with that of molecular CO gas and cool dust which was measured at a wavelength of 1.3 mm. This is precisely what one would expect if the infrared emission from the PAHs originates in dust-rich regions, as has been observed in the Milky Way.

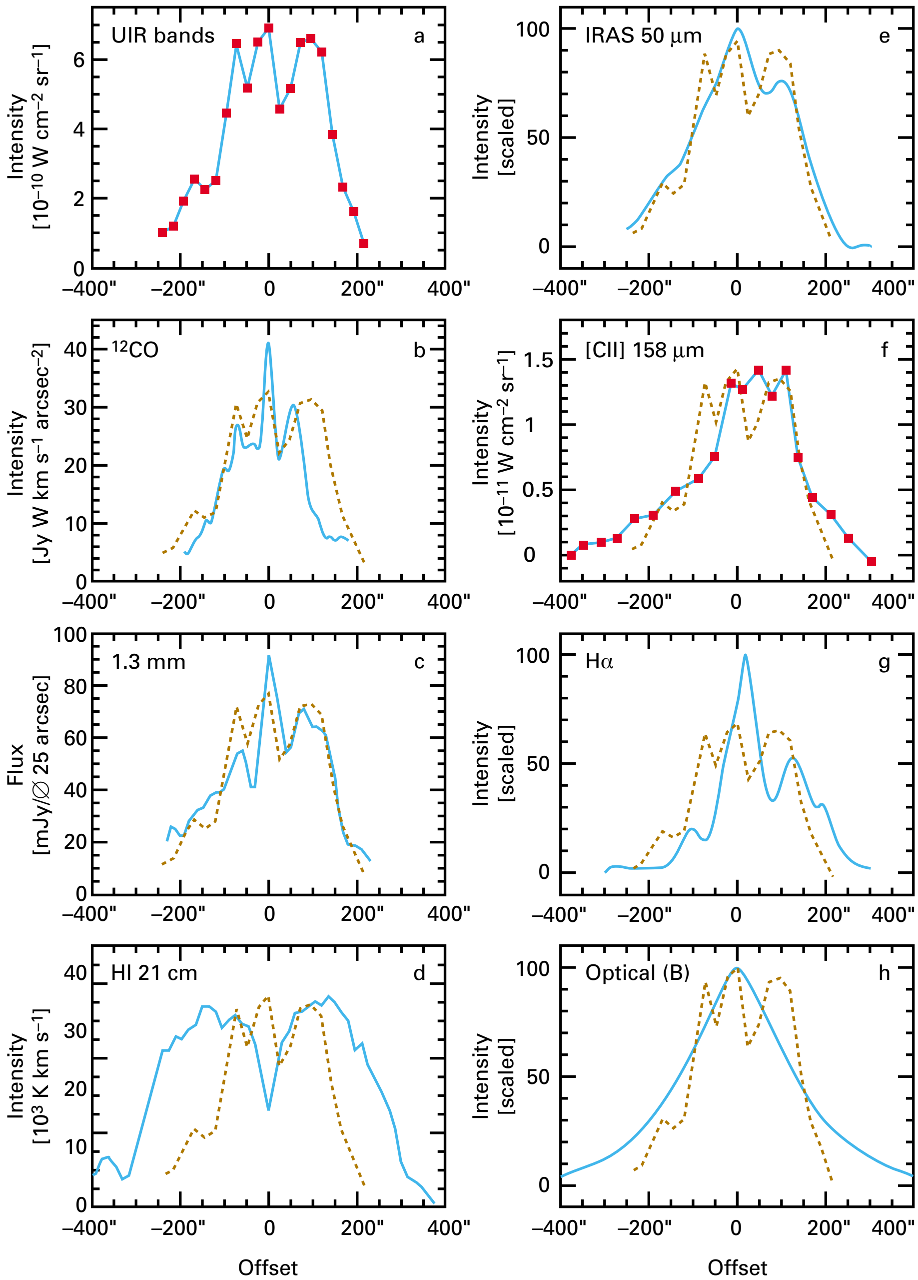

Fig. II.15: Intensity distribution of various components of the interstellar medium along the major axis of NGC 891. The distribution of infrared bands **(a)** more or less follows that of carbon monoxide **(b)**, but not (for example) that of ionized hydrogen (Hα, (g)). The broken lines each reproduce the distribution of the infrared bands from **(a)**.

On the other hand, the IR distribution just described differs significantly from that of the ionized components of the interstellar medium such asH^+ and C^+. This is somewhat astonishing since general opinion has it that the PAHs are excited by UV radiation at wavelengths below 400 nm. One might therefore expect, for example, that the distribution of C^+ more or less follows that of the interstellar UV radiation field, and hence that it also more or less corresponds to that of the PAHs. The fact that this is not the case suggests special properties of the PAHs in the interstellar medium.

Properties of the PAHs

If we wished to explain the fluxes which were measured with ISOPHOT in the emission bands of the near IR by thermal radiation from dust particles, their temperatures would have to be 100 K or more. This is ruled out in view of the radiation fluxes which are present there. To this extent, the ISOPHOT data support the suspicion that PAHs generate the emission bands. However, the intensity ratios of the lines lead to some puzzles. In areas with a very intensive UV radiation field, such as those in hot HII regions and planetary nebulae, the lines of the PAHs in the range from 11 µm to 13 m are weaker than those at 6.2 µm and 7.7 µm. In weak radiation fields such as for the interstellar cirrus or the diffuse clouds, the intensity ratios should be precisely reversed. However, this is not observed. The intensity ratios, for example *I*(11.3 µm)/*I*(7.7 µm), are about 0.24 in the diffuse interstellar clouds, about 0.4 in the cirrus and about 0.2 to 0.3 in planetary nebulae, HII regions and reflection nebulae – even though the radiation fields differ in intensity by as much as a factor of thousand. In the case of NGC 891, this intensity ratio could even be determined along the central axis. Here, it rises almost continuously from 0.2 to 0.5, from north to south.

This behaviour on the line intensities contradicts the theory, and it has provided much material for discussion, leading to a variety of possible solutions. For example, it has been suggested that the PAHs may lose hydrogen atoms due to the action of intensive UV radiation, as a result of which the radiation properties of the molecules would change. However, this hypothesis could not be reconciled with all the observational data. There is abetter correlation on objects such as NGC 891 if additional account is taken of the existence of ionised PAHs, in which case the ionisation level is a balance between ionisation in the UV radiation field and recombination with free electrons (i.e. the electron density).

These two mechanisms - loss of hydrogen atoms and ionisation – could possibly explain the intensity ratios of the line bands which were measured in the mid IR. In any case, more and more indications suggest that these lines originate from PAHs. Accordingly, these substances which resemble small soot particles are widespread in space, and they play a very major role in the radiation balance in the interstellar medium. They could also be important in terms of cosmochemistry. For example, American scientists have exposed PAH’s coated in ice mantles to UV radiation of the sort which also occurs in the interstellar medium. Interestingly, these PAHs were converted into biogenic substances such as alcohols and ether in this process. Therefore, PAHs could also play a key role in the formation of complex organic molecules in space.

III Instrumentation Development

There are basically two ways of increasing a telescope's performance. On the one hand, we can improve the size and surface quality of the main mirror. This means that more light is collected, creating sharper images, which makes it possible to reach fainter objects. On the other hand, however, we can optimize the scientific instruments which register an image or spectrum of the observed region of the sky in the focal plane of the telescope. At the MPIA, a whole series of instruments have been developed and built over recent years, bringing about significant improvements to the efficiency of telescopes and enlarging their areas of use. In particular, these include the Wide Field Imager, a camera with an exceptional large field of view; the ALFA adaptive optical system, and MOSCA, the multi-object spectrograph.

These instruments are designed and built in the Institute's workshops in cooperation with large and small companies. The requirements set by the scientists often confront these companies with completely new tasks, and the know-how gained in this process strengthens their competitive edge on the global market.

The use of Charge Coupled Devices (CCDs) has also brought about major advances in astronomical research. CCDs are light-sensitive semiconductors which achieve quantum yields of between 60 % and almost 100 % depending on the wavelength of the incoming light.

These small plates, just a few square centimetres in size, consist of a large number of light-sensitive pixels (picture elements). The largest CCD's have several million pixels. The incoming light generates an electrical charge in the material, which is stored in the pixel. At the end of each exposure, a special electronic system reads out the CCD chip and a suitable computer program converts the charge image into an optical image. A decisive advantage for the astronomers is that the number of charge carriers generated is strictly proportional to the intensity of the incoming light.

Normal commercial CCDs cannot be used on a telescope. Only chips of the very highest quality are suitable for astronomy. These are produced by companies such as Philips or Rockwell, but detailed tests on their suitability have to be carried out at the MPIA's laboratories before they can be put to use on one of the telescopes.

There now follows an overview of the MPIA's more recent instruments and the current status in the reporting year.

ALFA, adaptive optics with an artificial star

In theory, the resolution of a telescope (that is to say, its ability to show separate images of two objects that are located close to one another) depends exclusively on the diameter of the main mirror and the wavelength of the light. In the visible range (wavelength of about 550 nm), a 3.5 metre telescope has a theoretical resolution – also known as the diffraction limit – of 0.03 seconds of arc; at 2.2 µm, the figure is 0.13, or four times less. This would make it possible to see details of up to 300 metres on the moon. In practice, however, the turbulence of the air blurs images with longer exposures so heavily that the typical resolution is only one second of arc. This means that no large telescope will achieve better resolution than a 15 centimetre one!

In collaboration with colleagues at the MPI of Extra-Terrestrial Physics in Garching, astronomers and engineers at the MPIA have built an adaptive optical system for the near infrared range, which makes it possible to correct image fluctuations during the exposure (cf. 1997 Annual Report, p. 11). It operates approximately as follows: a plane wave of stellar light reaches the Earth's atmosphere and is distorted in it, like a cloth in the wind. When it arrives at the telescope, it shows »hills and valleys« with a height of about one micrometer. Inside the telescope, the wave is split into two subbeams by a beam splitter. While one sub-wave falls on a small adaptive mirror and enters the camera from there, the other reaches a so-called wave front sensor. This device analyses the form of the wave, and forwards this information to a computer. The computer uses the information to calculate how the surface of the flexible adaptive mirror must be deformed in order to correct the form of the other sub-wave. These commands are put into practice by small adjusting actuators on the rear of the adaptive mirror.

This procedure only works if the mirror can be adapted so quickly that the incoming wave trains are not already being deformed in a different way to the wave train which has just been analysed. Theory shows that for a wavelength of 10 m and good seeing, about ten corrections per second are needed. In the range from 1 to 2.5 µm, in which ALFA is used for observation, about 200 readjustments per second are required for a good correction.

On ALFA, a central part is played by the wavefront sensor which analyses the light wave. To enable it to operate fast enough, it needs a reference star of at least magnitude 13.5. If the celestial body that is to be imaged is too faint for this purpose itself, another must be found, which has to be no further than 30 seconds of arc from the object of interest.

If this condition cannot be met, the astronomers must have recourse to a trick: they shoot a laser beam towards the sky, parallel to the direction in which the telescope is pointed. At a height of about 90 kilometres, this beam encounters a layer that is enriched with sodium atoms. The wavelength of the laser is set so that it excites the sodium atoms to shine. In this way a spot of light or »artificial star« is created above the telescope, corresponding to a star of the 10th magnitude in an ideal case. The adaptive optics use it as a bright reference star during the image correction. In this way, ALFA can supply sharper images than the Hubble space telescope at comparable wavelengths. This development places the MPIA at the forefront of research.

Now, ALFA is supplying routinely diffraction-limited photographs and spectra in the near infrared with natural reference stars of up to magnitude 11. Virtually diffraction-limited images are still possible up to magnitude 13.5. This means that it has been possible to improve the resolution of the 3.5 metre telescope by a factor of about six.

During the reporting year, it was possible for the first time to obtain virtually diffraction-limited images with the laser reference star at a wavelength of 2.2 m (K-band). A Strehl factor of 23 % was achieved in this case. The Strehl factor denotes the ratio between the light intensity in the centre of a star image and the intensity which the ideal, diffraction-limited image would have. With normal seeing of one second of arc, the Strehl factor is only about 3 % in the near infrared, and in an ideal case it is 100 %. There is currently only one other system in the world which achieves comparable quality to ALFA with a laser guide star.

The efficiency with which the laser guide star can be used basically depends on the meteorological conditions. In the reporting year, the yield was improved still further by flexible handling of the observation plan.

To optimise the use of the laser guide star even further, the time behaviour of the luminous sodium layer was observed with a LIDAR. To do this, a pulsed laser beam is shot into the atmosphere. This excites the sodium atoms in the upper atmosphere to shine, and the photons emitted from there are registered again with the 3.5 metre telescope. The travelling time of the signal makes it possible to determine the height of the sodium layer.

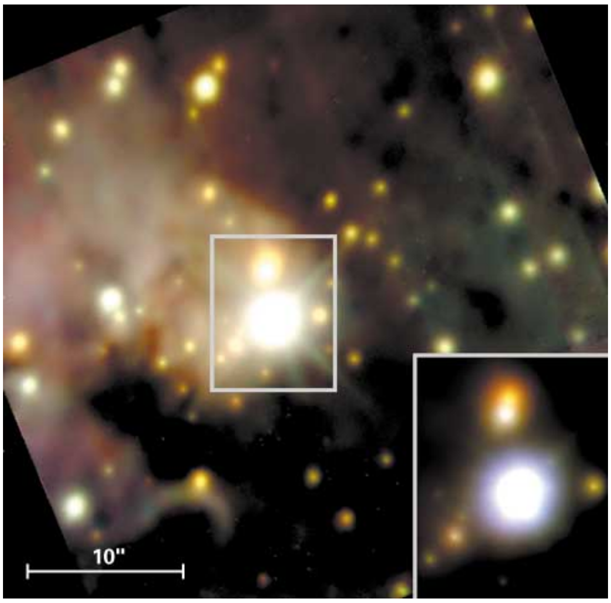

Fig. III.1: The Lagoon nebula around star Herschel 36 at a distance of 5000 light years.

A LIDAR of this sort was used to verify for the first time that the focal point of the artificial star is at a height of 90 kilometres. However, due to turbulence and other meteorological influences the position of this focal point may fluctuate within a few tens of seconds, and also from night to night, by several hundred metres up to 1.5 kilometres. At the same time, it was possible to observe on two nights that the thickness of the sodium layer in the mesosphere varied between 10 and 20 kilometres. Fluctuations of this sort can feign a defocusing of the telescope. With a regular LIDAR observation system it would be possible to detect them very quickly.

A whole series of brilliant scientific results were obtained with ALFA during the reporting year. During observations in the Lagoon nebula, a known star forming

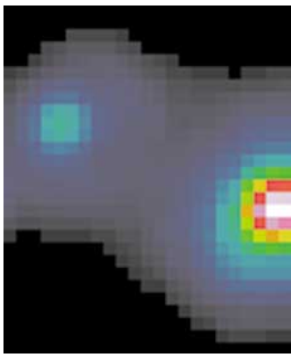

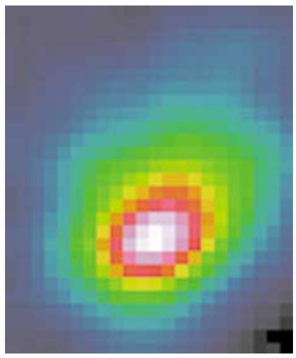

Fig. III.2 (left): The two components of T Tauri at a distance of only 0.″6 from each other are clearly separated by ALFA.

Fig. III.3 (right): The active core region of the galaxy NGC 1068 was resolved spatially with ALFA.

region, ALFA was able to detect the dust atmosphere over a previously known protoplanetary disc in the infrared for the first time (Fig. III.1). This gas and dust shroud is excited to shine by the nearby star Herschel 36. Dust discs of this sort are subjects of current interest because they are regarded as birthplaces of planets.

Moreover it was possible e.g. to achieve a clear separation of images of the components of the young star T Tauri which are only 0.7 seconds of arc distant from each other (Fig. III.2). Observations at different wavelengths therefore make it possible to determine the spatial distribution of molecular hydrogen in this region. The core region of the active galaxy NGC 1068 was observed at a resolution of 0.25″. This stellar system, only 45 million light years away, offers an ideal chance for detailed study of the central region, which probably contains a black hole (Fig. III.3).

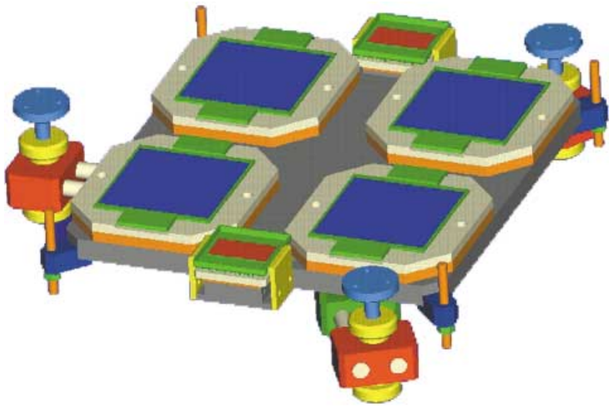

Fig. III.5: Arrangement of the four CCDs in the focal plane. The two small CCDs above and below the mosaic are used for tracking.

LAICA – the wide field camera for Calar Alto

Focal reducers such as CAFOS or MOSCA which were developed and built at the Institute in recent years have a relatively large field of view, of about ten minutes of arc in diameter. But for the future, it is hoped that much will be learned from research projects involving searches for faint clestial bodies in large fields. For this reason, it was decided to built a new wide-angle camera for the 3.5 metre telescope on Calar Alto. This Large Area Imager for Calar Alto, or LAICA in brief (Fig. III.4), will work in conjunction with the three-lens corrector in the telescope's primary focus. In this optical configuration, the aperture ratio is *f*/3.9, yielding a usable, error-free image field of 44 minutes of arc, corresponding to an edge length of 115 mm. A field of this size cannot be covered with one single CCD. For this reason, a mosaic of CCDs from Lockheed Martin (USA) was selected, each with 4096 × 4096 pixels (Fig. III.5). The imaging scale will be 0.225 seconds of arc per pixel.

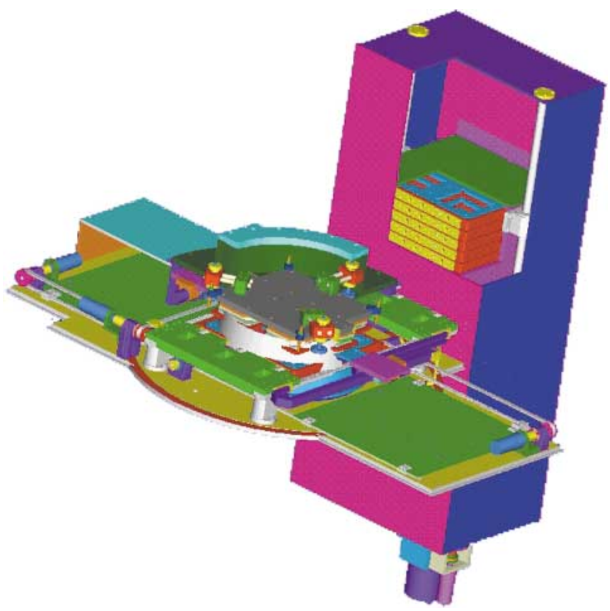

Fig. III.4: Computer drawing of LAICA on the K3 corrector in the primary focus of the 3.5 metre telescope. The light is coming from below. The shutter is clearly visible with the filter module in the background.

For production reasons, the CCDs cannot be linked to each other without joints, and this leaves a gap of about 50 mm. This corresponds to the CCD width minus an overlap of about 30 seconds of arc. A disadvantage of this arrangement is that it is impossible to image a closed area of the sky in one single shot. However, this can be compensated without major outlay by making three more photographs with different positions. A set of four photographs covers a composite field of one square degree, corresponding to about five times the area of the full moon. The overlap makes it possible to check astrometry and photometry. There are also numerous observation projects whose objective is merely to record the largest possible area of the sky, which does not necessarily need to be a closed region. However, one drawback is that distortion effects occur to a greater extent than with a single CCD, which only covers the central area of the image field; this is because in LAICA the image field exactly covers the CCD array, and so deformations which only occur in the edge area of the image field will fall in the outer areas of the CCDs. However, the deformation reaching into the corners of the field is less than 2 %.

An advantage of this CCD arrangement is that four small filters can be used instead of one large one. Smaller filters are substantially lighter, and they can be obtained at lower prices than a large one. The filter holder resembles the magazine of a slide projector. The magazine contains 20 filters, which are taken out by a grabber and pushed into the beam path. The shutter will enable exposure times of as little as one second, and a uniform exposure time with a maximum inhomogeneity of 0.5 % should be achieved for the entire CCD surface. Two smaller CCDs are used exclusively for tracking; there are two because they also make it possible to determine image rotations, of the sort which can occur during long observations in particular. These can be corrected because the camera can be rotated by several degrees during the imaging.

A start on building LAICA was made early in 1999. The CCDs were delivered to the Institute at the beginning of 2000. The first integration tests should be conducted in November this year so that the first images from the telescope should be obtained towards the end of 2000.

CONICA – High Resolution Infrared Camera for the VLT

CONICA is a high-resolution camera for the infrared. It is currently being built under the coordinating leadership of the MPIA in collaboration with the MPI of Extra-Terrestrial Physics in Garching and it will operate on one of the telescopes of the Very Large Telescope, VLT. The European Southern Observatory, ESO, is currently setting up the VLT on the 2630-metre-high peak of Paranal in Chile's Atacama Desert. When fully completed at the end of 2000, this facility will consist of four large telescopes, each with a mirror of 8.2 metres in diameter, and three smaller auxiliary telescopes (as they are known) with 1.8 metre apertures. By the end of 1999, three of the 8 metre telescopes and several measuring devices were already in operation.

Each of the four telescopes has three outputs which will be equipped with extremely powerful cameras and spectral instrumentation. CONICA will operate on the Nasmyth focus of the third of the four commissioned telescopes, named Melipal (Southern Cross), and it will supply diffraction-limited images with a resolution as low as 0.026 seconds of arc in the near infrared from 1 to 5 μm, in conjunction with the NAOS adaptive optical system. The commissioning of CONICA together with the adaptive optics built in France is planned for March 2001.

It will be possible to use CONICA for all current areas of research. Special emphasis is given to investigations of areas where stars are being formed and to protoplanetary dust discs, the galactic centre, the gaseous envelopes around red giants, and the search for extrasolar planets. In the extragalactic field, high priority will be given to observations of the central regions of active galaxies and the study of remote infrared galaxies. In return for their services, the astronomers at the two institutes will have45 nights' guaranteed observation time with CONICA available to them.

An infrared array with 1024 × 1024 pixels is used as the detector, and the imaging scale can be adapted between 0.014 and 0.11 seconds of arc per pixel. For each of these scales, two camera systems are available, operating in the two wavelength ranges from 1 to 2.5 m and from 2 to 5 m. Depending on the selected variant, the image field has an extent of between 14″ by 14″ and 56″ by 56″, and a diameter of 73″ at the lowest resolution.

CONICA is a multi-functional instrument with a Fabry-Pérot interferometer (2 to 2.5 μm), a set of 20 stan-

Fig. III.6: CONICA during tests in the Institute's laboratory.

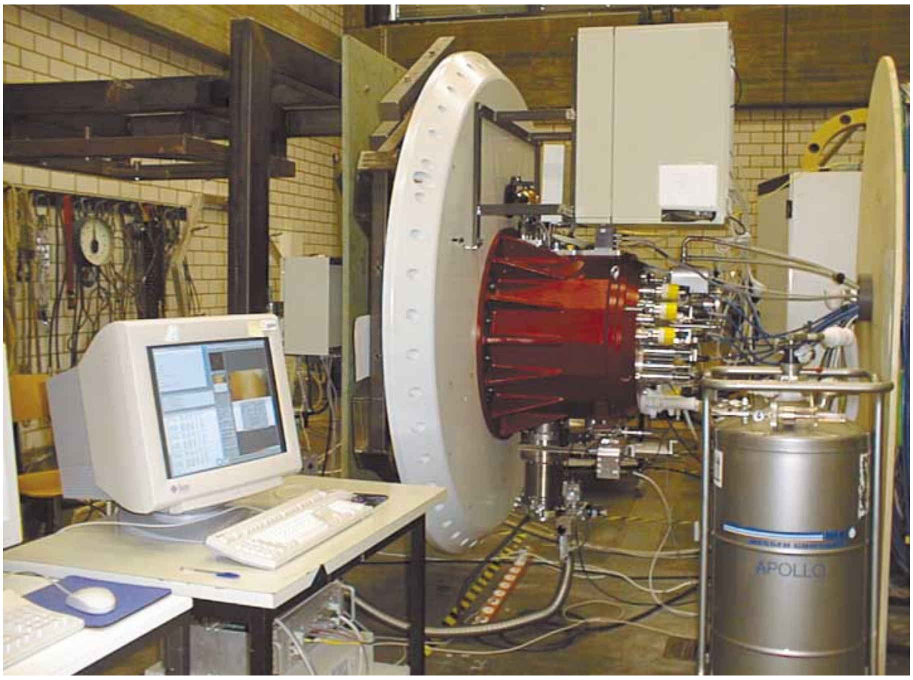

dard filters and 15 narrow-band filters, as well as Wollaston prisms and polarisation filters to measure the linear polarisation of extensive objects. Furthermore, three grisms provide the possibility of two-dimensional spectral investigations with an average spectral resolution.

In the reporting year, work on the infrared camera for the adaptive optics reached a stage which enabled the final InSb detector (Aladdin) to be installed and a start to be made on the final optical tests (Fig. III.6). For this purpose, all the modes of this instrument will be subjected to a thorough optical and mechanical test. In addition, the software for controlling the instruments was completed. Handover to ESO is planned for summer 2000. CONICA will then be transferred to the French consortium which is developing the associated adaptive optics. A first joint test is planned for autumn, 2000.

MIDI – Infrared Interferometer for the VLT

In the near future, the VLT will also operate as an interferometer. For this purpose, the beam paths of two or more telescopes will be combined and coherently superimposed in one common image plane. An interferometer of this sort has the spatial resolution of one single telescope with a mirror whose diameter would be equivalent to the basic length of the two telescopes linked by the interferometric coupling. Two of the VLT's telescopes, separated by a distance of 130 metres, will then be capable of achieving a resolution of a few thousandths of a second of arc in the near infrared range.

One of three interferometers, named MIDI, is being developed and built under the coordinating direction of the MPIA. The project also involves colleagues from the Netherlands and France, and from the Kiepenheuer Institute of Solar Physics in Freiburg and the Thuringian State Observatory, Tautenburg. MIDI is intended to enable interferometry with two telescopes at a wavelength of 10 µm, and it will mean a quantum leap in astrophysical research as far as spatial resolution is concerned. At the moment, it is planned to use MIDI in particular to observe active galactic cores (black holes), young stars, extrasolar planets, circumstellar dust envelopes and protoplanetary discs, as well as double stars.

The path lengths of the collimated beams arriving from the two telescopes must correspond precisely to within fractions of a wavelength, equivalent to about one micrometer, in the common image plane. Most of the difference in path lengths, which is principally due to geometry, will already have been compensated before the beams enter the instrument. Inside MIDI, the remaining difference in path lengths will be compensated by means of movable piezo-electrically driven mirrors. A beam splitter combines the beams to create the interference image. At the same time, however, it must also be possible to measure variations in the brightness of the observed celestial object due to air turbulence or clouds. For this purpose, part of the two beams will be diverted out of the interferometric beam path so that continuous separate measurements of the brightness can be taken.

In the reporting year, a start was made on manufacturing the instrument. At the end of July, the »Final Design Review« for the optics was conducted at ESO, and it was completed without any difficulties. At the end of the year, preparations were in train for the Final Design Review for the rest of the instrument, which is planned for February 2000.

At the NFRA, our partner Institute in Dwingeloo, a start was made on the design of the cooled optics (Fig. III.7). A prototype for the development of the adjusting mechanisms was produced and successfully tested; the accuracy of these mechanisms is critical for the combination of the beams. The design for the non-cooled section of the optics was completed, and optimized in collaboration with colleagues from the Kiepenheuer Institute. The piezomotors for the internal path length adjustment were tested successfully: speed, stability and precision equalled or exceeded the required values. The specifications for the most sensitive part of the instrument, the beam combiner, were verified and the order was issued to the Präzisionsoptik Gera company.

The detector, an Si:As-IBC-Array (IBC = impurity band conduction) with 320 × 240 pixels was ordered from the Raytheon company. A first test-quality specimen has already been delivered. Work on the read-out electronics was continued, and a test Dewar was also produced to examine the temperature behaviour and vibration sensitivity under the most realistic conditions possible. It emerged that the envisaged arrangement of cooler and instrument on separate heavy tables reduces

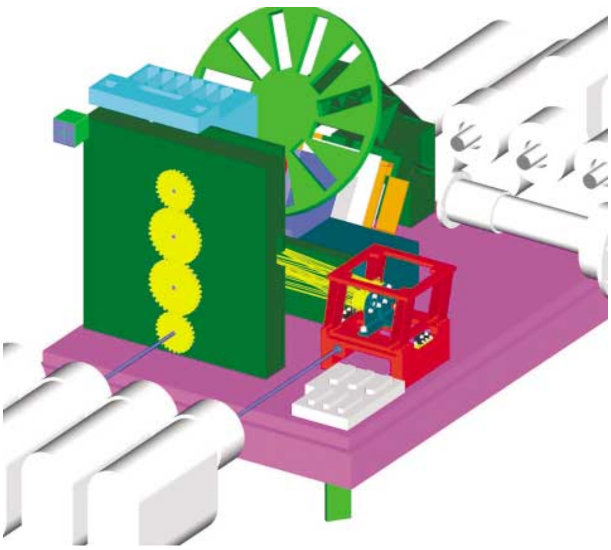

Fig. III.7: Design for the mechanics of the cold section of the optics of MIDI with various adjusting units.

the anticipated vibrations to tolerable proportions. The final cryostat has been designed, and the construction of the calibration sources for laboratory tests is under way. Extensive work has begun on the software for the instrument, both for the instrument control in Heidelberg and the data evaluation in Paris and Leiden. The Sterrewacht Leiden is coordinating this work.

Once the instrument has been tested in Heidelberg, it is planned to ship it to South America late in the autumn of 2001, and then to install it on Paranal mountain.

PACS – Infrared Camera for FIRST

In the year 2007, the European Space Agency (ESA) intends to launch FIRST, the Far-Infrared and Submillimeter Space Telescope. This is the ESA's fourth major cornerstone mission. FIRST will be provided with a 3.5 metre mirror and three scientific instruments which are intended to cover a wavelength range from 60 to 700 µm. These are being built by international consortiums of scientists. FIRST will therefore link up to the field of radio astronomy at long wavelengths. One focal point of the research programme will be the observation of protostellar dust clouds and protoplanetary dust discs. It will also be possible to detect the infrared radiation from very remote young galaxies in the submillimetre range.The MPIA will be participating in the construction of PACS (Photoconductor Array Camera and Spectrometer), one of the instruments. This project is being led by the MPI of Extra-Terrestrial Physics in Garching (MPE).

PACS is being designed for photometric and spectrometric investigations in the wavelength range between 60 and 210 µm. The MPIA will be making major contributions towards the development of the cameras, the pre-amplifiers, the focal plane chopper and also towards the data centre. In 1999, it was decided that the Institute will participate in the detailed planning of the structure of the FIRST ground segment, and in particular the control centre for PACS. Based on experience with ISO, it was possible to make major contributions towards the design of a flexible command system for the instruments. It was decided that the Institute will be responsible for all aspects of the calibration of PACS during flight.

In the reporting year, the major contribution to PACS was the construction of a prototype for the chopper. An optical device of this type has the following task: during infrared observations, a disruptive background signal of greater or lesser strength may occur, for example due to the telescope's heat radiation. So that this can be taken into account, the object and an empty section of sky are exposed alternately. The latter supplies the background which is subsequently subtracted from the actual image. The alternating observation of two areas of the sky is achieved by positioning a mirror in the beam path which continuously tilts to and fro (or »chops«).

The main mirror of FIRST will probably have a temperature of about 90 K, so that considerable heat radiation may be expected as from a wavelength of about 50 µm. Chopping will therefore be a very important aspect of observations in this wavelength range. Thanks to ISO, the Institute has already been able to gather experience with choppers at very low temperatures where most conventional materials and technical systems fail: several million tilting cycles were executed without material fatigue over more than a thousand hours.

For PACS, the requirements are even higher – at a temperature of 4 K, 630 million cycles should be possi-

Fig. III.8: A prototype of the PACS chopper with a mirror of 25 mm. Two semi-conductor plates (field plates) made of InSb/NiSb operate as position sensors in each air gap.

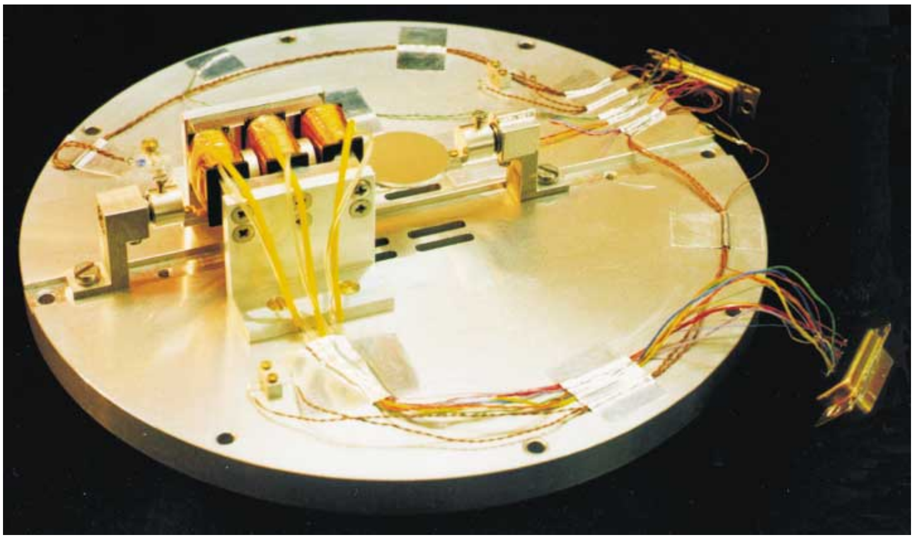

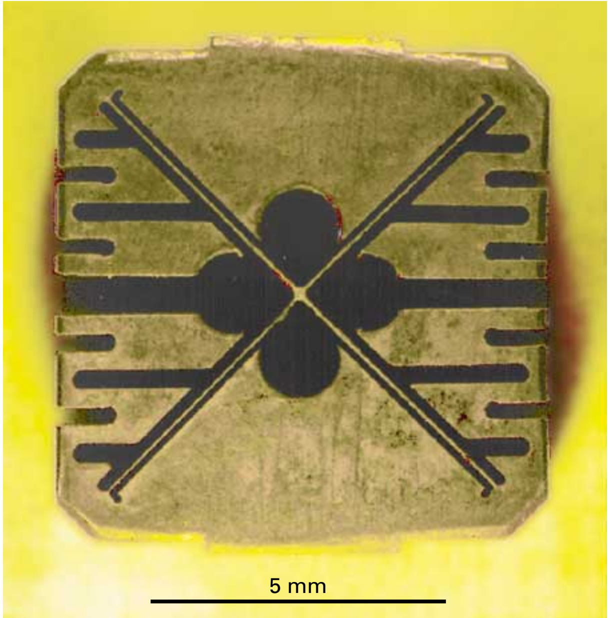

Fig. III.9: Prototype of a cross spring joint on which the chopper axle is mounted.

ble. The mirror has a diameter of 25 mm, and it must be possible to chop it over an angle of nine degrees. It must also direct the light from two internal calibration sources to the detectors. At the Institute, it was decided that the chopper should have an electromagnetic drive with the minimum of moving mechanical components, to generate virtually no heat.

The drive comprises three parallel Cryoperm cores (Fig. III.8). These three metal cores are surrounded by coils which generate a magnetic field in each of the two air gaps. If an alternating voltage is applied to the coils, a Lorentz force is created in the air gap, moving the drive magnets to and fro. This linear movement is transmitted to an axle via joints, so that it is converted into a rotary movement. The chopper mirror sits on this axle.

The axle itself is mounted on so-called cross-spring joints which function without wear and entirely without lubricants, even at low temperatures (Fig. III.9). They consist of two flexible leaf springs arranged as a cross. If the axle rotates, these leaves are bent into an s-shape. Due to their high elasticity, axle rotations of up to 9 degrees are possible.

The prototype manufactured in the laboratory has already been able to demonstrate impressively that this system is suitable in principle. Computer simulations also indicate that the maximum power loss of 4 mW specified by the ESA can also be achieved. To minimize the ohmic heat loss from the drive coils, the Institute examined various materials with high electrical conductivity which are suitable for cryomechanics, such as silver, aluminum and copper with exceptional purity levels of about 99.999 %, and superconductors.

Finally, in the reporting year three industrial offers for the construction of the flight model chopper were obtained, together with a lifetime, qualification and flight replacement model, and preparations were made to conclude a contract.

A new secondary mirror for the UKIRT

For years, the institute has participated in the United Infrared Telescope (see Chapter I). A few years ago, a decision was taken to improve the technical aspects of the telescope in conjunction with the Royal Observatory in Edinburgh, Scotland. Under the auspices of this agreement, the MPIA took on the construction of a complete secondary tip-tilt mirror unit, including a new front ring for observations in the infrared. In 1996, the Institute delivered a system of this sort to Mauna Kea, Hawaii. In the reporting year, a new secondary mirror was produced with further improvements to the surface. Since then, it has been used to attain the theoretically possible resolution on the UKIRT.

The secondary mirror unit can perform three different tasks at the same time. On the one hand, the mirror is installed on the front ring with a hexapod mount. As a result, it can be moved slowly (at maximum frequencies of 1 Hertz). This active optical system makes it possible to adjust the mirror optimally during observations in any position, and to compensate for focusing errors.

Secondly, the mirror is mounted on a platform which can be tilted very quickly (at frequencies of up to 220 Hertz) by means of piezo-crystals. This allows adaptive correction of tilting movements of the incoming wavefront provoked by turbulence in the atmosphere during the exposure (see also the article on ALFA, p. 31). At the same time, when observations are being made in the middle infrared, the piezo-platform carries out the chopping function described above.

Since the mirror with its diameter of 31 centimetres is moved very rapidly to and fro in certain observation modes, it was necessary to select a special lightweight structural design. A honey-comb pattern was elaborated from the solid mirror blank made of Zerodur, a kind of glass ceramic. The remaining walls of the honey-comb and the disc-shaped mirror support were then only 4.5 millimetres thick in each case. This made it possible to reduce the weight from 5.5 kilograms to 2 kilograms (Fig. III.10).

The system has been operating very successfully since 1996. However, in order to attain the targeted maximum possible resolution (diffraction limit) of 0.3″ at a wavelength of 2.2 µm maximum variances of the surface of the secondary mirror from the specified shape had to be less than 125 nm. This was not altogether the case on the first mirror, because sharp edges or microfissures occurred in the surface of the glass ceramic while the honey-combs were being mechanically ground down, and

Fig. III.10: The rear of the secondary mirror, showing the honey-comb structure which reduces the weight.

this led to local tensions in the material so that the honey-comb structure left a slight impression in the surface of the mirror.

For the second mirror, a process developed by the Carl Zeiss company of Oberkochen was used: a layer of 0.2 mm was removed from the rear of the mirror support by applying an aggressive acid. This caused all the microfissures and tensions in the material to disappear, as a result of which no further traces of the honey-comb structure were visible on the surface of the mirror. The entire surface of the secondary mirror now only showed a maximum deviation from the ideal shape of 110 nm. The success was so convincing that the first secondary mirror is due to be post-treated with the new etching procedure in the near future.

IV Scientific Work

IV.1 Galactic Astronomy

Dust around Young and Massive Stars – Envelopes or Discs?

Circumstellar gas and dust discs play a decisive part in many astrophysical processes. Young stars similar to the Sun, so-called T-Tauri stars, are surrounded by discs of this sort, in which planets are probably formed at a later stage. The situation with more massive stars (known as Herbig-Ae/Be stars, after the man who discovered them) is less clear. They also display a series of phenomena which are associated with the existence of discs. In some cases, for example, intensive infrared radiation has been found which must originate from the dense circumstellar dust. Thanks to the Iso infrared observatory, it has been possible to observe seven Herbig-Ae/Be-stars simultaneously in the middle and far infrared. In almost every case, they displayed radiation distributions which are characteristic of circumstellar discs.

The term »Herbig-Ae/Be stars« is used to denote the young progenitors of the later A and B stars. Their masses are in the range from about two to eight solar masses. The spectra of these pre-main sequence stars show strong emission lines. The stars are almost always located in the dark cloud in which they have been formed, and they are surrounded by reflection nebulae. It has also been possible to detect a wind of fast particles near the Herbig-Ae/Be-stars. In some cases, the outward flow is bipolar, and sometimes it even takes the form of closely collimated particle beams, or »jets«, as they are known. In these cases, it is assumed that the particle wind leaves the star perpendicularly to a circumstellar disc which is not directly visible.

Strong indications of two discs which surround the two components of the Herbig-Ae/Be double star Z Canis Majoris were recently found by astronomers at the Institute with the help of speckle infrared polarimetry (see the 1998 Annual Report, p. 16). The radii of these discs must be less than 100 AU. In 1997, American astronomers observed some Herbig-Ae stars using high-resolution interferometry in the millimetre range, where carbon monoxide can be detected. Some stars had extended envelopes with total masses (dust and gas) of between 0.005 and 0.034 solar masses, corresponding to 5 to 34 Jupiter masses. In the case of star AB Aurigae, the emission of carbon monoxide gas showed an ellipsoid envelope with a major semiaxis of 450 AU, whose radial velocity field can most simply be explained in terms of a rotating disc (Fig. IV.1).

The Herbig-Ae/Be stars observed with Iso are located at distances of between 2000 and 7000 light years. Although their suspected discs are more or less the same size as that of AB Aurigae, they have an angular extent of about one second of arc, so that they cannot be resolved spatially with Iso. Accordingly, all the information must come from the spectral energy distribution of the thermally radiant dust.

Now, Iso has also offered the opportunity to observe some Herbig-Ae/Be stars in the far infrared, where cooler dust radiates from the outer regions of the envelopes or discs, and where the entire radiation distribution reaches its maximum. Moreover, it was possible to measure the infrared radiation throughout a large wavelength range for the first time. Astronomers at the MPIA in conjunction with colleagues from the Jena

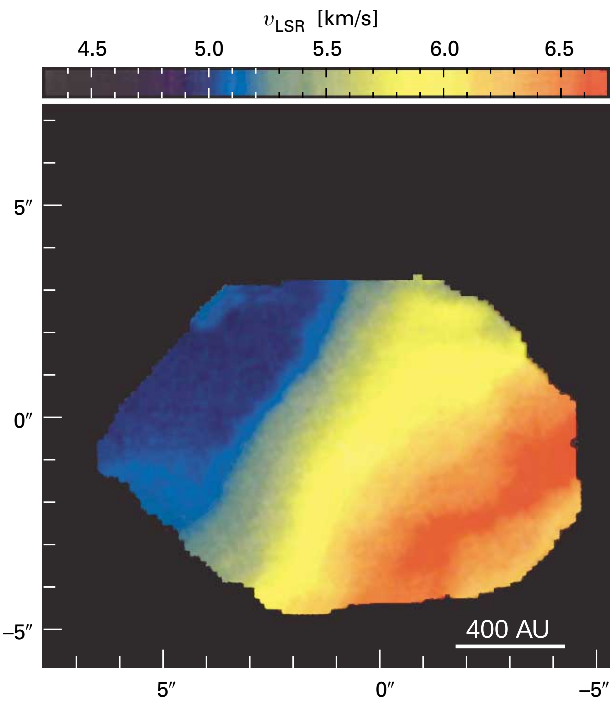

Fig. IV.1: The distribution of carbon monoxide in the presumed disc around AB Aurigae. The velocity field is color-coded : blue areas are moving towards us, red ones are moving away from us. (Mannings, Sargent, CIT)

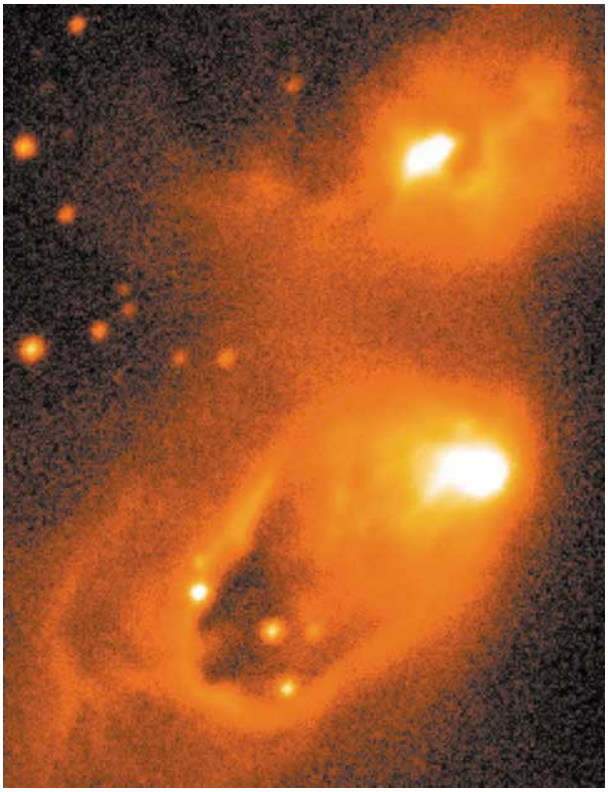

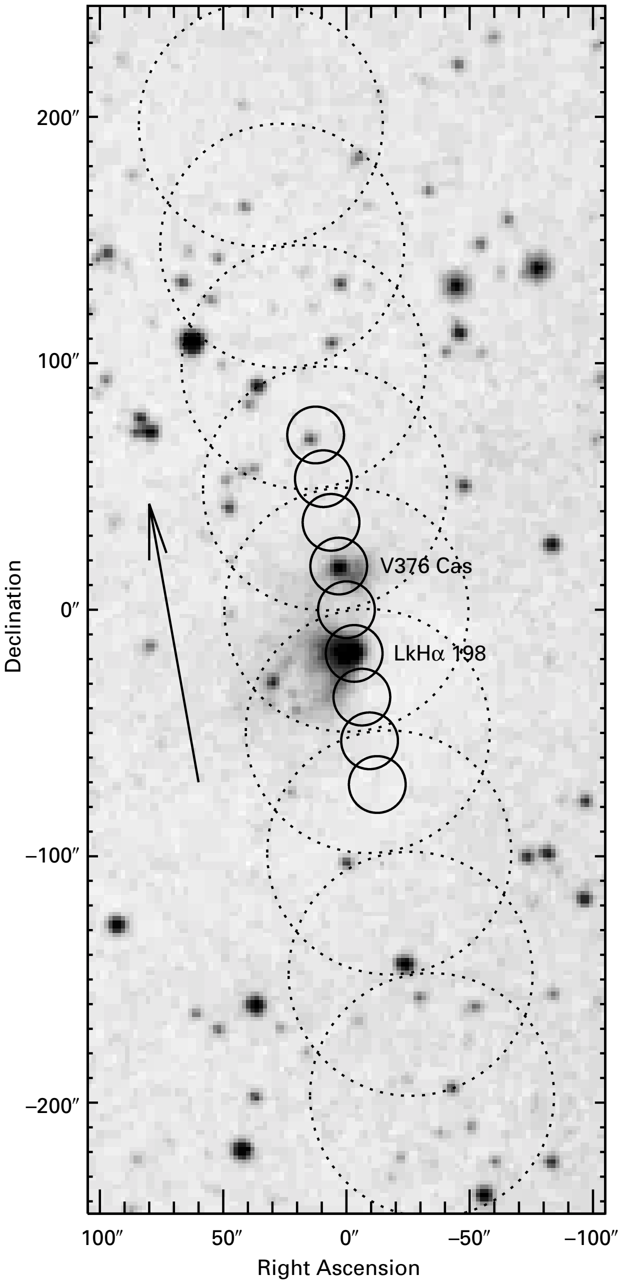

Fig. IV.2: Above – an optical image of the reflection nebula LkHα 198 (Photo: T. Ray, Dublin). **Right** – the positions of the ISOPHOT observation apertures in the area around LkHα 198 and V 376 Cas in the dark cloud Lynds 1265.

University Observatory were able to examine a total of seven Herbig-Ae/Be stars in the wavelength range from 5 to 200 µm.

The difficulty of these investigations is shown by the example of the two stars LkHα 198 and V 376 Cas, at distances of 2000 light years. The two stars are only half a minute of arc away from one another in the same dark cloud in which they had probably formed, at about the same time. Various observations, including some by scientists of the MPIA, had shown that the two stars are probably surrounded by discs. In the case of LkHα 198, it was even possible to prove the presence of a jet – a strong indication for a disc. However, final confirmation was still awaited. The situation is complicated by two more sources which can only be discerned in the infrared. One is situated 6 seconds of arc north of LkHα 198. This is also likely to be a Herbig-Ae/Be star. It sits so deeply inside the cloud that the dust attenuates the stellar light in the visible range by about 35 magnitudes, corresponding to a factor of 10^{14}. There is also another object 19 seconds of arc to the north-west. It is so cool that it only appears at wavelengths of about 1 mm.

As Fig. IV.2 shows, ISOPHOT was used to place a scan over both objects, and the aperture diameter for wavelengths of 5 to 20 µm was 23 seconds of arc (unbroken circles). LkHα 198 and V 376 Cas could be resolved individually here. At 60 and 100 µm, the aperture had a diameter of 99 seconds of arc (dotted circles). A planar background emission from the dark cloud first had to be subtracted before the two sources could be described by a distribution function. At wavelengths of 150 and 200 µm, one pixel corresponds to an angular resolution of 90 arc seconds . Here too, an intensive background emission had to be subtracted, but in this case the resolution is not sufficient to separate the sources. Moreover, the submillimeter source located 19″ to the north-west probably appears here too.

These data could be used to produce the spectral energy distributions of the two Herbig-Ae/Be stars (Fig. IV.3). For V 376 Cas, the intensity rises to longer wavelenghts, reaching a maximum at about 100 µm. This wide energy distribution is caused by the emission of dust at different temperatures. Now, it is possible to deduce from the new ISO data that the cool dust must have a temperature of about 33 K at a great distance from the star. The total luminosity in the range from 1 µm to 1000 µm proves to be 430 solar luminosities. Since ISOPHOT made it possible to cover the entire spectrum between 16 µm and 100 µm for the first time, this means that the luminosity has also been determined reliably for the first time.

Interestingly, the increase in the emission up to 100 µm can be described by a power law very similar to the one for dust discs around T-Tauri stars which are similar to the Sun. In this case, the emission in the near and middle infrared originates from the inner region of the disc, and the power law suggests that the material is optically thick there. The maximum at around 100 µm then identifies that area in the disc where the dust be-

Fig. IV.3: The spectral energy distributions of the six Herbig-Ae/Be stars. For LkHα 198, the contributions of two nearby companions were taken into account. For MWC 1080, substantial radiation components of an extended source probably contribute in the far infrared; a causal connection between these and the star seems unlikely.

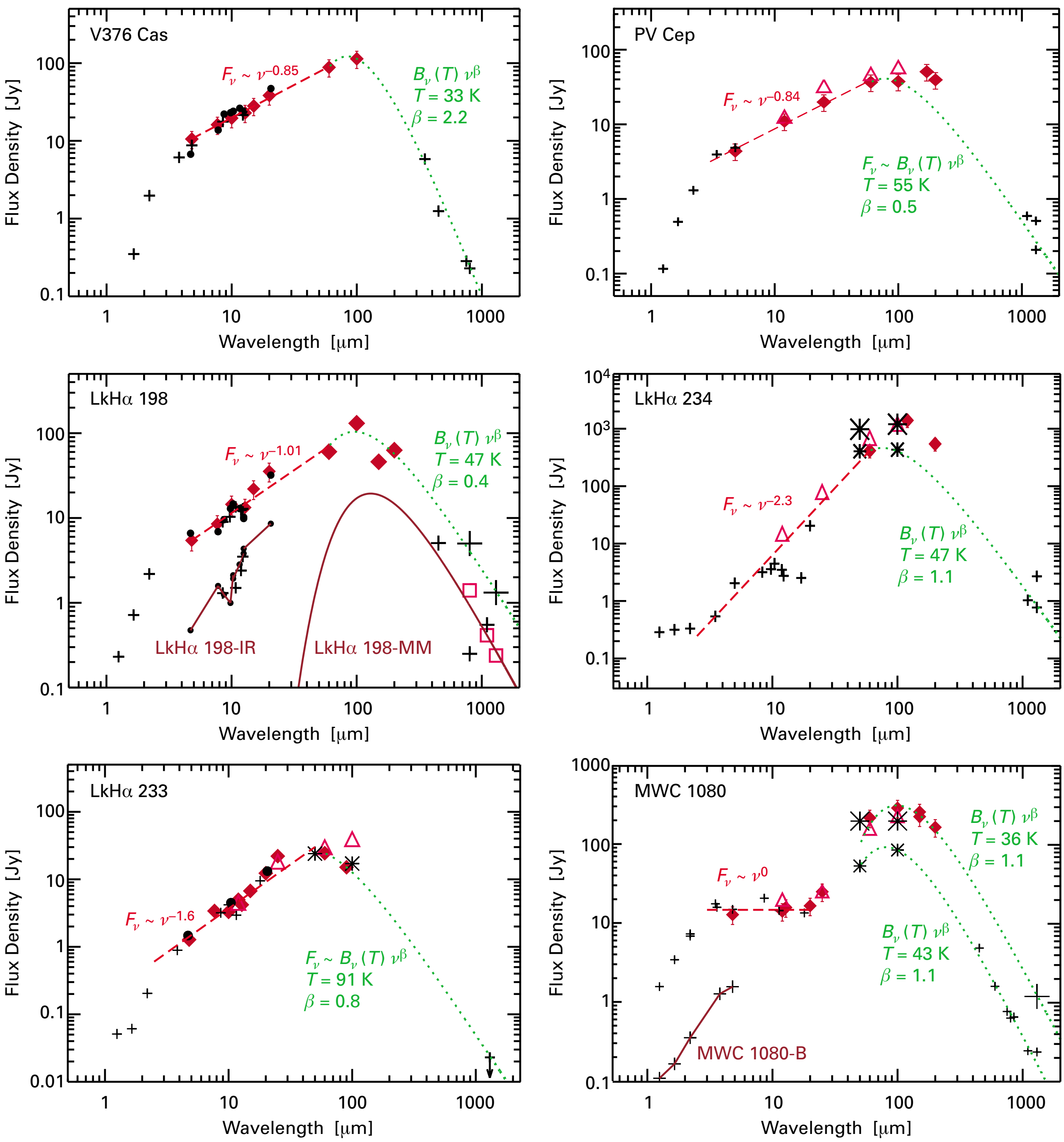

comes cooler and optically thin. Although this energy distribution does not make it possible to prove the existence of a disc around V 376 Cas, it is an indication that one may be present.

The case of LkHα 198 is more complex, since the nearby infrared sources contribute more to the signal as the wavelength increases. However, the three stars mentioned at the outset cannot be separated. If further observation data are also used, it becomes possible to give an approximate description of the measured intensity distribution by means of three Planck curves (Fig. IV.3). This means that LkHα 198 also has a spectral energy distribution which can be described by a power law up to the maximum. The best adaptation of the temperature of the cool dust proves to be 47 K here, and the total luminosity in the range from 1 μm to 1000 μm is between 60 and 350 solar luminosities. This value is uncertain due to the contamination from the two adjacent sources.

The other Herbig-Ae/Be stars have been analyzed in a similar manner. On average, the temperatures are 50 K, placing them in the range of the dust discs around T-Tauri stars. They are lower than for the discs around stars of the »Vega type« (see »The age of the disc stars Vega, Fomalhaut and Beta Pictoris«, p. 53). These are about 60 – 120 K. The power laws derived for the other Herbig-Ae/Be stars also resemble those for T-Tauri stars.

Ultimately, though the observed spectral distributions of the Herbig-Ae/Be stars can be explained by the existence of dust discs, this interpretation is not without ambiguity. The observation data also fit models with spherical dust envelopes and models in which a disc is surrounded by a very extended envelope. Nevertheless, the ISO data are a major contribution to the total complex of star formation, since it has been possible for the first time to observe the spectral energy distribution of these young stars in the range around the maximum, which has not been explored until now. This has yielded the temperatures in the cool areas of the envelopes or discs, and reliable values have been derived for the total luminosity of the dust envelopes. These are all valuable physical variables which are incorporated into the theoretical models. As compared with IRAS, the significant progress includes not only the extended wavelength range but also the substantially higher sensitivity and the possibilities for spectroscopy. In view of the fact that only 15 per cent of the entire ISO data have been evaluated so far, the astronomers are still expecting many more results from this successful mission.

In the more distant future, the researchers are placing their hopes in the aircraft-borne telescope SOFIA and the next major European FIRST satellite mission, in which the Institute will again be participating (see Chapter III).

Migrating Young Planets

At the end of 1995, two Swiss astronomers discovered the first extra-solar planet. Since then, about 40 dark stellar companions have become known, most of which are probably planets. Almost all of these planets are at least as massive as Jupiter and they orbit around the star at distances of less than one astronomical unit. This contradicts previous opinion, according to which planets similar to Jupiter can only form at distances of at least 4 AU from the star. With the help of computer simulations, theoreticians from the Institute have been able to demonstrate that massive proto-planets lose angular momentum due to interaction with the gas/dust disc in which they are created. As a result they approach the central star on a spiral path.

The extrasolar planets are so close to their central star in the sky, and are so faint, that they cannot be observed directly. So far, their presence can only be proven indirectly through their gravitational effect on the star: the planet and the star orbit around a common centre of gravity which is located somewhat outside of the centre of the star (Fig. IV.4). The effect of this is that the star oscillates to and fro with the orbital period of the planet. High-resolution spectrographs make it possible to measure the radial component of movement (the one located in the direction of the line of sight) with an accuracy of a few metres per second.

The mass of the star and the observed period and amplitude of its orbit around the centre of gravity of the system make it possible to calculate the masses and orbital radii of the planets. However, only lower limits are obtained for the mass values, since the spatial orientation of the orbit is unknown. If it is perpendicular to the celestial plane, the star is only deflected in the radial direction, and the mass value that is determined is exactly correct. In all other cases, the movement of the star also includes a component in the celestial plane that is not recorded, so that the actual planetary mass is larger than the figure derived from the radial velocity.

Values obtained so far nevertheless indicate clearly that most cases actually involve planets whose mass is many times that of Jupiter. Bodies with more than about 13 times the mass of Jupiter are brown dwarfs (see »From Low-Mass Star to Brown Dwarf«, p. 46). The lower limits for the mass values of extra-solar planets which have been determined so far are between 0.34 and 13 times the mass of Jupiter. The star HD 209458, where the planet moves in front of the star as we see it, is the only case where it has been possible to determine the mass as precisely 0.7 times the mass of Jupiter and the radius as 1.5 times the Jovian radius. The satellites are located at a distance of 0.04 to 2.5 AU from their central star, and the eccentricity of their orbits is between 0 (circular) and

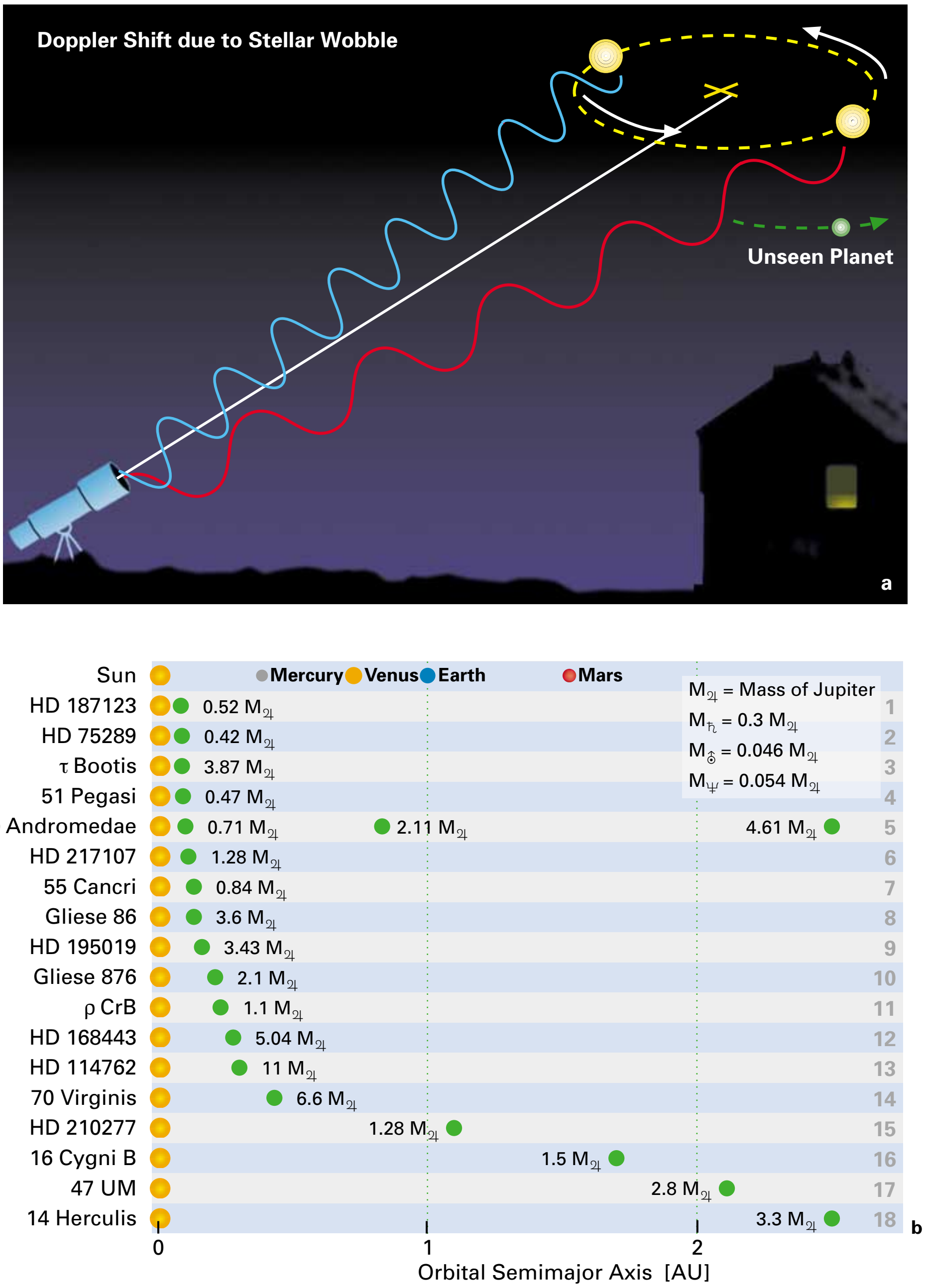

Fig. IV.4: (a) A star orbited by a planet moves back and forth, which is measurable as a Doppler shift in the spectrum. **(b)** The extrasolar planets that are known so far are closer to the star they orbit than had been expected previously.

0.67 (elongated ellipse). Accordingly, all the planets are closer to their central star than might be expected according to present theories on the formation of planets.

Planets beyond the Snow Limit

Planets are formed in circumstellar discs made of gas and dust. While the material condenses to form a star in the centre, it agglomerates in the outer areas to form planets. According to present ideas, this process takes place in several stages. First, dust and gas are mixed and the solid particles continue to grow as they collide and remain attached to each other. The particles continue to become heavier in this way, and then they sink to the central plane of the disc due to gravitational force; here, they form a relatively thin disc of dust. Since the density of the dust has increased due to this process, the particles now collide with one another more frequently and continue to grow until they have attained diameters of as much as a few kilometres. This process is known as coagulation. The planetesimals ultimately grow into objects with a size of up to ten times the mass of the Earth, due to collisions caused by gravitational interactions. The gravitation of the bodies which have been formed in this way is now large enough to attract (or accrete) more matter from the surrounding area, especially gas, which they bond to themselves.

At a distance of about 5 astronomical units from the star, it takes up to a million years for a planet the size of Jupiter to form. This period falls within the lifetime of the protoplanetary discs, which has been determined as several million years on the basis of observations. Astronomers from the MPIA played a decisive part in obtaining these results (see the 1998 Annual Report, p. 11). According to this work, the period for planetary formation derived from the theory lies within the empirically determined lifetime of the discs - which shows that our understanding of planetary formation is already quite complete. However, there is still one problem.

According to model calculations, the first stage in the formation of a gas planet similar to Jupiter is the formation of a solid rocky core with about 10 to 15 times the mass of the Earth. This accumulates gas from the nearby areas, and surrounds itself with an atmosphere. This procedure evidently has to start before the gas has disappeared from the disc, i.e. within about 10^7 years. However, at short distances from the star, neither the time nor the quantity of matter in the disc are sufficient to allow the formation of such massive cores for the later gas planets. This is only possible at a distance of at least 4 AU from the star, beyond the so-called ice condensation radius, also known as the snow line. The temperature there is so low that volatile gases condense to form ice. The formation of these solid particles from the gas phase increases the coagulation rate so that the massive cores which are the predecessors of the gas planets form more quickly than they would without this process.

If this theory is correct, it contradicts the observations of extra-solar planets. This contradiction could be resolved if a mechanism were found which causes planets to migrate towards the star from greater distances. One possibility here is an interaction between the protoplanet and the dust disc, as a result of which the body loses part of its angular momentum.

How a planet loses angular momentum

Earlier calculations had already indicated that the gravitational field of the planet introduces a disturbance into the circumstellar dust disc, leading to the formation of spiral density waves. These recall the arms of spiral galaxies.

There is also an interesting exchange of angular momentum between the disc and the planet. The particles within the planetary orbit move around the star faster than the planet itself. The planet therefore brakes them with its gravitational force or, in other words, the particles lose angular momentum and migrate further inwards. On the other hand, the particles beyond the planetary orbit are slower than the planet, from which they gain angular momentum causing them to migrate further outwards. In this way, a ring-shaped gap is created in the disc, along the path of the planet.

The planet gains angular momentum due to this interaction with the inner disc, and it would migrate outwards as a result. At the same time, it loses angular momentum to the outer disc. These two effects could cancel one another out in the long run, but this is not actually what happens. In reality, the particles in the inner disc lose angular momentum and fall into the central star. This causes a constant reduction in the mass of the inner disc, so that the loss of angular momentum to the outer disc is greater for the planet than the gain from the inner disc. Accordingly, the planet should migrate inwards.

Computer simulations were intended to verify whether these qualitative considerations are correct. It was also the aim to determine the period within which the planet migrates towards the star, how this process affects the eccentricity of the orbit, and how much matter the planet accumulates from the disc while it is taking place. It was assumed that a planet with one Jupiter mass had already formed at a distance of 5 AU from the star. Two more Jupiter masses of matter were assumed to be present within the initial planetary orbit. A typical value was assumed for the turbulent viscosity of the protoplanetary disc.

First of all, the simulation of a system of this sort clearly showed how the spiral arms form in the disc, and that the gap in the disc was created after about 200 orbits by the planet, corresponding to 2000 years (Fig. IV.5). A detailed image (Fig. IV.6) clearly shows the gas flow in the surroundings of the protoplanet. (It should be noted here that the reference system revolves with the planet around the star.) At the same time, the planet does actually migrate inwards, as expected. As Fig. IV.7 (left) shows, after about 2000 orbits, the planet is 40 % closer to the star than it was at the start of the simulation. A large part of the inner disc has already disappeared by this time.

During this phase, the planet has accumulated disc matter. At the outset, this process takes place quickly, but as soon as the gap has formed, less material is available to the planet. Nevertheless, it continues to accrete until the end (Fig. IV.7, right). As can be seen, it has more than doubled its mass after 2000 orbits.

This computer run was calculated with a high resolution so that the details could be examined reliably as well. In order to be able to study the long-term behaviour within appropriate computing periods, calculations at lower resolution were required. The reliability of various computing codes was tested here. Certain physical parameters, such as the planet's accretion rate,

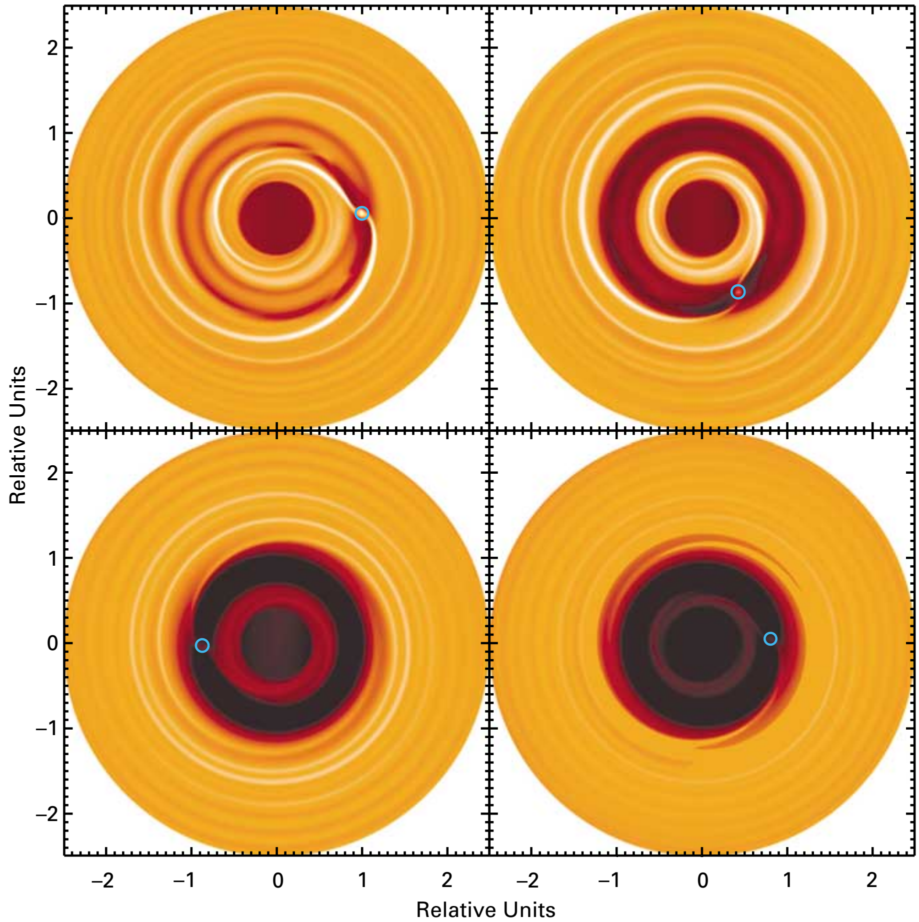

Fig. IV.5: Evolution of a protoplanet in a circumstellar disc during 527 orbits. The circle represents the position of the protoplanet. Areas of the disc with low matter density are dark while those of high density are light.

were also varied. Although some differences emerged in detail, the planets nevertheless migrated inwards in every case. And in a period of between about 100,000 and 200,000 years, they had reached the star and – theoretically – were bound to fall into it. This means that the time scale for the inward migration is about one magnitude smaller than that for the formation of large gas planets.

In this way, the migration movement described can also be used to explain the existence of massive extrasolar planets which orbit around their stars at very short distances. At the same time, a new question arises: what stops the migration before the planet disappears into the star? Several possibilities are conceivable here.

For example, more than just one planet will generally be present in the disc. On the one hand, they change the structure of the disc and, on the other, they influence one another due to their gravitational force. It is known that three large planets of this sort can disturb one another so

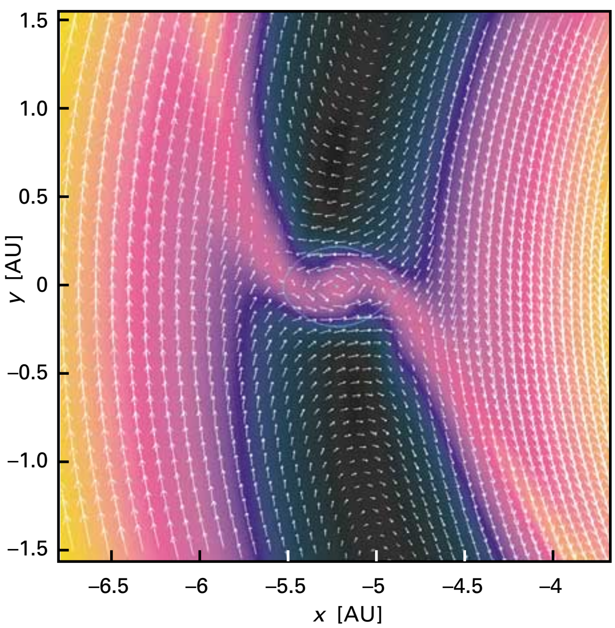

Fig. IV.6: The flow in the vicinity of the protoplanet, in relation to the planet. The blue line symbolizes the Roche volume of the planet.

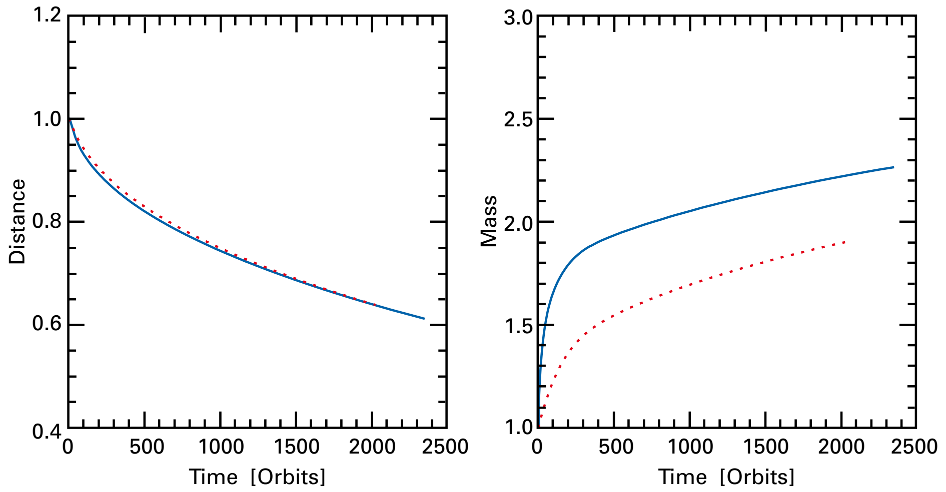

Fig. IV.7: The evolution of the orbit (left) and the increase in mass (right). The blue line denotes a lower-resolution model and the red line shows a model with higher resolution. In both cases, it was assumed that a gap is present at the start of the calculations.

much that their paths take on a chaotic course, and one of the bodies can be thrown into an orbit close to the star. It is also conceivable that giant planets are formed even further out. From a distance of 20 AU, the body would require about one million years in order to migrate into the inner zone. By then, the disc would have vanished and no further transfer of angular momentum would be possible. It is also possible that stellar magnetic fields could stop the inward movement.

The theoreticians now intend to refine their models by including other physical effects such as radiation cooling of the disc, or the effect of magnetic fields.

From Low-Mass Stars to Brown Dwarfs

The masses of the stars span a wide range from about one tenth of a solar mass to about one hundred solar masses. Precisely how far this scale extends at either end, and which characteristics the stars there possess, are questions which have not been fully clarified in either empirical or theoretical terms: for example, where is the start of the area of the brown dwarfs, whose interiors have ceased to ignite the nuclear fusion which generates energy, and where is the transition to the planets? Observations of two close stellar systems have made it possible to determine luminosity and mass very accurately. In this case, three of these celestial bodies proved to be stars of extremely low mass (0.07 solar masses). This is the region in which the theoreticians suspect that the transition to the brown dwarfs lies. In another investigation, it was possible to prove periodic luminosity variations in a brown dwarf. Conceivable explanations for this phenomenon include dust clouds surrounding the celestial body, or magnetic activity. Finally, a third study in the open star cluster M 35 revealed a series of candidates for brown dwarfs.

The study of stars with extremely low masses was boosted a few years ago by the discovery of brown dwarfs. But due to their extremely low luminosities, these heavenly bodies are difficult to discover. For example, the Gliese catalogue published in 1957 by the Astronomisches Recheninstitut in Heidelberg contains stars at distances of up to 20 parsec (approx. 65 light years). It comprises 915 single and double stars with a total of 1094 components. Within this group, the star density at a distance of 12 light years is apparently three times greater than at 65 light years. If we assume that the stars are in fact more or less uniformly distributed, we must conclude that the fainter stars can no longer be discovered, even at this relatively short distance. This means that in a spherical volume around the Sun with a radius of 65 light years, there are more than 3000 stars, about two-thirds of which have not even been discovered yet.

The faintest star in the Gliese catalogue is a red dwarf at a distance of 20 light years, with an absolute visual magnitude of 18.5. Hence this low-mass star only has about 1/20,000 of the Sun's luminosity. But does the stellar mass scale end here? Theoretical models predict that stars below a specified mass have such a low central temperature that the fusion of hydrogen to form helium – the »burning« of hydrogen – no longer takes place on a significant scale. For a short period after it is formed, a body of this sort can probably go on burning deuterium and tritium. But then this process will cease too, and the body will slowly cool off as a brown dwarf.

According to the latest calculations, the transition from a star to a brown dwarf occurs at about 0.075 solar masses. At about 0.013 solar masses (corresponding to about 13 Jupiter masses), present knowledge suggests that the transition to a planet takes place. It is difficult to decide whether an object of about 0.08 solar masses is a brown dwarf or a red dwarf star of extremely low mass. All young brown dwarfs are of spectral type M, and it is virtually impossible to distinguish them from normal stars of extremely low mass. It is only when a brown dwarf is older than about one billion years that it falls below the temperature range of low-mass stars.

Together with other colleagues, astronomers at the MPIA succeeded in carrying out a detailed investigation of two stellar systems of extremely low mass. This project, which has run for many years, has made it possible to arrive at an accurate determination of important stellar quantities, and to compare them with models. Three of the celestial bodies also emerged as the stars with the lowest masses known in the environment of the Sun. Above and beyond this, it was possible to demonstrate impressively that dust is formed in the outer areas of these cool stars, and its optical attributes play a major part in determining the stellar masses, to give only one example.

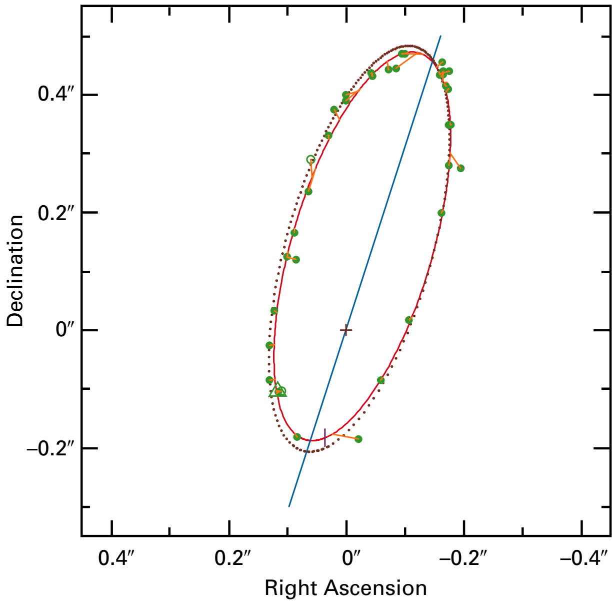

Fig. IV.8: The orbit of Gliese 866 AB (continuous line). The dotted line identifies a previously determined orbit.

The Triple System Gliese 866

For thirty years, star number 866 in the Gliese catalogue was regarded as a single star. In 1986, astronomers at the MPIA discovered a companion at an angular distance of only 0.4 seconds of arc from the main star, with the help of high-resolution speckle interferometry. They immediately recognised that it would be possible to determine the masses of the two stars if they could follow their orbits. Four years later, the first figure was already available. Accordingly, the mass of the two stars together comprises 0.38 solar masses. However, star models based on the photometric data for the two components yielded masses of 0.14 and 0.11 solar masses respectively – adding up to a much smaller total. During recent spectroscopic examinations of G 866, French astronomers have discovered a third and hitherto unknown companion. Was this the solution to the discrepancy between the two mass determinations?

In order to pursue this question, the MPIA researchers decided to study this interesting system more closely, in conjunction with colleagues from the Astronomisches Recheninstitut in Heidelberg and from the USA. For the period from 1990 until 1998, they observed Gliese 866 several times with the 3.5 metre telescope on Calar Alto, and also with other ESO telescopes on La Silla and with the Hubble space telescope. This resulted in 37 independent data points from which it was possible to reconstruct the orbit of the two brighter components (Fig. IV.8).

At a distance of 11.2 light years, it emerged that there was an elliptical path (eccentricity e = 0.437) with a major semi-axis of 1.2 AU and an orbital period of 2.25 years. From this it is possible to use Kepler's second law to calculate the total mass as (0.336 ± 0.026) solar masses; the majority of the error is due to the uncertainty about the distance. This means that the mass figure was corrected downwards in relation to 1990, although it was still significantly above the value derived from the photometric measurements.

The question as to whether at least one of the components is a brown dwarf cannot be answered on the basis of kinematic data alone. However, photometric and spectroscopic investigations suggest that all three components have very similar effective temperatures. Since they are very probably of the same age, they must therefore have similar masses as well. Ultimately, masses of 0.11 each were obtained for the three stars. Even with an error of 10 to 20 %, it seems certain that none of the members of Gliese 866 is a brown dwarf. Hence the initial problem of the lack of mass is solved by the third companion.

This work is very important, especially in terms of stellar astronomy, since it was possible to determine the movements of the components and hence the total mass, beyond doubt. Since these stars are at the lower end of the mass scale, they will serve as standard references for stellar models in the future. The situation is very similar with the multiple system LHS 1070, which has also been examined in great detail.

The quadruple system LHS 1070

Approximately speaking, celestial bodies at the transition between low-mass stars and brown dwarfs should be of spectral type M8 or later. Since about 1995, more and more of these interesting objects have been found. Spectroscopic investigations have recently made it clear that spectral classes M9 and later should be redefined and designated as spectral type L. A characteristic feature of this class is that the molecule lines of titanium oxide (TiO) and vanadium oxide (VO) (on which the definition of class M is actually based) are unexpectedly weak or even absent. Instead, lines of the alkaline elements potassium, sodium, rubidium and caesium are stronger. The cause of this phenomenon only became apparent recently: in their photospheres, dwarf stars with effective temperatures of up to 2600 K only show temperatures of about 1500 K – cool enough for dust to form. Then, elements such as titanium (Ti) or vanadium (V) condense on the dust particles, while the more volatile alkaline elements remain in gaseous form.

An interesting question is what happens to the dust. It is possible that it forms clouds and drops down into the photosphere, or that it forms a layer of vapour around this star where it exerts a greenhouse effect. Another question which arises here concerns the extent to which stars and brown dwarfs differ from one another as regards the supposed formation of dust.

In the near solar environment, we currently know of only two star systems in which there are objects of the late M or early L types, and for which the orbital parameters can be determined. One of these is LHS 1070. In 1994, astronomers at the MPIA were for the first time able to use speckle interferometry to determine the spatial arrangement of three stars at 2.2 m (Fig. IV.9). Accordingly, the two components A and B were then separated from one another by 1.1″, while component C was located 0.27″ to the north of B. In a second observation in 1998, C had migrated 69 degrees counterclockwise, and was 0.36″ away from B. In recent spectroscopic investigations, American astronomers have

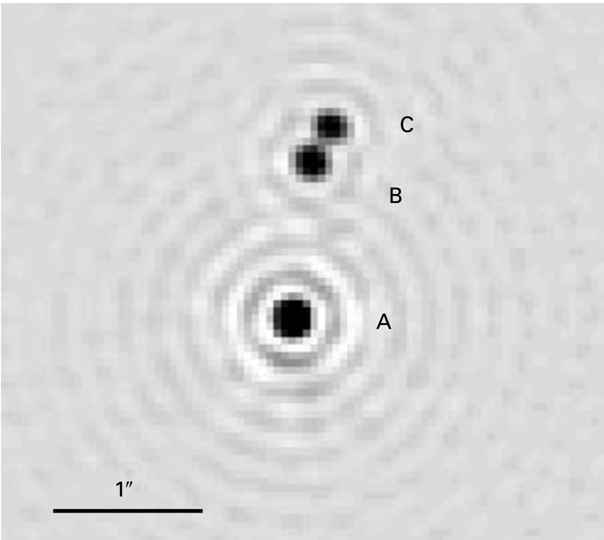

Fig. IV.9: The LHS 1070 system in the infrared at a wavelength of 2.2 m.

Table IV.1. Basic parameters of the components of the triple star LHS 1070 at a distance of 28.7 light years.

Component	Spectral type	Absolute magnitude (visual)	Effective-temperature [K]	Mass [$M_\odot$]
A	M5.5 – 6	15.63	2950	0.1
B	M8.5 – 9	18.96	2400	0.08
C	M9 – 9.6 (L0)	19.35	2300	0.08

used the Hubble space telescope to detect a fourth component at a distance of only 0.05″ from A.

LHS 1070 is therefore an ideal study object for low-mass stars. Spectroscopic and photometric observations with Hubble formed the basis for a detailed analysis which was then carried out with a stellar atmosphere model. This model can be used in a temperature range of 1500 to 3000 K, and in addition to the normal radiation transport, it also takes account of the formation of more than 600 types of gaseous and dust-like particles, and the opacities of different types of dust, insofar as they are known from laboratory experiments.

The spectral classes were determined on the basis of various criteria, and the interval of about one half of a magnitude in absolute magnitude shows the uncertainty in this range of the mass scale (Table IV.1). Whereas the astronomers are also familiar with similar representatives in the cases of components A and B, component C shows a very unusual spectrum. In the new classification scheme, C would be assigned to spectral class L0. The absolute magnitudes are critically related to the assumed distance. For LHS 1070, parallactic measurements produce a value of 24.1 light years. However, this value is considered uncertain due to the multiplicity of the system. In the work described here, the best matches between the models and the spectra were obtained at a distance of 28.7 light years, which was also used in the subsequent analyses for this reason.

Using this model, the spectra yielded masses for the single components as follows: 0.08 solar masses for B and C, and 0.1 solar masses for A. In all probability, this means that A is a low-mass star and not a brown dwarf. B and C are precisely in the transition zone. These values are based on an assumed age of five billion years and a solar element abundance. If, instead, we take an age of one billion years and if we reduce the abundance of heavy elements by a factor of three, the masses that are obtained only change by a few thousandths of a solar mass. A notable feature of LHS 1070 is that components B and C (and also D, as far as is known) are the faintest stars within a distance of 65 light years from the Sun for which a mass determination should be possible on the basis of orbital motions in the coming years (as for Gliese 866). The orbital period is below 20 years.

Using the new stellar atmosphere model which also takes dust formation into account, it has generally been

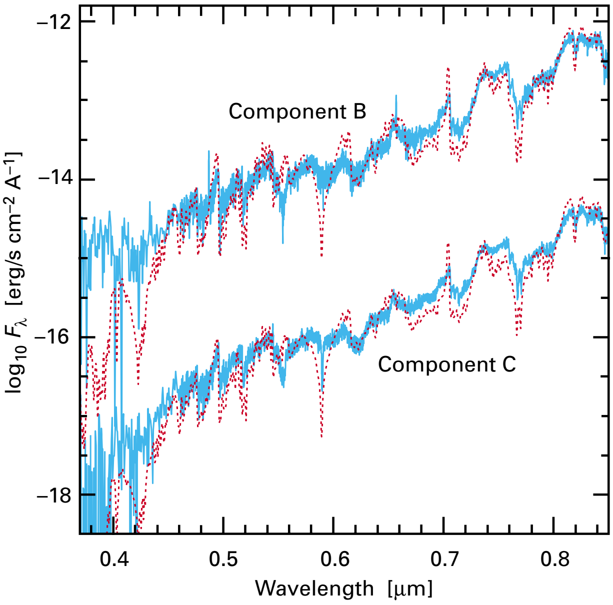

Fig. IV.10: Spectra of components B and C of LHS 1070 as compared to a model (dotted line).

possible to reproduce the spectra very well (Fig. IV.10), something which was hitherto impossible. It emerged clearly that the brightest component A is too hot to form significant quantities of dust. On the other hand, B and C are the most dust-rich stars known at present. The form in which the dust is present is still unknown. However, the data suggest that the particles accumulate in thin layers which then fall slowly into the photosphere. More information about this question is probably concealed in observational data which the astronomers have already obtained with the Hubble space telescope and ISO in the near infrared.

Dust Clouds in the Sky of Brown Dwarfs?

The first brown dwarfs were discovered in the open star cluster of the Pleiades, at a distance of 380 light years. In 1999, astronomers at the MPIA examined six members of this cluster, three of which are certainly brown dwarfs, with two stars of very low mass and one star whose nature has not yet been clarified. Using the 2.2 metre telescope of the Calar Alto observatory, the researchers looked for luminosity fluctuations from the six celestial bodies. If they occur periodically, they are very probably associated with the rotation of the objects. This important stellar variable depends on the age or the mass of the body, so it provides some indications about the formation and evolution of the brown dwarfs.

Brightness fluctuations due to magnetic activities are also conceivable. At least for more massive stars, theoretical models suggest a correlation between the velocity of rotation and the magnetic activity. It is entirely unclear whether such a relation exists for the least massive stars as well. However, also magnetic activity can cause star spots which result in broghtness variations with the period of rotation. In this case, such luminosity fluctuations ought to occur mainly in the light of the hydrogen line, Hα.

In the first investigation described here, it was possible to exclude luminosity variations with amplitudes of between 0.025 and 0.07 magnitudes in the time interval between about half an hour and about a hundred hours, for five of the six stars. The astronomers' search was only rewarded in the case of the low-mass star designated as 2M 1145 (Fig. IV.11). Here, they discovered a periodic variation with a time of 7.12 hours and an amplitude of 0.04 mag.

The cause of this variation is not known, but it can probably be ascribed to rotation. For an assumed radius of 0.1 solar radii, the rotation period corresponds to an orbital velocity at the equator of 17 km/s. This places the object in the range from 2 to 32 km/s which has been determined for M dwarf stars in the solar environment. However, it is below the range from 37 to 65 km/s which was determined for nine M dwarfs in the Pleiades.

It is not yet clear how this new result can be integrated here. If the luminosity fluctuation can be attributed to magnetic activity, then it should appear in the Hα emission in particular. However, it is also conceivable that dust clouds form in the atmosphere of 2M 1145, obscuring a greater or lesser part of the stellar disc. If they rotate with the star, they could also cause the variations in luminosity. The astronomers at the MPIA intend to undertake further observations in various filter ranges in order to get to the cause of this phenomenon.

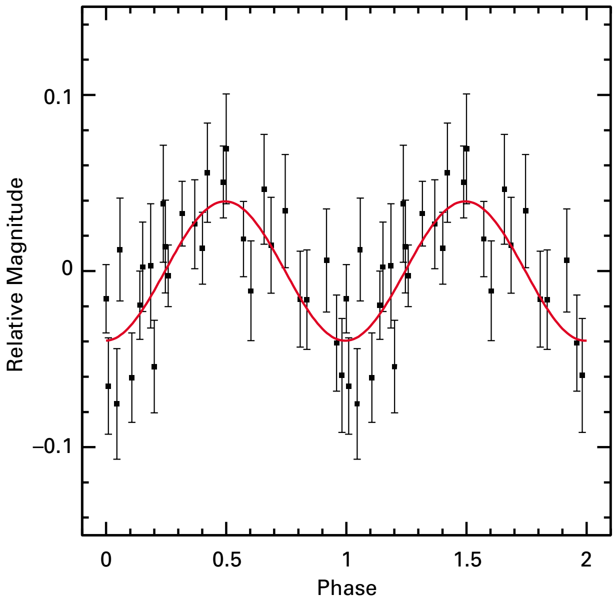

Fig. IV.11: The light curve of the L dwarf star 2M 1145. The period is 7.12 hours.

Brown Dwarf Candidates in the Open Star Cluster M 35

Until now, only a few brown dwarfs have been identified unambiguously. In order to determine the frequency and characteristics of these faint heavenly bodies, considerably more of them will have to be found. An opportunity to do so is offered by a photometric study which has been undertaken by an MPIA researcher on the Canada-French-Hawaii telescope on Mauna Kea, where he succeeded in obtaining deep images of the open star cluster M 35 through two filters in the red (R) and infrared (I)wavelength ranges.

At a distance of some 3000 light years, M 35 is among the most beautiful star clusters which are still visible to the naked eye (Fig. IV.12). Its apparent size in the sky more or less corresponds to that of the full moon. According to the latest analyses, it is 125 million years old, the same age as the Pleiades (see the next chaapter »New age scale for star clusters«); but with an estimated total mass of 1000 to 3000 solar masses, it is considerably more massive.

The main goal of the work was to determine the luminosity and mass function of the stars. For this purpose, the first important task is to separate the members of the cluster from those stars which are only located in the same direction by chance. This is done by producing a colour-luminosity diagram of all the stars (Fig. IV.13). Since the distance of the cluster is known, the main sequence (on which the members of M 35 must lie) can be entered in the diagram. In fact, two groups emerge: one comprises the members of M 35 on this curve and the other contains the field stars, which are an average of four magnitudes fainter. Although the separation between field stars and cluster stars is not ent-

Fig. IV.12: The open star cluster M 35

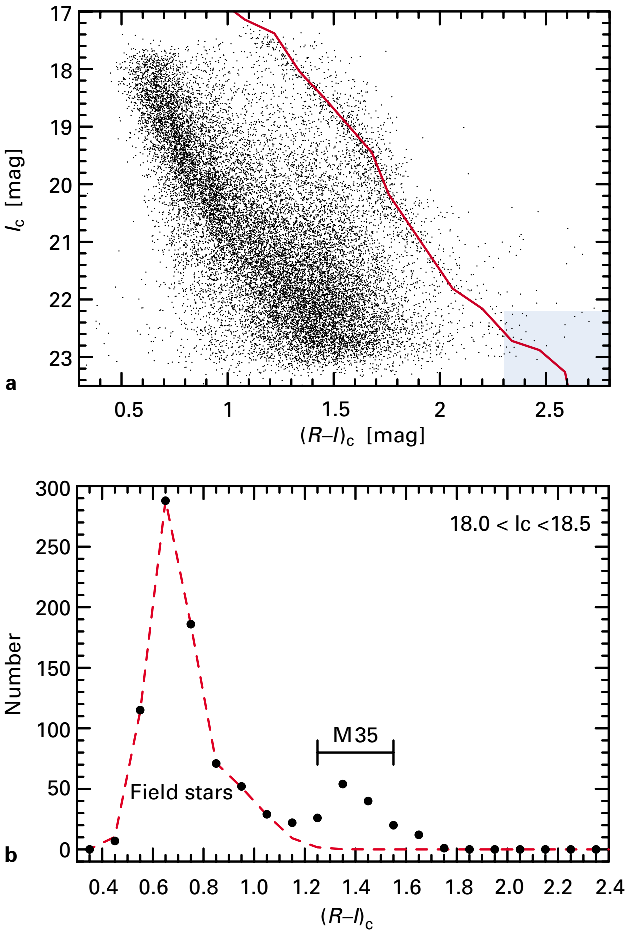

Fig. IV.13: (a) Colour-magnitude diagram of stars in M 35 and field stars. Stars belonging to the cluster are seen in close vicinity of the main sequence.The brown dwarf area is marked. **(b)** Histogram of field and cluster stars.

irely without a transition, a statistical method has ultimately made it possible to separate the members of the cluster with a high level of probability.

The luminosity function of M 35 now proved to be almost identical with that of the Pleiades, which indicates that the star formation rate for stars of different mass is not dependent on the size of the star formation area (M 35 contains substantially more stars than the Pleiades). The dataset for M 35 is complete up to the 19th absolute magnitude in the infrared. Not all the fainter stars were recorded, and the proportion of unrecognised field stars also increases in their case. For a cluster age of 125 million years, the range of the brown dwarfs would be about I = 22.2 mag and (R-I) = 2.3 mag. As can be seen in Fig. IV.13a, there are about 20 objects in this range. Future observations should provide a clear picture of their nature.

A New Age Scale for Star Clusters

Determining the age of stars is one of the central tasks of astrophysics. For example, the age of the stellar population in the Milky Way can be used to draw conclusions about the formation and evolution of our galaxy. For young star clusters, a precise knowledge of the age is very important if brown dwarfs are being sought in them. This is because their temperatures, luminosityes and colours are critically dependent on their age. A new method of determining age is based on the fact that lithium is destroyed in low-mass stars. This means that as the age increases, the proportion of lithium in their atmospheres will decrease. This criterion has helped to re-determine the age of the open star cluster IC 2391, the Pleiades and NGC 2516. According to this work, these clusters are considerably older than had previously been assumed.

There are various methods of determining the age of stars, most of which are based on the theory of stellar evolution. For young stars inside which the nuclear fusion processes have not yet begun and which have not yet reached the main sequence, the age is obtained from their position in (for example) a colour-magnitude diagram, in conjunction with theoretical models of star formation and protostellar evolution. But if a star has reached the main sequence, it is very difficult to determine its age since it hardly moves at all in the colour-magnitude diagram during the main sequence stage.

It is easier to determine the age of a star cluster. In this case, it is assumed that all the members were formed at about the same time. Since the lifetime of the stars (the time for which they remain on the main sequence) decreases as the mass increases, the upper mass limit of the member stars located on the main sequence moves downwards as the age of the cluster increases: the older the cluster, the lower the mass of the most massive star on its main sequence. This is a good criterion for determining age, but even this method depends on the stellar evolution models.

The Lithium Depletion Method

Only a few years ago, a new procedure was suggested which has an altogether different basis. This is known as the lithium depletion boundary method. It is based on the following idea: for a long time, it has been known that the nuclear reactions in the interior of low-mass stars and brown dwarfs destroy lithium, but do not form it. This means that the lithium abundance becomes lower and lower as the age of these bodies increases. The destruction rate depends on the mass: the more massive the star, the faster it eliminates its lithium. Among the low-mass members of a star cluster of the same age, there is consequently a boundary between the more massive stars which have already eliminated their lithium altogether, and the less massive stars which have not yet reached this stage. As age increases, this lithium depletion boundary moves towards less and less massive members. This provides another criterion for the age of a cluster. This method is also dependent on a model, but it offers the prospect of supplying very sharp boundaries for the age of a cluster.

Until very recently, this method could not be used because it was impossible to detect sufficiently low-mass stars and brown dwarfs. It was not until 1998 that this method could be used to determine the age of the Pleiades for the first time (Fig. IV.14). The result was surprising: the lithium method yielded an age of 125 million years, substantially more than the previous standard figure of 70 million years. Encouraged by these results, researchers at the MPIA used the 4-metre telescope of the Cerro Tololo Interamerican Observatory in Chile to examine the open star cluster IC 2391. At a distance of just 500 light years, this is the fifth nearest open star cluster and it can easily be recognised by the naked eye in southern skies. Its angular extent in the sky is about four times that of the full moon.

Earlier investigations had indicated a low age, but accurate dating was not possible. It was only with more sensitive detectors that several dozen stars of extremely low mass and probable brown dwarfs could be tracked down in IC 2391. The candidates were identified with the help of photometric images in the red and infrared wavelength ranges. A total of three hours' exposure time in the red and two hours in the infrared were required in order to cover most of the extensive cluster. But in order to carry out the lithium test, spectra are needed in a range around 670.8 nm wavelength where there is a strong lithium absorption line. It has been possible to obtain spectra of 19 objects which have been unambiguously identified as members of IC 2391; this called for exposure times of between 10 minutes and 4.5 hours.

Fig. IV.15 shows three examples which clearly demonstrate how the lithium absorption line of a faint star (CTIO-038) with an infrared magnitude of 16.29 disappears through a rather brighter one with $I = 16.14$ to an even brighter star with $I = 15.83$. The lithium line could also be detected in two other stars which are even fainter than CTIO-038. According to these observations, the lithium depletion boundary is located at an apparent

Fig. IV.14: The Pleiades, an open star cluster, shown here in an image from the Calar Alto observatory, are possibly a good deal older than was previously assumed.

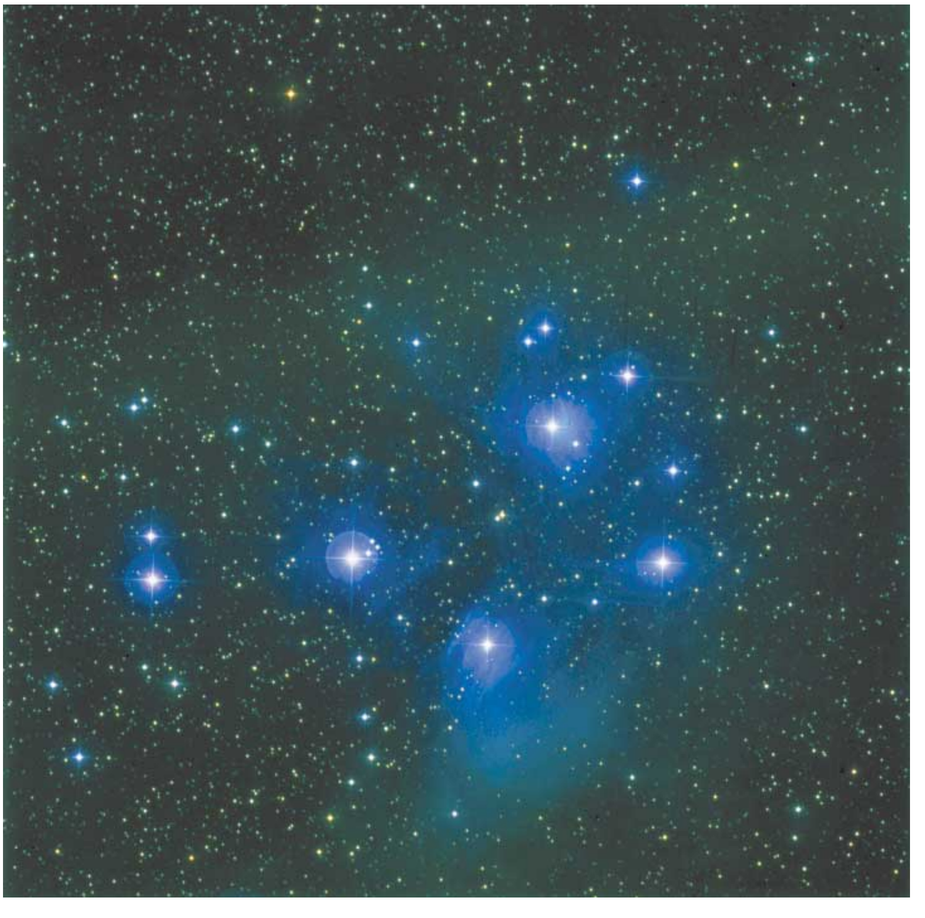

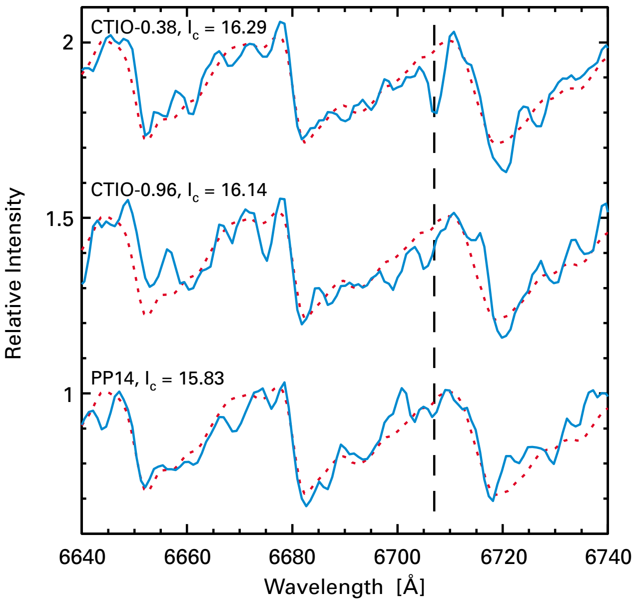

Fig. IV.15: Spectra of three faint stars in IC 2391. The lithium absorption line at 6708 Å becomes increasingly fainter from the faintest star (top) to the brightest one (bottom).

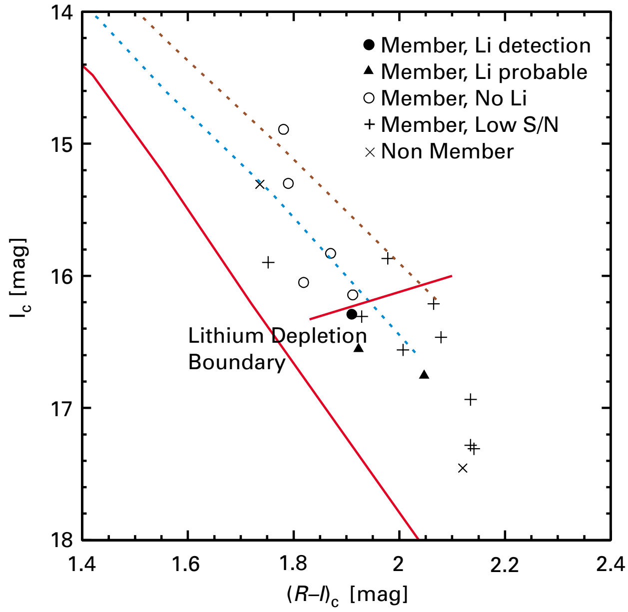

Fig. IV.16: The lithium depletion boundary obtained from the spectra for IC 2391.

Fig. IV.17: As the age of the star cluster increases, the lithium depletion boundary migrates towards fainter and less massive stars.

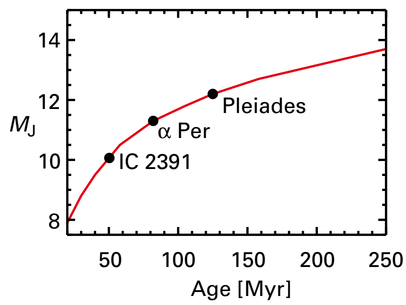

magnitude in the infrared of between 16.0 mag and 16.3 mag (Fig. IV.16). This yields an age of 53 million years, which is again considerably higher than the previously assumed value of 35 million years. This discrepancy could be due to imperfections in the stellar evolution models which form the basis for previous determinations of age.

The new age also gives a new magnitude limit for brown dwarfs. At the present age of 53 million years, a celestial body at the transition boundary between a star and a brown dwarf (assumed to be about 0.075 solar masses) should have an absolute magnitude of 11.15 mag in the infrared. If this is so, then the two faintest objects that were observed must actually be brown dwarfs.

Fig. IV.17 shows how the lithium depletion boundary migrates towards fainter stars as the age increases; shown are data for the three open star clusters on which this method has so far been used with success. The cluster around Alpha Persei was also included here, and in this case too, the lithium method yielded a higher age than had previously been supposed: 85 million years instead of 50 million.

For all the open clusters examined so far, the new method therefore results in an age which is about 50 % higher than the figure obtained by the standard methods. If these findings were to be confirmed in the future, a new age scale for these star clusters would have to be considered. This would have a whole series of consequences. Firstly, the stellar evolution models would have to be revised, and then the search for brown dwarfs would be made more difficult, because they are born as hot celestial bodies which subsequently cool down slowly. The older a cluster is, the cooler it is, and hence the redder and fainter are the brown dwarfs which it contains.

The Age of the »Disc Stars« Vega, Fomalhaut and Beta Pictoris

In the mid-1980's, astronomers came across intensive infrared radiation from the stars Vega, Fomalhaut and Beta Pictoris. Subsequent investigations then showed that this originated from dust discs which surround the stars. The term »Vega phenomenon« was coined immediately. More recent investigations revealed that the discs evidently disintegrate in the course of several hundred million years. Astronomers at the Institute played a decisive part in reaching this result (see 1998 Annual Report, p. 11). One difficulty with these investigations is the question about the age of the stars. For Beta Pictoris, for example, the estimates fluctuate between ten and several hundred million years. A study undertaken at the MPIA has now been

able to make this matter more clear. For Vega and Fomalhaut, it yielded an age of 200 million years, and for Beta Pictoris the figure was 20 million years.

The origin of these discs has not been conclusively clarified. On the one hand, they could be remains from the period when the star was formed. But on the other hand, it is conceivable that the dust particles are produced continuously, and the disc is constantly being renewed. An argument in favour of this second possibility is the fact that several influences such as the star's particle wind and the stellar light act on the particles and destroy the disc. At the same time, the accretion of the particles could form larger bodies, even planets, a process which also uses up the dust reserves in the disc (see »Young planets on their travels«, p. 42). The result of these procedures should be that a disc is already destroyed before the star reaches the main sequence stage.

The dust is possibly topped up by planetoids and comets, as is the case in our own solar system. Here too, the interplanetary dust is constantly being used up and produced again. About two-thirds of the interplanetary particles are created during planetoid collisions, and the remainder originates from comets. It is altogether feasible that there are already planetoids and comets which generate dust in the dust discs around Vega, Fomalhaut and Beta Pictoris. From the viewpoint of planetary formation and stellar evolution, these processes are extremely interesting. One of the key variables in the understanding of how such discs develop is, of course, their age.

Beta Pictoris

In the recent past, determinations of the age of Beta Pictoris (for example) based on stellar evolution models have led to completely different values. In 1995, theoreticians arrived at an age of about 12 million years. Other attempts led to values of 20 to 40 million, 100 million and even 300 million or more years. It is equally unclear whether Beta Pictoris is already in the main sequence, or just before it.

The new study undertaken at the MPIA is based on a totally different approach. In this case, it is assumed that the star under examination was formed at the same time as the other stars in a cluster. This makes it conceivable that other cluster members will be found whose age can be determined more easily. In the case of the three Vega-type stars, however, it has so far been impossible to prove membership of an open star cluster. For this reason, attempts were made to discover whether these disc stars might belong to a moving group. These are open star clusters whose members have already moved far apart from one another in space. They can only be recognized because they have virtually identical spatial velocities.

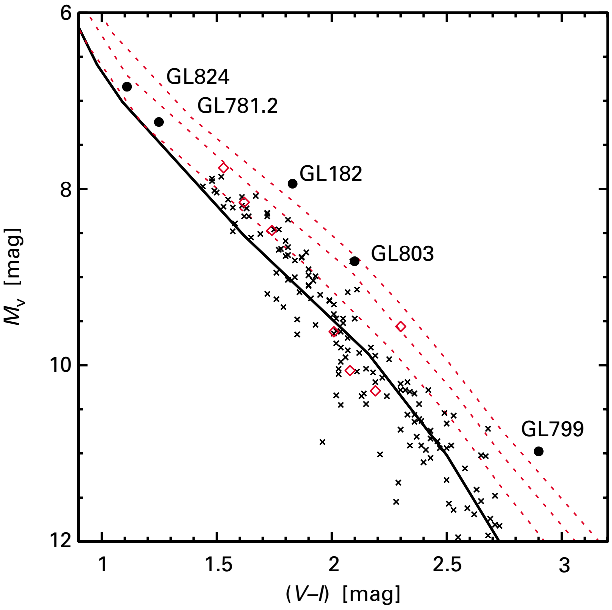

Fig. IV.18: Colour-magnitude diagram with the main sequence (marked as a continuous line) and isochrones for stars aged 20, 30 and 50 million years.

The search for moving clusters is extremely laborious, because they cannot be recognized as accumulations of stars in the sky. In one of the best-known examples, the Ursae Majoris cluster, the members are strewn across the entire sky. The Sun is situated in the middle of this cluster although it does not belong to it. In the MPIA study, the astronomers referred back to previous work in which companions to Beta Pictoris were suspected but not ultimately identified. The distances and intrinsic motions of these stars were initially determined, using the star catalogue of the HIPPARCOS European Astrometry Satellite and the PPM catalogue of the Heidelberg Astronomisches Recheninstitut. The radial velocities had also been known since 1995. From this dataset, the researchers now determined the spatial motions of the stars and compared them with that of Beta Pictoris. This initially left six candidates as possible companions for this disc star. One was rejected because it is evidently a good deal older than Beta Pictoris, and another could not be included in the analysis because observation data were lacking. This left only four stars.

These candidates were compared in a colour-magnitude diagram together with theoretical paths of evolution for young stars (Fig. IV.18). Accordingly, two of them (GL 799 and GL 803) are 20 million years old and the other two (GL 781.2 and GL 824) are 40 million years old. Another argument in favour of this low age is that at least the two stars GL 803 and GL 799 show strong X-ray activity on images from the ROSAT satellite telescope. On the other hand, GL 824 does not show any intensive X-radiation, so it should be older. These investigations lead to an age of (20 ± 10) million years for the Beta Pictoris moving group. Hence this disc star is younger than most previous studies have indicated.

Fomalhaut and Vega

At the start of the 1990's, it was already suspected that a group of 18 stars including Castor, one of the two Twins, form a moving group. It even seemed possible that Vega and Fomalhaut belonged to it. The MPIA researchers included these 18 stars as well as 26 other candidates in their new investigation, first using the HIPPARCOS and PPM catalogues to determine their luminosityes in various spectral ranges, as well as their intrinsic motions and distances. The radial velocities were also known already. With the help of this extensive data material, it was possible to rule out some stars as members of the Castor moving group.

Fig. IV.19 shows the two galactic velocity components U and V of the remaining candidates; a virtually identical V-component (parallel to the galactic disc in the direction of motion) was considered as the strongest criterion in favour of membership of a moving group. Other criteria included the positions of the stars in a colour-magnitude diagram, and their stellar activity in the range of the hydrogen emission (Hα) and in the X-ray range. Ultimately, only 8 stars remained from the group which originally comprised 44, including Castor, Vega and Fomalhaut.

At first, an attempt was made to determine the age of these stars in the colour-magnitude diagram, with the help of theoretical evolution models. In this case, how-

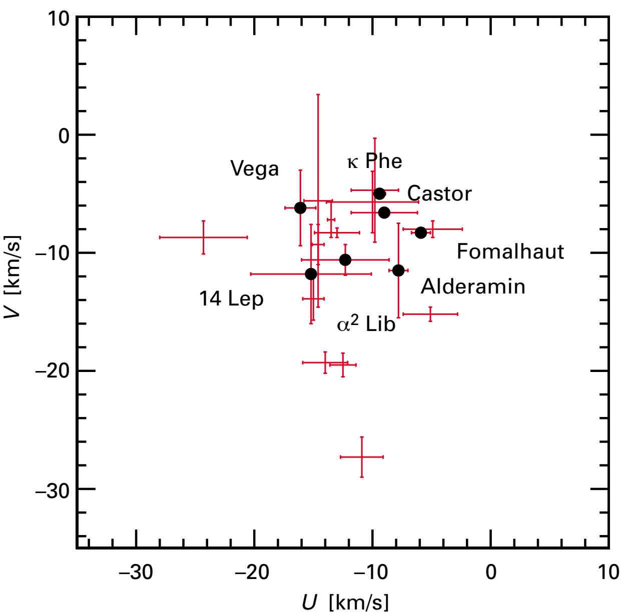

Fig. IV.19: The candidate members of the Castor moving group in a diagram of the galactic velocity components *U* and *V*.

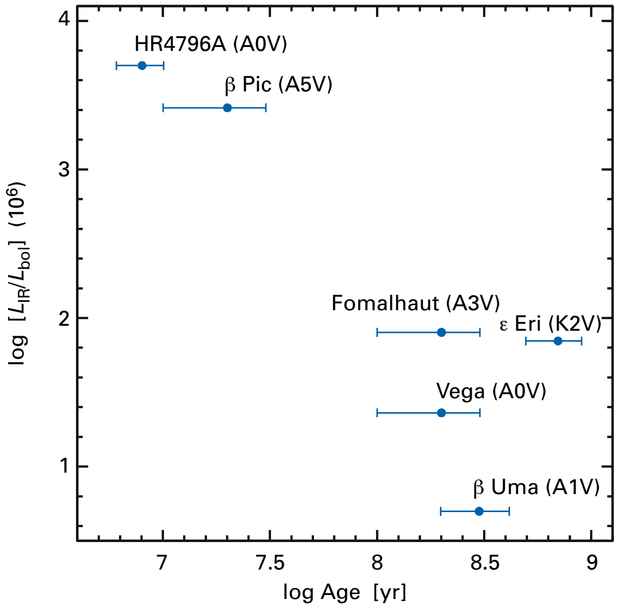

Fig. IV.20: Decrease of infrared luminosity as the age of the stars increases.

ever, this method is very inaccurate, because the proportion of heavy elements is not known. This only yielded a minimum age of 35 million years. As long ago as 1993, astrophysicists had attempted to derive the ages of Vega and Fomalhaut directly from evolution calculations of this sort. At that time, they arrived at figures of 400 and 200 million years respectively.

However, the MPIA researchers used a new method which had already proven its merits in other cases: the lithium depletion boundary method (see »A New Age Scale for Star Clusters«). The basis is that low-mass stars destroy lithium, but do not form it. This means that the lithium abundance decreases as the age increases. The destruction rate also depends on the mass: the more massive the star, the faster it destroys lithium. Hence among members of a star cluster with the same age, there is a boundary between the more massive stars which have already destroyed their lithium completely, and the less massive ones which are not yet at this stage. As the age increases, this lithium depletion boundary migrates towards constantly less massive members, which can be used as the criterion for the age of a cluster.

Applied to the Castor moving group, this method results in an age of 200 ± 100 million years. And this should also be the age of Vega and Fomalhaut. In this way, we can now check whether the dust masses in the circumstellar discs decrease with increasing age. As Fig. IV.20 shows, this does actually seem to be the case. Accordingly, these discs disintegrate within several hundred million years. They then attain a state in which the destruction and supply are in equilibrium, and an unchanging, low-mass disc has become established, as can be observed in the case of the Sun at present.

The Bar Structure in the Interior of the Milky Way

Over the last ten years, a series of astronomical investigations has reinforced the suspicion that the Milky Way system belongs to the barred spiral galaxy type. But since the solar system lies within this galaxy, it is extremely difficult to determine the structure, size and orientation of the bar. Thanks to the European astrometry satellite, HIPPARCOS, it has been possible to measure the velocity distribution of many stars in the vicinity of the Sun. The structure of this distribution can be explained by the influence of the galactic bar, whose rotation period is accordingly half as long as the period in which the Sun orbits around the galactic centre.

In the classification scheme originated by Edwin Hubble, a distinction is drawn between two types of spiral galaxies. In the normal types, the spiral arms directly adjoin a central area which is more or less strongly defined. In the bar spirals, the centre is crossed by a wide bar consisting of gas and stars. The spiral arms adjoin it almost vertically (Fig. IV.21). Investigations in the optical spectral range show that there is a bar in about 30 % of all spiral galaxies. There is no conclusive explanation of how these structures are formed. They evidently represent disruptions in the disc, which could arise due to external influences such as the gravitational effect of a nearby galaxy, or equally because of processes in the interior.

The bars exert a strong influence on the evolution of a galaxy. The rotation of the bar (as a rigid structure) is superimposed on that of the disc, which results in a redistribution of matter and angular momentum. In specific terms, matter reaches the centre from the outer areas. At the centre, the large matter flows can trigger the formation of stars, or they may also »feed« a central black hole.

In the interior of the Milky Way, radio-astronomical investigations have revealed an asymmetrical velocity distribution for the neutral hydrogen. This led to the conclusion that a galactic bar was exerting an effect. Analyses of the surface brightness in the near infrared also suggested a structure of this sort. This bar could then be responsible for a flow of matter which has been observed, of the order of 0.01 solar masses per year, coming from the outer areas and flowing into a region at a distance of 500 light years from the galactic centre. Previous observations indicated a bar which extends over an area at an approximate distance of between 300 light years and 10,000 light years from the centre of the Milky Way.

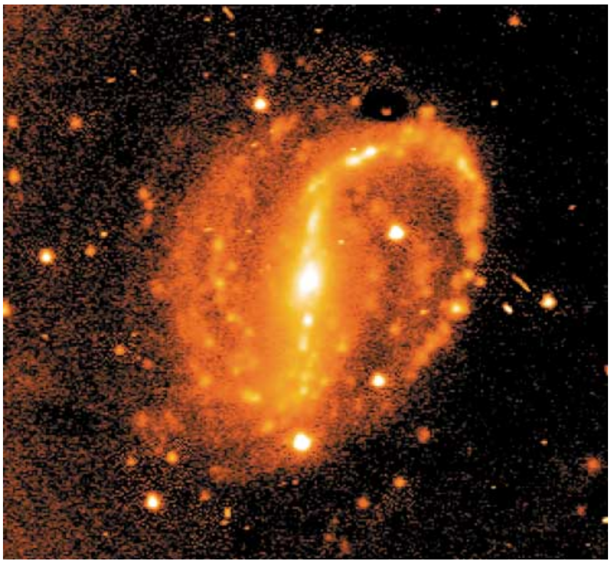

Fig. IV.21: NGC 7479, a typical barred spiral galaxy.

Galactic Bar Explains HIPPARCOS Data

A new chance to learn more about the galactic bar has now been offered by the star catalogue of HIPPARCOS, the astrometrical satellite. From its data, astronomers at the MPIA selected a set of more than 14,000 stars in the solar environment, avoiding selection effects which would have caused systematic errors in the analysis. For these stars, HIPPARCOS only determined the distances and intrinsic motions, but not the radial velocities, and so the three-dimensional velocity vector of individual stars cannot be reconstructed. Nevertheless, with the help of a statistical procedure, it has been possible to determine the distribution of the stars through the three velocity components u, v, and w (these are the components of the velocity in the direction of the galactic centre, in the direction of rotation and in the direction of the galactic north pole, i.e. perpendicular to the disc). The velocities are referred to the local standard of rest, the origin of which is the Sun.

For the 6,000 or so red-coloured stars, most of which are old, this distribution surprisingly shows a marked dual split (Fig. IV.22). Most stars are to be found in the upper area (red ellipse). As well as our Sun, this area also contains several well-known star clusters such as the Pleiades and the Hyades. Hence the velocities of these stars which are distributed over the entire sky do not deviate greatly from that of our Sun. Below this area, we find an area (blue ellipse) in which only 15 % of all stars are located. Its characteristic feature is an average negative velocity component u. So these stars are moving less in the direction of the galactic centre than away from it.

As opposed to the group with the low velocities (red ellipse), no blue-coloured stars, i.e. primarily young stars, are to be observed in this group (blue ellipse). This rules out the usual explanation of structures of this sort as indications of a young star cluster. The idea of a star cluster falling in from the halo of the Milky Way is also very improbable, and it cannot explain the observed metal abundances in the stars concerned. As astronomers from the MPIA have been able to demonstrate, the diagram can be explained quite naturally by the effect of the galactic bar.

For this purpose, it is necessary to consider the dynamic effects of a bar on the motion of the stars. They occur with particular clarity at so-called resonances, and they can be understood as follows: the stars orbit around the centre on epicyclical paths (Fig. IV.23). A path of this sort can be represented by two components: a large, circular one around the centre, described by the orbital frequency Ω_φ, and another smaller elliptical path whose central point is moving along the large circle. This is designated as Ω_r. The superimposition of these two components of motion results in an epicyclic path. Now, resonances may occur between the angular velocities of these path components and those of the bar Ω_B. One resonance of this sort is the outer Lindblad resonance:

$$\Omega_B = \Omega_\varphi + {}^1/_2\, \Omega_r .$$

A star whose orbital parameters fulfil this condition moves around the centre in phase with the bar. This means that after each complete orbit on its ellipse, the star is at the same point again in relation to the bar. As a result of this, this star is always influenced by the gravitation of the bar at the same point on its orbit, and is pushed onto another orbit. In this way, it can assume the observed high velocity component u in the direction of the galactic centre.

The dual division determined with the help of HIPPARCOS can also be explained in qualitative terms if the orbit of the Sun lies somewhat beyond the outer

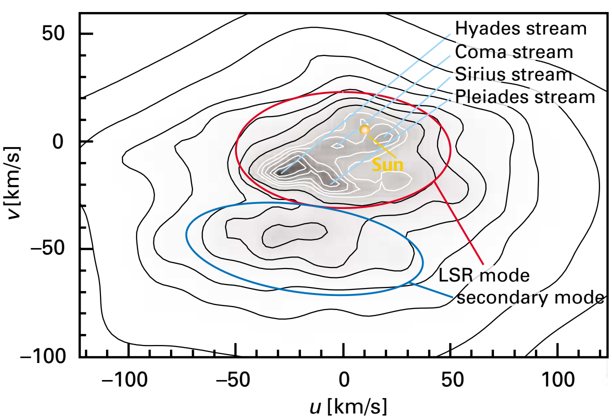

Fig. IV.22: The velocity distribution of 6000 red stars in the solar environment, determined with HIPPARCOS. The position of the Sun is centered at $v = 5$ km/s und $u = 10$ km/s.

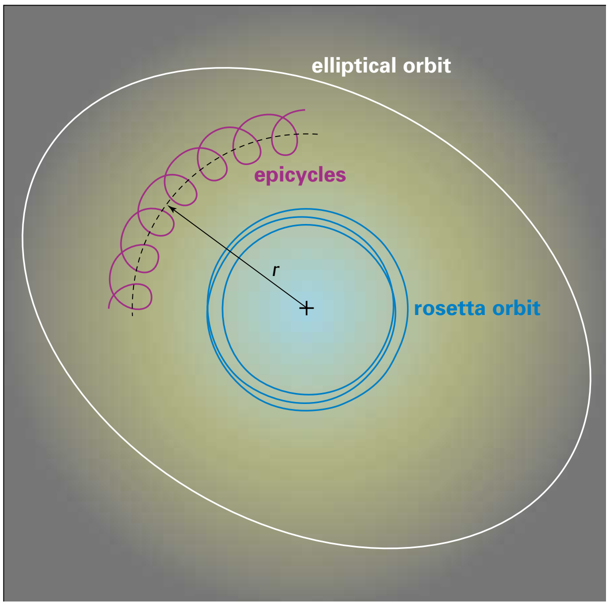

Fig. IV.23: Illustration of epicyclic stellar orbits in spiral galaxies.

Lindblad resonance. In this case, the depletion of the stars between the two areas (red and blue ellipses in Fig. IV.22) attests the presence of orbital paths which lie precisely on the outer Lindblad resonance. The measured velocity component *v* of this depletion, amounting to approximately –13 km/s, suggests an outer Lindblad resonance about 3000 light years within the orbit of the Sun.

In order to arrive at a more accurate determination of certain physical parameters relating to the galactic bar, a numerical model was calculated in which consideration was given to the fact that the outer Lindblad resonance – that is to say, the borderline between the two velocity zones – depends on four variables:

- the distance of the Sun from the outer Lindblad resonance
- the angle φ between the line connecting the galactic centre with the Sun and the longitudinal axis of the bar
- the rotatonal velocity of the stars around the galactic centre, and
- dthe form of the rotation curve of the Milky Way.

The numerical models assumed a bar which moves in the interior of an initially axisymmetrical disc, whose material density decreases exponentially from the centre outwards. Using reasonable parameter values, this model partially gave a very good reproduction of the observed velocity diagram from the HIPPARCOS data (Fig. IV.24). The best matches between the model and the observation were found for the case where the Sun orbits beyond the outer Lindblad resonance. Following this, models were calculated in order to determine the

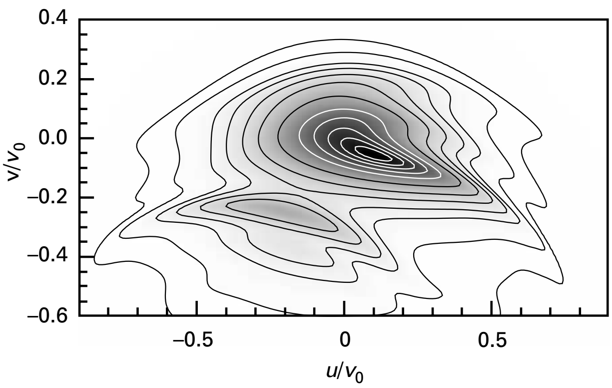

Fig. IV.24: One of the models calculated at MPIA, explaining the double split of star velocities due to the influence of a galactic bar.

angular velocity of the bar Ω_B and the distance of the Sun from the outer Lindblad resonance ΔR. For this purpose, the angle φ was varied between the currently accepted values of 15 and 45 degrees, and four different distances of the Sun from the galactic centre R_0 and corresponding orbital velocities v_0 were assumed. In this instance, it emerged that the values for Ω_B and ΔR did not depend too greatly on these parameters.

For the current standard values, R_0 = 8 kpc (26,000 light years) and v_0 = 227 km/s, this yielded an angular velocity for the bar of 53 $\pm$ 4 km s^{-1}/kpc, and the outer Lindblad resonance is approximately at a distance of 7.4 kpc (24,000 light years) from the galactic centre. Accordingly, the bar must rotate in the zone of the outer Lindblad resonance at an orbital velocity of 392 km/s, making it twice as fast as stars orbiting there.

Consequently, these simulations prove that the velocity distribution of the stars which has been observed with Hipparcos can be explained in a natural way by the effect of the gravitational force of the galactic bar. The physical parameters of this structure should be determined even more accurately in the future with the help of improved modelling.

CADIS Supplies Knowledge of the Structure of the Milky Way

For some years, astronomers at the Institute have been working on the Calar Alto Deep Imaging Survey, CADIS (see 1997 Annual Report, p. 18). This long-term project involves imaging of an area of the sky covering one third of a square degree in about 40 wavelength ranges, with the aim of searching for the youngest and most remote galaxies. During the automatic evaluation, however, numerous stars are also discovered and classified. This data material reveals information of hitherto unique sensitivity about the structure of the Milky Way and the luminosity function of the stars. In a first interim report, the CADIS Team describes how it has found a stellar population outside the classical region of the galactic disc, in the so-called »thick« disc. Moreover, the investigations contradict the supposition that the number of stars decreases as from an absolute magnitude of about 12 mag.

CADIS, the Calar Alto Deep Imaging Survey, is a programme set up for at least five years, with which astronomers from the MPIA search for the protogalaxies in the universe (see 1997 annual report, p.18). For this purpose, they photograph several selected fields of the sky with areas of 100 to 150 square arc minutes each (corresponding to one quarter of the area of the full moon) through a series of colour filters. 10 % of the total annual observation time on the 2.2 and 3.5 metre telescopes is made available for this ambitious project.

As well as a large image field, the CADIS images have two other decisive advantages: one is that the photometric images have virtually spectroscopic quality on account of the large number of colour filters used, and the other is that the long exposure periods of several hours mean that even very faint objects are visible. The data already available can therefore be used not only for the search for the youngest galaxies; they are also ideally suitable for identifying and classifying stars, and hence for the study of the structure of our Milky Way system.

The Structure of Our Galaxy

Modern mass distribution models of our galaxy take account of several components which differ from one another in terms of dynamics and the average age of their stars. Accordingly, the central area contains the flattened central bulge (thickening) with a diameter of 16,000 light years, at whose centre is the core with a diameter of about 500 light years. Adjoining the bulge is the disc, with a diameter of about 100,000 light years. This primarily contains young stars. Their mass density reduces not only radially, from the centre outwards, but also perpendicularly upwards and downwards from the central plane, on an exponential basis.

In recent times, it has been realized that another thick disc exists as well as this thin one. It has a similar radial extent to the thin disc, but it has a considerably greater scale height of about 3000 light years perpendicular to the disc plane. The stars it contains rotate at about 40 km/s less than those in the thin disc, and they are rather older. It is estimated that the thin disc contains about ten times more stars than the thick one. However, many questions remain to be clarified here. For example, there is discussion about the scale height of this component (decline of star density to 1/e), its absolute star density and also its origin.

The disc is surrounded by an almost spherical halo with a radius of about 70,000 light years. This includes the spherical star clusters as well as individual stars. Above and beyond this, the astrophysicists suspect the presence of dark matter in the halo, perhaps with ten times more mass than the stars, gas and dust nebulae together.

Classification of 300 Stars

The images of the two fields at 9^h and 16^h right ascension have been obtained at the 2.2 metre telescope of the Calar Alto Observatory with the CAFOS focal reducer, and at the 3.5 metre telescope with the MOSCA camera and the Omega Prime near infrared camera. Images have been obtained through ten filters; for the star classification, however, it was sufficient to use images in three filter ranges around wavelengths of 461 nm (blue), 649 nm (red) and 815 nm (near infrared). The exposure times were between 30 minutes and 8.5 hours. Since the fields of the sky are located at high galactic latitudes, extinction due to interstellar dust is negligible.

The images of the two fields of the sky contain about 10,000 objects. First, therefore, it was necessary to write a computer programme that could be used to separate the galaxies from the stars. This is done on the basis of the colour and the form (stars appear as points). Using spectroscopic re-observations of 245 celestial bodies selected at random, including 55 stars, it was possible to prove the reliability of this method: only one galaxy had been erroneously classified as a star. This means that the photometric data for 300 stars up to magnitude 23 are available – a unique dataset. The classification of the stars was carried out by taking the spectra of standard stars from a catalogue as reference and transferring them to the filters used on CADIS.

In this way, it was possible to classify about 300 stars with apparent magnitudes in the red of between 15.5 mag and 23 mag. In order to determine the spatial distribution of the stars, we need their distances. These are obtained by deriving the absolute magnitude from the measured apparent magnitude. This problem can be solved as follows: the astronomers may assume that all the objects are main sequence stars. An unambiguous relation between the colour and the absolute magnitude applies to these stars. Fig. IV.25 shows a colour-magnitude diagram of this sort, in which the difference in magnitude in the blue and red spectral ranges was selected as the colour. In this instance, an uncertainty arises because this relation refers to stars with solar element abundance. Since the blue stars in the halo of the Milky Way generally contain less heavy elements than the Sun, a correction of the main sequence is required for them. This consists of a shift to weaker luminosityes by about 0.75 magnitudes (dotted line in Fig. IV.25).

Thin and Thick Galactic Disc

The absolute luminosities obtained from the colours can now be converted into the distances (Fig. IV.26). We find two stellar populations whose boundary is located on a colour index (blue – red) = 0.7. The red stars ($b - r > 0.7$) are objects in the disc of the Milky Way and the other stars are mainly located in the halo. In the two fields of the sky, there were a total of 95 halo stars and 178 disc stars. This is about twice as many disc stars as were theoretically expected.

The distances could now be used to determine the density distribution of the stars as well. A point to be considered here was that the star count is only complete down to a specified minimum luminosity. After this correction, the star density was obtained in relation to the height above the galactic plane. If we first consider all the stars in the disc population only ($b - r > 0.7$ mag), we obtain a distribution as shown in Fig. IV.27. As the nearest stars in the CADIS catalogue are still 650

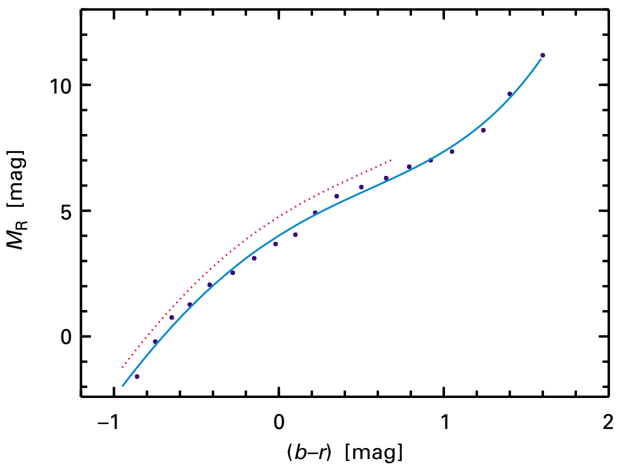

Fig. IV.25: Colour-magnitude diagram for stars with solar (continuous line) and sub-solar abundances of heavy elements.

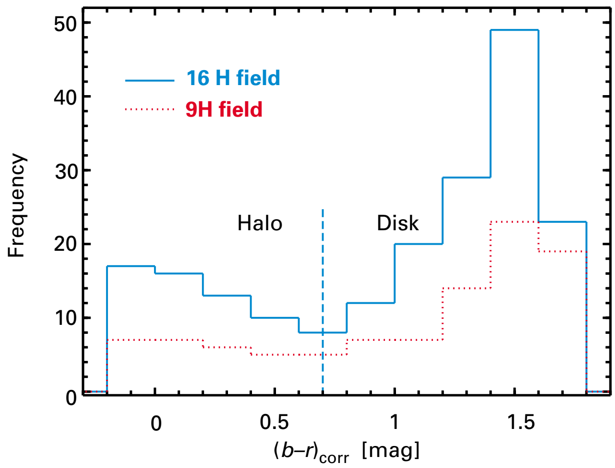

Fig. IV.26: The distribution of stars according to their colours reveals a double split into halo stars ($b - r < 0.7$) and disc stars ($b - r > 0.7$).

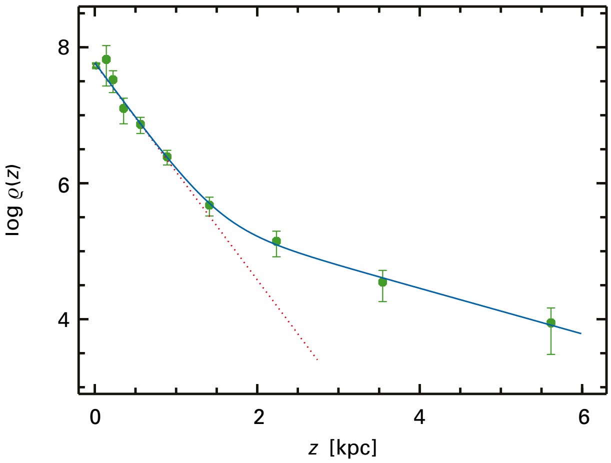

Fig. IV.27: Density of the disc stars in relation to their height above the Galactic plane in the 9h field. Broken line: fit to the thin disc; continuous line: fit to thin and thick disc.

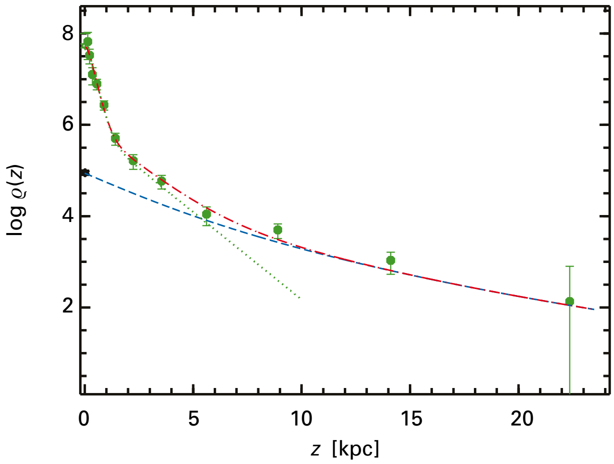

Fig. IV.28: Density of all stars versus height above the Galactic plane in the 9h field. Dotted line: adjustment for the disc; broken line: de Vaucouleurs profile; broken and dotted line: total of the two profiles.

light years away, the dataset was expanded by adding stars from the so-called Fourth Catalogue of Nearby Stars (CNS 4). This was compiled at the Astronomisches Recheninstitut in Heidelberg on the basis of HIPPARCOS data, and it contains stars up to distances of 65 light years from the Sun.

When the star density was being determined, the possibility arose to distinguish between disc and halo stars, and to differentiate the individual components more clearly. As a first step, the disc stars were considered on their own. As can clearly be seen in Fig. IV.27, there are two areas in the star density: up to a height of 5000 light years to 6500 light years (1.5 kpc to 2 kpc), the density distribution can be described with an exponential law (dotted line in Fig. IV.27). This is adjoined by a second distribution which follows an exponential law with a different gradient. The continuous line shows the superimposition of the two functions. These two star populations identify two components of the Milky Way system which have been under discussion for some time: the thin and thick discs.

The CADIS data now allow us to determine certain parameters for the thin and thick discs. For example, a scale height has been obtained for the thick disc of about 890 light years, placing the MPIA result exactly in the middle of the range currently under discussion, which is from 650 to 1000 light years. The scale height of the thick disc turns out to be about 4200 light years, which is within the range of present-day models.

The Halo

In a second step, the halo stars were now incorporated into the analysis as well. Fig. IV.28 shows the density distribution up to a distance of 70,000 light years above the Milky Way plane. Hence, even stars in the outer area of the halo were tracked down. However, the data suggest that the halo may possibly contain fewer stars than hitherto supposed. In any case, in relation to the number of halo stars, the CADIS study found twice as many stars in the disc as were predicted by present models.

The three components (thin and thick disc, halo) are clearly visible in Fig. IV.28 and they must be described by three different distribution functions, which again underlines the existence of the thick disc as an independent population. At hights of between 5,000 and 15,000 light years, it clearly dominates the star density distribution. Between 18,000 and 50,000 light years, the halo can be excellently described by a classic de Vaucouleurs profile. But within current error limits, a density drop with the third power of the distance would be possible. In this case, it is also possible to determine the spatial extent of the halo. The best fit turns out to be an ellipsoidal halo with an axial ratio of about 2 : 3.

The Luminosity Function

The luminosity function is a central astronomical variable. It describes the number of stars per luminosity interval, thus forming the empirical basis for the mass function (the number of stars per mass interval) and for the rate at which stars are formed. The shape of the luminosity function is known least accurately in the range of the faintest stars. A particular point in dispute at present is whether the number of stars actually does decrease as from an absolute magnitude of 12 mag, as (for example) was first deduced in 1998 from a study with the Hubble space telescope. The CADIS investigation was also able to supply a partial answer to this question.

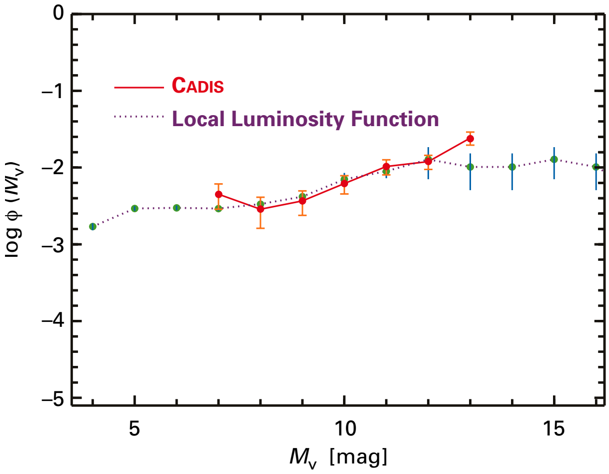

Fig. IV.29: Luminosity function of stars from the CADIS study (continuous line) and of stars close to the Sun from CNS 4 (dotted).

In order to be able to use a homogeneous and complete group of stars for the analysis, the researchers only chose members of the thin disc at distances of up to 5,000 light years. The luminosity function determined from the two fields of the sky is shown in Fig. IV.29. In the range of the stars of 8th to 12th magnitude, an excellent match is apparent with the stars from the CNS 4 (dotted line), which reinforces confidence in the CADIS data and their evaluation. Then, however, the distribution obtained from the CADIS data continues to rise as far as the 13th magnitude, in contrast to that of the CNS-4 stars. This result also contradicts the aforementioned study using the HST. In the range of faint stars, it is probably true to describe the dataset obtained from the CADIS study and the Hipparcos catalogue as the best luminosity function in the world at present.

The observed luminosity function can also be converted into a mass function with the help of an empirical relation. For a range of 0.2 to 1.1 solar masses, it then emerges that the number of stars per mass interval increases in approximately inverse proportion to the mass.

Only the Beginning

This analysis is based on a quarter of all the CADIS data. The researchers ultimately hope to have a catalogue at their disposal containing 1200 stars up to an apparent magnitude in the red of 23.5 mag. By then, standard spectra should also be available for main sequence stars with low element abundances, which will lead to an improved classification of the halo stars. By then we should be able to measure the scale heights of the thin and thick discs or the shape of the halo more accurately. And, in particular, it should be possible to determine the luminosity and mass functions down to the 14th magnitude.

IV.2 Extragalactic Astronomy

Random Sampling with ISO Provides an Important Catalogue of Galaxies

In connection with a serendipity survey, the ISOPHOT camera developed at the MPIA has been used on the ISO infrared satellite to research a section of the sky in the far infrared range. In the current years, the astronomers will be able to use this unique dataset to compile a catalogue that will probably contain more than a thousand galaxies and an as yet unknown number of cold dust clouds in the Milky Way. In the reporting year, it has been possible to publish a first partial catalogue containing 115 galaxies. It became apparent that practically all spiral galaxies contain large quantities of cold dust which had remained undiscovered until now. The mass of this dust is 10^6 to 10^9 solar masses. This exceeds previous estimates based on observations with the IRAS satellite by factors of two to ten. ISO has therefore made it possible to track down a significant dust component.

ISO, the European infrared observatory, was launched on 17.11.1995 and it operated faultlessly until April 1998. In almost 29 months of observing time, astronomers carried out some 26,000 individual observations with ISO. ISOPHOT, one of the scientific instruments, was built under the direction of the MPIA in cooperation with Dornier Satellitensysteme GmbH, DASA and the Carl Zeiss company. Unlike its predecessor IRAS, ISO observed selectively targeted infrared sources. Moreover, ISOPHOT extended the covered wavelength range up to 240 µm, detection sensitivity was increased one hundred times, and high-resolution spectroscopy and polarimetry of very faint sources was also made possible for the first time.

First Catalogue of Galaxies

Since ISO was used to investigate individual objects, the instrument had to be shifted from one position in the sky to the next during the observations. In order not to waste the slew time, the C200 camera of ISOPHOT was switched on during the shift, providing scans of the entire sky with a width of about three minutes of arc, in the infrared range at 170 µm – a wavelegth range in which observations had never been carried out prior to the ISO mission. This new method makes it possible to detect point-like and extended sources. Thus, during 12,000 slews throughout the entire mission it was possible to make use of about 550 extra hours, corresponding to five per cent of the total observation time. During the course of the ISO mission, the satellite scanned an area of 150,000 degrees in the sky, corresponding to a coverage of about 15 % of the sky.

In order to incorporate an object in the galaxy catalogue, three selection criteria had to be met (among other requirements): the signal-to-noise ratio had to be greater than 5 in all the pixels of the detector; the object had to be at least 15 degrees from the dust-rich Galactic disc, and it had to be croß-identified in existing galaxy catalogs.

The result is a catalog comprising 115 galaxies, in which all galaxies with redshifts of more than 0.005 (corresponding to distances of more than about 100 million light years) are listed with precise positions, distances (redshifts), and optical brightnesses from earlier studies. In addition, the absolute infrared fluxes at a wavelength of 170 µm, measured by ISOPHOT, are listed. This hitherto unique dataset allows some far-reaching statements about cold dust in galaxies.

Cold Dust in Spiral Galaxies

In the spiral galaxies, which also include our Milky Way system, about 90 % of the total visible matter takes the form of stars. The interstellar gas accounts for just about 10 %, while the dust only contributes 0.1 %. Nevertheless, the dust component is very important since it makes a highly effective contribution towards the galaxy's energy radiation: dust particles absorb the stellar light at short wavelengths causing them to heat up and radiate in the long-wave infrared range. In this way, the dust shields the interior of large clouds against high-energy stellar radiation, and molecules can form under the protection of the absorbing dust. As has been known for a long time, new stars are formed in the interior of large clouds of molecules.

But the existing infrared telescopes only made it possible to see the relatively warm dust with temperatures above about 20 Kelvin. With ISO, dust at temperatures as low as about 12 Kelvin became visible for the first time. Only recently, astronomers at the MPIA were able to use ISOPHOT to detect cold dust in the Andromeda galaxy and in its companion galaxy NGC 205 (see 1998 Annual Report, p. 68). It has also been possible to prove the presence of this hitherto unknown dust component in a few very close galaxies. However, it was unclear whether this cool matter is only present in a few galaxies, or whether it is in fact part of the »normal inventory«. The result of the serendipity survey provides a clear answer to this question: about half

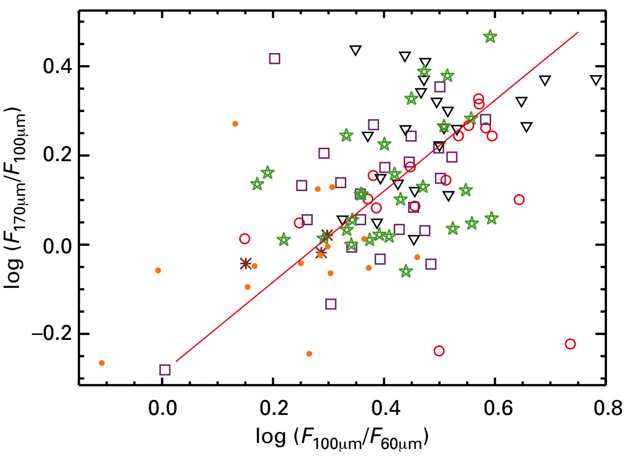

Fig. IV.30: The colour-colour diagram shows a linear correlation between the emission of warm and cool dust. All types of the galaxies shown here behave identically: open stars = normal spiral galaxies, open circles = type Sa, triangles = type Sab, squares = Sb, stars = irregulars, dots = not classified.

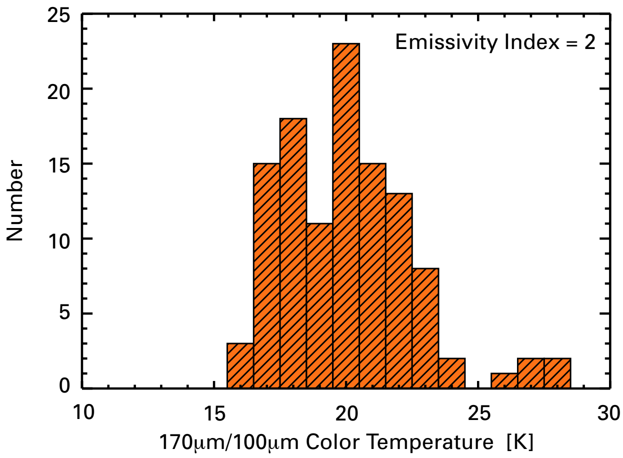

Fig. IV.31: Temperature distribution of the dust in the various galaxies.

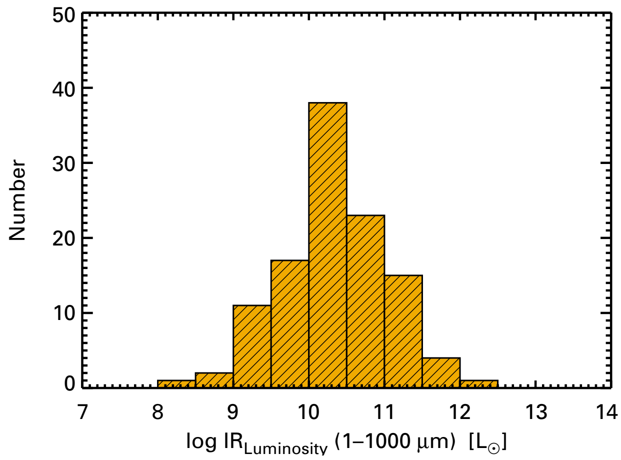

Fig. IV.32: Infrared luminosities of the dust in the various galaxies.

of all registered galaxies contain significant quantities of dust at temperatures below 20 K, while rather warmer dust could be detected in the other half.

The data can be used to compile a colour-colour diagram showing the flux ratio 170 µm/100 µm (cold dust) against the ratio 100 µm/60 µm (warm dust) (Fig. IV.30). If both variables are plotted logarithmically, a linear relation is obtained with a slope of about 1. This means that the intensity ratio of the radiation of cold and warm dust remains constant, while the intensities themselves vary within a factor of 8.

Interestingly, it is evident that all types of spiral galaxies fulfil this relation equally – in marked contrast to the situation at shorter wavelengths, where a clear separation had become apparent in 1986, with bar spiral galaxies showing stronger emission than normal spiral galaxies at a wavelength of 25 µm. This was attributed to an increased star formation rate due to the bar structure. Accordingly, it is conceivable that the cold dust component radiating at 170 µm is present in all galaxies to more or less the same extent, whereas the amount of warm dust depends on the current star formation rate.

The data shown in Fig. IV.31 make it possible to determine a temperature distribution for the dust, with some plausible assumptions about the physical behaviour of the dust particles. There is a relatively narrow distribution between 15 and 25 K. This solves a question which was still disputed until recently: all spiral galaxies contain a significant component of cold dust. Now, how large a proportion does it make up?

Assuming thermal emission, Planck's Radiation Law can be used to calculate the total luminosity of the cold dust for the wavelength range from the infrared to the millimetre range (1 to 1000 µm) (Fig. IV.32). This gives values of between 109 and 1012 solar luminosities. Hence the most luminous objects extend to the range of the ultra-luminous infrared galaxies (ULIRGs), whose total luminosity is dominated by the infrared.

Also on the basis of the luminosities the masses can be calculated (Fig. IV.33). They cover a range from 106 to 109 solar masses. This is higher by factors of two to ten than had been estimated using observations with the IRAS satellite. ISO has therefore made it possible to track down a significant dust component. Likewise, no difference between normal spiral galaxies and bar spirals is apparent in the mass distribution. Only two galaxies with less than 10^7 solar masses occur – and these are dwarf galaxies.

For about half of the galaxies in the ISOPHOT catalogue, radio observations are already available from which the masses of the molecular hydrogen can be deduced. This also makes it possible to determine the gas-to-dust ratios for these objects. In the Milky Way, this value is 160. For other spiral galaxies, the IRAS data had yielded very high values between 500 and 2000 which could not be explained. Now the situation has become

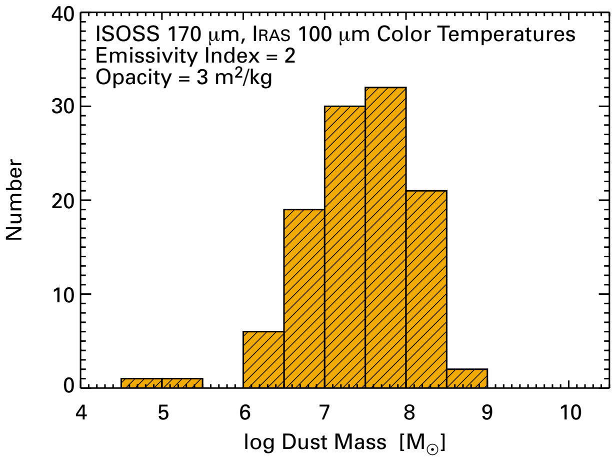

Fig. IV.33: The mass distribution of the dust in the galaxies

clear: IRAS had not recorded a large part of the dust emission at all. The new ISOPHOT data now lead to a broad distribution of the gas-to-dust ratio with values between 10 and 1000. However, the most frequent value is about 250. Taking into account of the uncertainties, this fits well with the »canonical« value that is valid for the Milky Way system. If this value is also valid in other spiral galaxies, it opens up the possibility of estimating the gas masses of the galaxies on the basis of the measured far infrared fluxes. This method was practised in the past, but with no knowledge of whether the value used for the gas-to-dust ratio even applied to any other galaxies. Now for the first time, the new ISO data create confidence in this procedure.

Nevertheless, the broad scatter of the data is remarkable, and it probably cannot be attributed solely to experimental uncertainties. Rather, the gas-to-dust ratio could vary with the chemical composition of the matter. Hence the higher the proportion of heavy elements is, the more gas might condense into dust. It would also be conceivable for the gas-to-dust ratio to depend on the star formation rate in the galaxy.

This ISOPHOT point source catalogue is only the start. In its final form, it will probably comprise more than a thousand galaxies, so that a series of questions can be approached on a systematic basis. At the same time, the group at the MPIA (in collaboration with astronomers from Budapest and Helsinki) will search the serendipity survey for slightly extended sources. These comprise very cold dust clouds, prestellar cores, globules and other objects in our Milky Way. This catalogue will include abundant information about young star formation regions.

When Dwarf Galaxies Lose their Gas

Dwarf galaxies are inconspicuous star systems. Edwin Hubble did not even know about them when he made his classification of galaxies. They are only a few thousand light years in size, their masses are from 10^7 to 10^{10} solar masses, and they are difficult to detect on account of their low surface brightness. The best-known examples are the Magellanic Clouds and M 32, a companion of the Andromeda Nebula. For a long time, it was not clear why dwarf systems in dense galaxy clusters contain less gas on average than those in less rich clusters. A theoretical study at the MPIA now proves that the hot intergalactic medium blows the interstellar gas out of most dwarf galaxies within a few billion years.

Dwarf galaxies are interesting research objects for a number of reasons. Nowadays it is considered certain that there are substantially more dwarf galaxies than large ones. However, their proportion of the total mass of the universe is not known because they are difficult to detect. Several types of dwarf galaxies are known today. The two most frequent types are dwarf irregular galaxies, which are irregular in appearence and usually gas rich, and dwarf elliptical galaxies that are gas-deficient. These properties resemble those of their more massive counterparts, the spiral and elliptical galaxies. Interestingly, this morphological difference only relates to the interstellar gas in the case of the dwarf galaxies. Observations have in fact revealed that elliptical and irregular dwarf galaxies have very similar stellar populations. This may allow us to conclude that these two types of dwarf galaxies possibly have a common origin.

How the two classes came into being has been the subject of a study lasting several years by the theory group at the Institute. Since dwarf galaxies have a substantially lower gravitation potential than their massive counterparts, supernovae are much more prominent features of the dwarf systems. These high-energy explosions whirl up the interstellar gas, leading to the diffuse appearance of the irregular dwarf galaxies, as the group was able to prove in 1998 (1998 Annual Report, p. 24).

In the simulations, however, the dwarf elliptical galaxies still contain a large amount of gas after ten billion years, while some of the observed systems no longer have significant gas reserves. The suspicion now arose that dwarf ellipticals were originally dwarf irregulars that lost their gas. Several years ago, it had already been discovered that dwarf galaxies in dense galaxy clusters contain less gas than those in extended clusters with sparse populations – a finding which is equally applicable to massive galaxies: in dense galaxy clusters, large galaxies lose gas as they move through the intergalactic medium at high speed. During this process, the intergalactic gas exerts high pressure on the interstellar gas in the interior of the galaxy, actually blowing it out. Since dwarf galaxies have a much lower gravitation potential than their larger sisters, this process of »ram pressure stripping« should proceed more effectively in their case. Using a numerical simulation, theoreticians at the MPIA in conjunction with colleagues from the University of Tokyo were hoping to discover the extent of the influence of such an intergalactic wind on the evolution of dwarf galaxies

Dwarf Galaxies in the Particle Wind

Present-day models of the origin of galaxies assume that the gas in the interior of the dwarf galaxies was very hot in the early universe. Two mechanisms may be responsible for this phenomenon: other young galaxies with strong star formation that were emitting intensive UV radiation, and supernovae that were heating up the surrounding medium due to UV radiation and particle winds. However, the cause is irrelevant to the models. The decisive factor is the general assumption that dwarf galaxies originally contained hot gas in their interiors, held together by an extended, massive halo made of dark matter. It was possible to detect the halos made of dark matter due to their gravitational effect (1997 Annual Report, p. 73). In the dwarf galaxies, they may account for 95 to 99 % of the total matter, so that they dominate the dynamic behaviour of these systems. The spatial density distribution of the halo has also been represented by a model produced at the MPIA. It was further assumed that the hot gas in the interior is in hydrostatic equilibrium corresponding to its temperature, which also justifies the assumption of an initially spherically symmetrical distribution.

For the simulations, three physical variables were varied within realistic limits: firstly, the speed at which a primeval dwarf galaxy moves through the intergalactic medium – the two values of 500 km/s and 1000 km/s were assumed here. Secondly, the density of the hot intergalactic medium at 10^7 K – this was selected between 10^{-3} and 10^{-5} particles per cubic centimetre. And thirdly, the mass of the halo made of dark matter – this was varied between 10^6 and 10^{10} solar masses.

Whether or not the interstellar gas is blown out of the interior of a dwarf galaxy during its movement through the intergalactic medium depends on whether the ram pressure, exerted when the two media collide, is stronger than the gravitational forces which hold the gas together. A simple analytical estimate already led to the suggestion that all galaxies of up to 109 solar masses lose their gas entirely within a few billion years.

The problem is complicated by instabilities which occur on the impact zone between the intergalactic and the interstellar medium. At first, so-called Kelvin-Helmholtz instabilities occur here. These are gas flows that (like convective flows) occur on the border layer between two liquids or gases that are moving against each other. They come from one of the two media and penetrate the border layer, playing a very major part in transporting gas from the interior of a dwarf galaxy into outer space. On the other hand, gas that is torn out of the galaxy on its windward side can flow around the galaxy and back into the interior on the rear. In order to include these processes as well, the ›gas stripping‹ was modelled numerically during the passage of a dwarf galaxy through the intergalactic medium.

Fig. IV.34 shows a simulation of this sort, using the example of a galaxy with 10^7 solar masses which moves at 1000 km/s through an intergalactic medium with a density of 10^{-4} cm-3. The time interval between the first and the last image is 90 million years, and the left column shows the density distribution with the pressure distribution in the right column. The arrows in the Figures in the right column indicate the direction of the gas flow.

When intergalactic and interstellar gas collide, a shock wave spreads out into the interior of the galaxy on the windward side, initially compressing the gas located there. At the same time, on the leeward side, a reverse shock is generated which migrates into the intergalactic medium. After about 40 million years (third figure), Kelvin-Helmholtz instabilities develop on the border layer. The interstellar gas is now pushed out of the galaxy by the ram pressure of the intergalactic medium, and the instabilities also contribute towards this process. Rayleigh-Taylor instabilities also occur (e.g. at $R = 0$, $z = 0.5$), but they do not develop very strongly because they are suppressed by the strong gravitational field of the galaxy. It can be clearly seen that the interstellar gas has been entirely blown out of the galaxy at the end of the simulation.

The second simulation in Fig. IV.35 shows the same conditions, except that the galaxy mass has been increased to 10^{10} solar masses. In this case, the whole time interval is about three billion years. At the outset, the conditions resemble each other, but since the gravitation potential is stronger in this case, the central pressure of the interstellar gas is greater and it withstands the ram pressure better. At first, only a slight depletion of the interstellar gas occurs due to incipient Kelvin-Helmholtz instabilities. However, the gas in the interior is compressed and it reacts to this by expanding laterally (perpendicularly to the flow – third figure). This increases the wind resistance surface, as a result of which the galaxy now loses more matter. Moreover, Rayleigh-Taylor instabilities are created. These lead downstream to the reverse flow of the gas into the interior of the galaxy, as already mentioned. Nevertheless, the galaxy loses about three-quarters of its gas in the course of a few billion years.

Fig. IV.36 shows how the gas content of the dwarf galaxies evolves in relation to the speed, the gas densi-

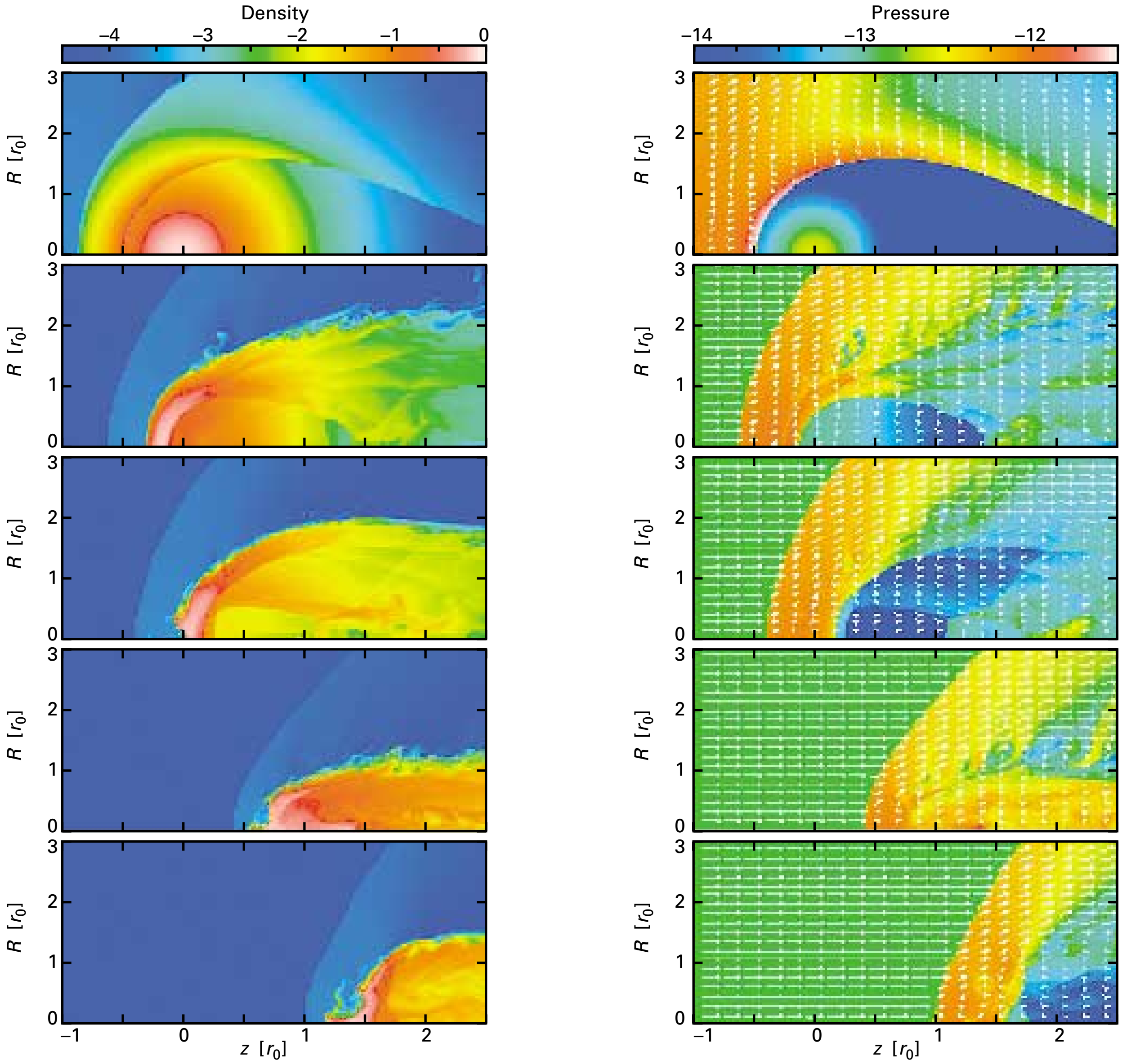

Fig. IV.34: Evolution over time of a dwarf galaxy with 107 solar masses which moves at 1000 km/s through an intergalactic medium with a density of 10^4 cm^{-3}. The density is shown on the left, the pressure and the gas movement on the right. The time intervals are: 5.6×10^6, 2.9×10^7, 4.6×10^7, 7.4×10^7 and 9.6×10^7 years.

ty of the intergalactic medium and the galaxy mass. It can be seen that all galaxies of up to 10^8 solar masses lose their entire gas reserves within one to two billion years. For more massive galaxies, the evolution depends on their speed and the density of the intergalactic medium.

In many galaxy clusters, it has been possible to determine the average density of the hot intergalactic gas with the help of ROSAT images. A good example of this is the Coma cluster. In this case, the gas density is 3000 cm^{-3}, whereas the average velocity dispersion of the galaxies is about 1000 km/s. According to the simulations, all the dwarf galaxies in the Coma cluster should have lost all of their gas within a few billion years. In reality, we find the gas-deficient dwarf ellipticals in the clusters and the more massive irregular dwarf galaxies outside them.

The simulations have shown that the ›gas stripping‹ plays a decisive part for dwarf galaxies in galaxy clusters. It would explain why these stellar systems contain less gas on average in dense galaxy clusters than they do in less intense clusters where the intergalactic gas also has very low densities.

This process must also have an effect on the chemical evolution of dwarf galaxies. During supernovae explosions, heavy elements reach the interstellar medium. This gas is initially hot. So that it can be incorporated into later generations of stars, it must first cool off and

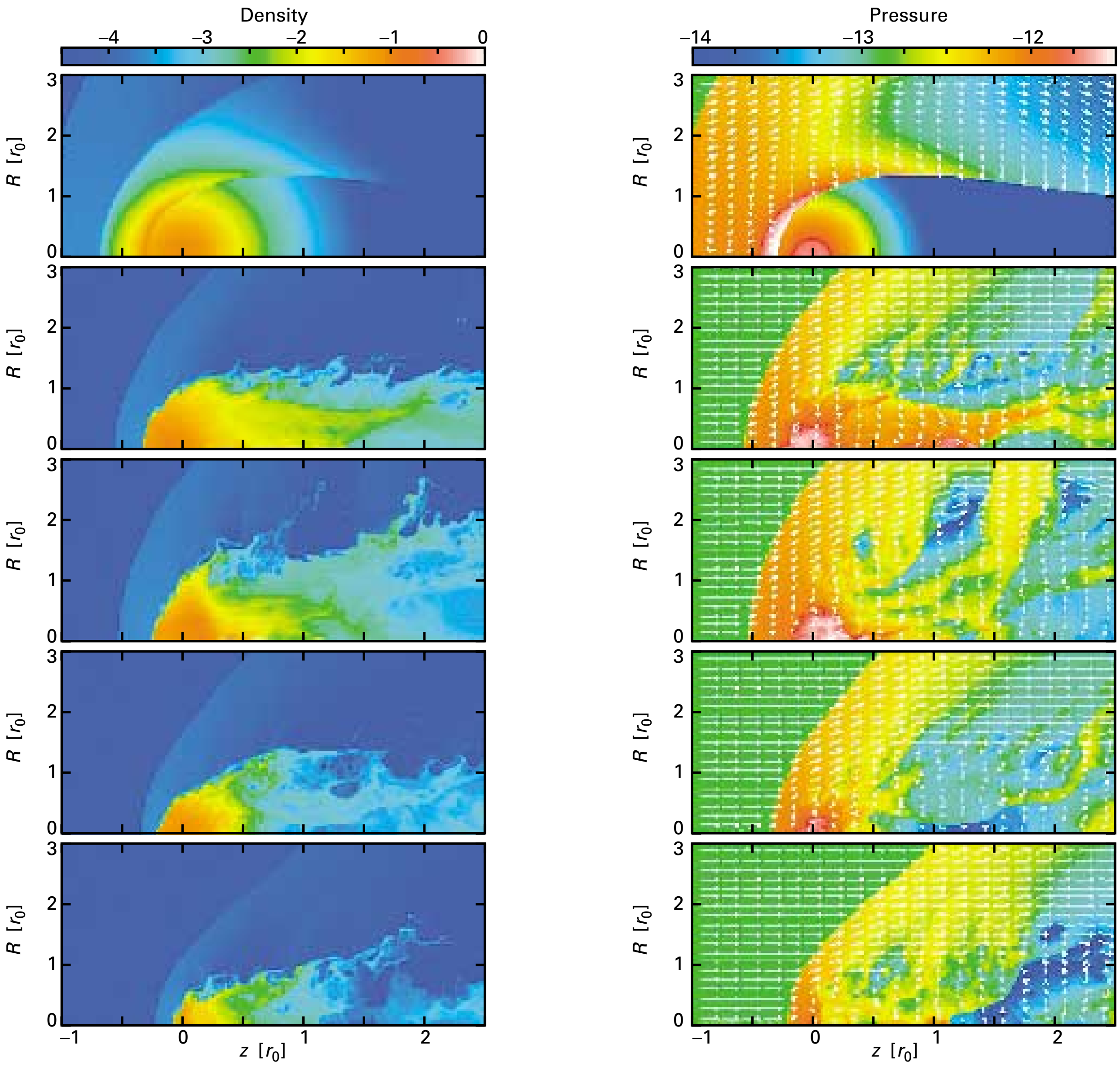

Fig. IV.35: Like Fig. IV.34, but with a galaxy mass of 1010 solar masses. Time intervals: 6.8×10^7, 7×10^8, 1.2×10^9, 2.2×10^9 and 3.3×10^9 years.

accumulate in dense clouds of gas and dust. According to the simulations shown, however, this process is impeded by the ›gas stripping‹. This means either that the enrichment of the interstellar medium with heavy elements took place very quickly in an early phase of galaxy formation, or else that the simulations neglected physical processes which delay the ›gas stripping‹ or even prevent it to some extent. The cooling of the gas could be a process of this sort. Radiation cooling is to be taken into consideration in future computer simulations.

How Spiral Galaxies Form Elliptical Galaxies by Merging

Until the mid 1980's, elliptical galaxies were considered to be rather boring stellar systems. Then, however, certain interesting characteristics were found: in their core areas, some elliptical galaxies contain gas and stars whose kinematic properties differ significantly from the other stars in the galaxy. In some cases, the core even rotates in the opposite direction to the rest of the galaxy. In the visible range, it was discovered that what appears to be an elliptical form in the interior of some of the galaxies is in fact slightly distorted. Boxy and disky isophotes were recognized. With the help of computer simulations, it was now possible to show that these two types can be explained by the fusion of spiral galaxies. The decisive factor in the shape of the elliptical galaxy that is created is the mass ratio between the two parent galaxies.

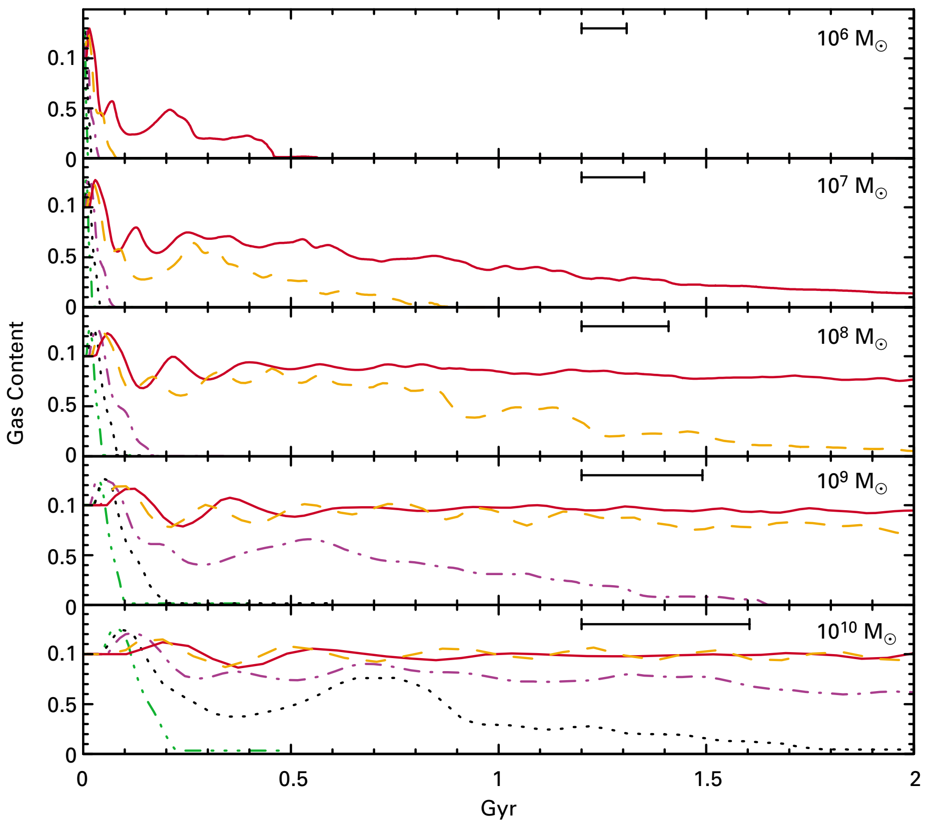

Fig. IV.36: Evolution over time of the gas content of dwarf galaxies between 10^6 and 10^{10} solar masses. The curves mean: dash-dot-dot-dash: $n = 10^{-3}$ cm^{-3}, $\upsilon = 1000$ km/s, dots: $n = 10^{-3}$ cm^{-3}, $\upsilon = 500$ km/s, dash-dot: $n = 10^{-4}$ cm^{-3}, $\upsilon = 1000$ km/s, dashes: $n = 10^{-4}$ cm^{-3}, $\upsilon = 500$ km/s, line: $n = 10^{-5}$ cm^{-3}, $\upsilon = 1000$ km/s..

Elliptical galaxies (Fig. IV.37) can be described by a triaxial form which resembles a rugby ball. Their degree of flattening depends on the angle from which the stellar system is viewed. If the observer looks in the direction of the longitudinal axis, then the galaxy appears to be circular, but from a perpendicular angle it seems very elliptical. Two types can now be distinguished on the basis of their luminosities. The first type comprises elliptical galaxies of low luminosity:

- they have an isotropic velocity field,
- they are flattened due to their marked intrinsic rotation,
- the velocities of the stars around the major axis of symmetry are low, and
- the isophotes (lines of identical brightness) in the interior deviate from the perfect elliptical form. They are elongated and rather disc-shaped or »disky«.

The second type are elliptical galaxies of high luminosity:

- They are flattened due to an anisotropic velocity distribution,
- they rotate slowly,
- they contain kinematically decoupled cores,
- the velocities of the stars around the major axis are high, and
- the isophotes are square or »boxy«.

Using some parameters that have been observed, Fig. IV.38 shows how elliptical galaxies of high and low luminosity differ from one another. Parameter a_4 describes the deviation of the isophotes from the elliptical form. Galaxies with $a_4 > 0$ have disky isophotes (open circles), and those with $a_4 < 0$ have boxy isophotes (filled circles). In general, disky elliptical galaxies rotate more quickly (higher υ/σ), have an isotropic velocity field (large $(\upsilon/\sigma))^*$), and they rotate less markedly around their large axis than boxy elliptical galaxies.

So far there have been several attempts to explain these differences. For example, it was assumed that elliptical galaxies are formed bs the merger of two spiral galaxies. Although this hypothesis was stated as long ago as the early 1970’s, detailed numerical simulations which included the spiral galaxies and their halos of dark matter were not possible until the end of the 1980’s. These showed that an event of this sort can in fact lead to a

Fig. IV.37: M 87 in the Virgo galaxy cluster is a typical elliptical galaxy.

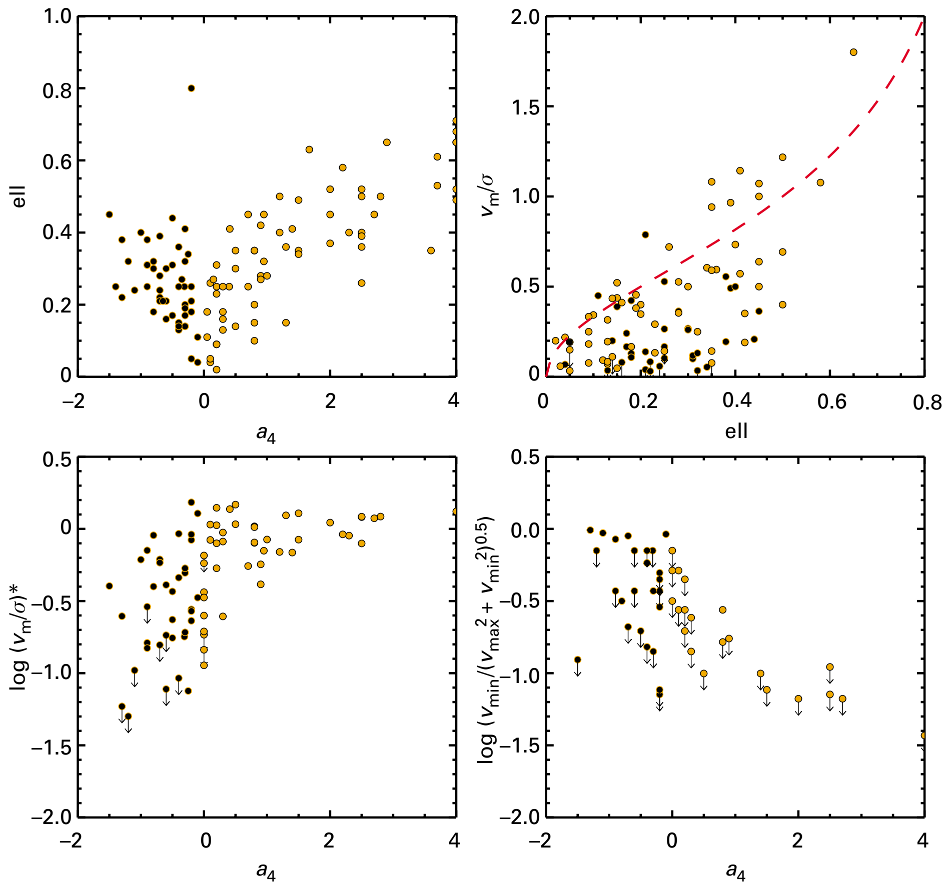

Fig. IV.38: Elliptical galaxies have various physical characteristics depending on their luminosity. Top left: apparent ellipticities of the galaxies towards a_4. Disky elliptical galaxies (open circles) have $a_4 > 0$, boxy elliptical galaxies (black dots) have $a_4 < 0$. Top right: the ratio of the rotation speed at the half-light radius (υ_m)) to the central velocity dispersion (σ) against the ellipticity. The broken line shows the values for a theoretical model of a rotating, isotropic and oblate ellipsoid. Bottom left: degree of velocity anisotropy $(\upsilon/\sigma)^*$ against a_4. Bottom right: strength of rotation along the minor semi-axis against a_4.

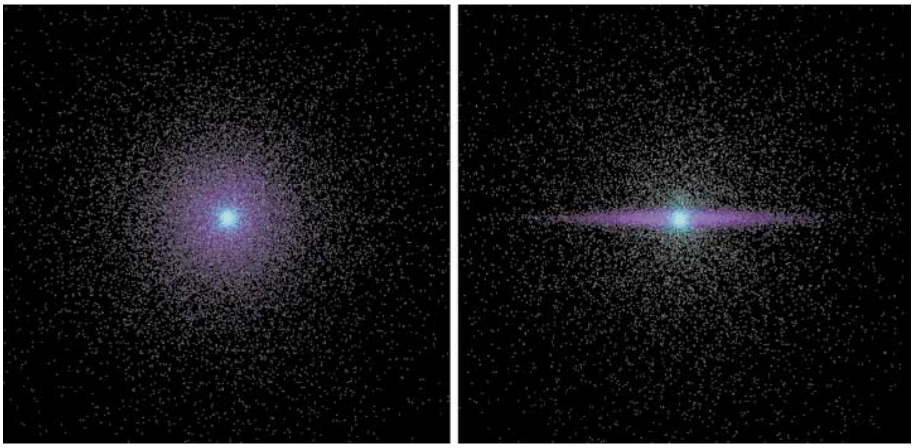

Fig. IV.39: Initial distribution of the test particles of a spiral galaxy prior to the start of a simulation.

slowly rotating, anisotropic spheroid system. Later work then attempted to explain the disky and boxy isophotes by suggesting that the elliptical galaxies formed by merging are merely viewed from different angles. However, this is contradicted by the observational fact that the two types have different characteristics in terms of radio and X-radiation.

Taking another approach, theoreticians suspected that the different gas masses in the original spiral galaxies lead to different isophotes in the elliptical galaxy that is formed. The behaviour of the gas component during the merging process can only be simulated with difficulty, so that this possible explanation could not be verified conclusively.

Fig. IV.40: Four steps in the fusion of two equally large galaxies to form an elliptical galaxy. The coloured lines show the orbits of the galaxies.

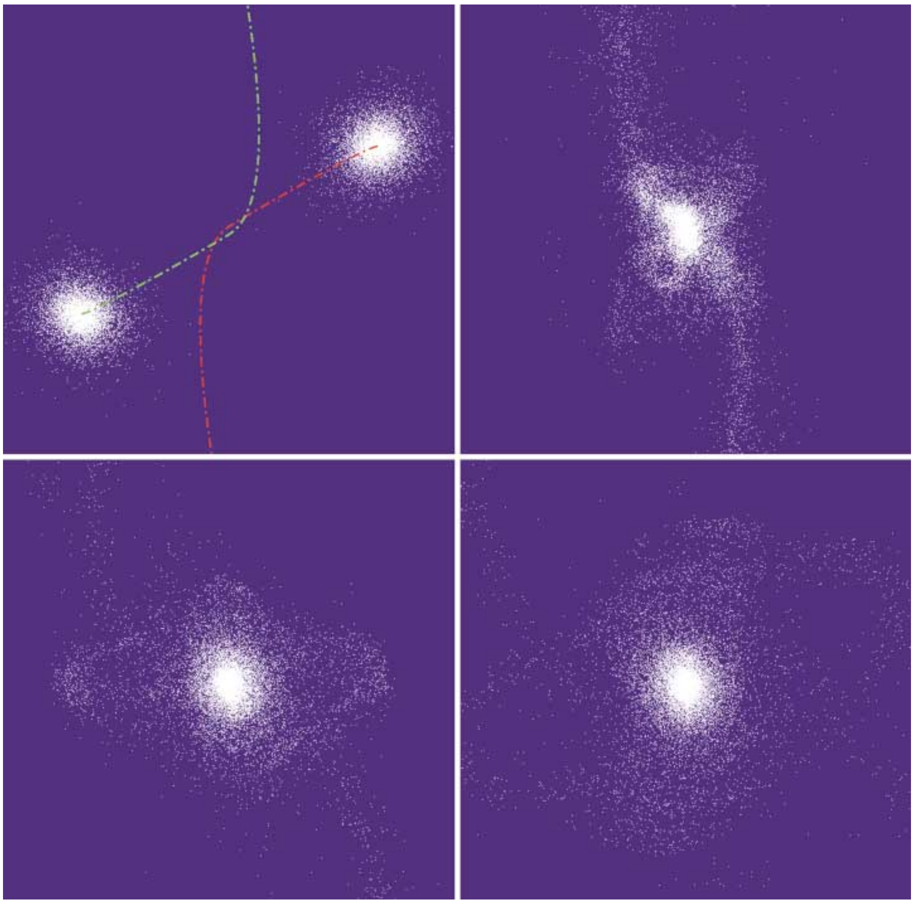

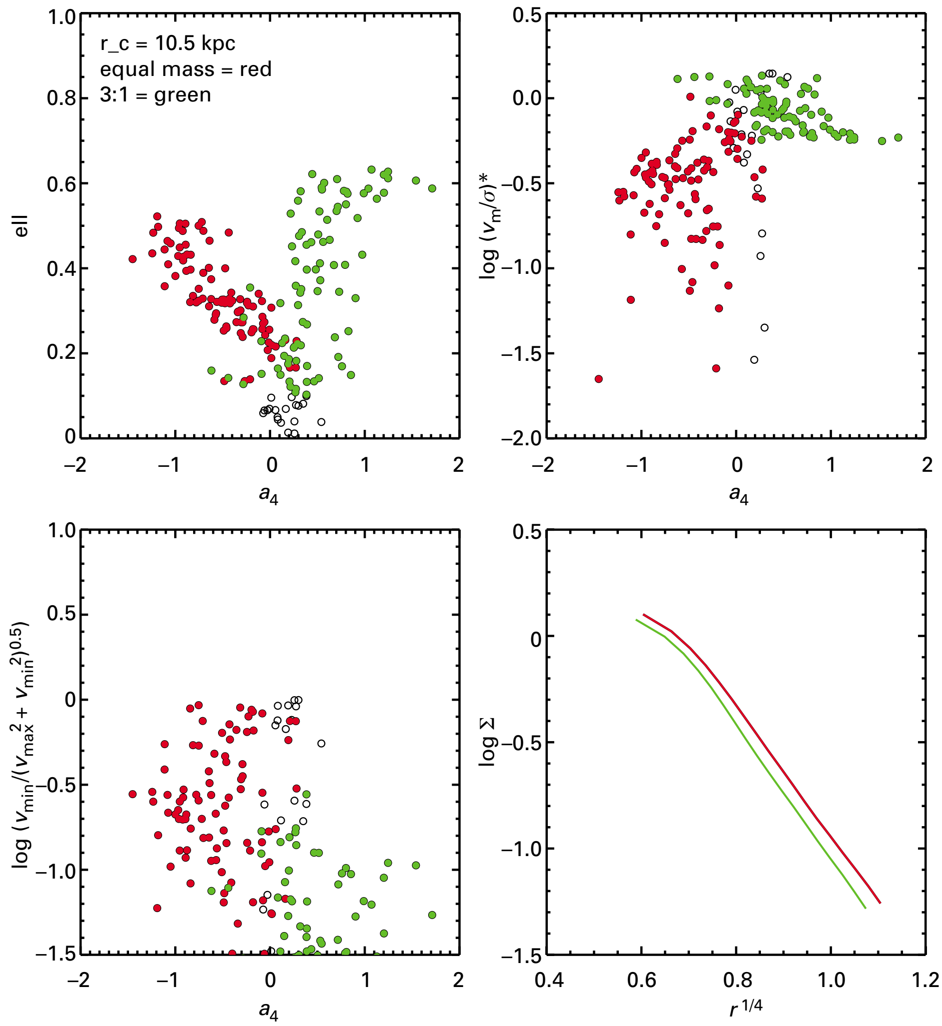

Fig. IV.41: Results of the model calculations compared with the observations. Three of the parameters discussed in Fig. IV.38 for the simulated galaxies. Bottom right: surface brightness of the simulated galaxies.

Astronomers at the Institute followed up another suggestion which is convincingly simple. According to this idea, luminous elliptical galaxies with boxy isophotes could be formed by a merger of two spiral galaxies of equal size, while the elliptical galaxies of low luminosity are formed with disky isophotes if a massive galaxy merges with one of low mass.

In order to test this hypothesis, two cases were simulated: one was the merging of two equally large spiral galaxies, and the other involved two spiral galaxies with a mass ratio of 3:1. The massive galaxies were each represented by 200,000 test particles, consisting of a central bulge (20,000 particles), a disc with an exponentially decreasing density profile (60,000 particles) and a spherical halo comprising dark matter (120,000 particles) (Fig. IV.39). In the case of the 3:1 model, the smaller galaxy contains one third of the quantity of particles. Only the dynamic behaviour of the particles was examined in the simulations. More complex processes in the gas component (compression, heating, star formation, etc.) were ignored.

Both systems approached one another on parabolic paths, and the two discs were inclined by 30 or –30 degrees relative to the orbital plane (Fig. IV.40). After the merging, an adequate period was allowed to expire so that the system that had been formed could be considered in a state of equilibrium. Then an »artificial image« was created to show how this galaxy would appear in a telescope.

In reality, the artificial system showed the external appearance of an elliptical galaxy, and the deviations of the isophotes from perfect ellipses were also present (Fig. IV.41). To investigate this more closely the average of 200 »observations« obtained from different angles of view was taken. The 3:1 model actually shows the disky isophotes and the 1:1 model shows the boxy ones. The numerically determined values match the actual figures very well. As in the case of the observations, the simulated galaxies with marked boxy or disky deviations also have the greatest ellipticity. Simulated disky galaxies are isotropic, and they only rotate slightly around their main axis. As with the observed ellipses, the surface brightness follows a $r^{1/4}$-law.

These simulations suggest that the two different isophote shapes that occur among elliptical galaxies can actually be explained by the fusion of two spiral galaxies, without having to consider the complicated interaction of the interstellar gas. This means a major simplification as compared with other models. However, it is known that in nearby colliding galaxies such as the Antennae galaxy, the gas very probably plays an important part in other aspects of a process of this sort. It is whirled up and locally condensed, so that star formation begins to be intensified. The extent to which these processes may possibly affect the inner form and dynamics of elliptical galaxies is to be shown by future simulations.

Dust in quasars

Quasars are compact galaxy cores with immense luminosities. Since they always appear as points in images of the sky, their inner structure is still a matter of great uncertainty. Their formation and evolution are also largely unknown. With ISOPHOT, astronomers at the MPIA have carried out infrared investigations on the question of whether all quasars contain significant quantities of dust, or whether there are dust-free quasars which might be at a later stage of evolution. In actual fact, the new data suggest that the quasars are surrounded by large dust masses. If we follow classical models, the activity of the suspected black hole in the centre of many of these celestial bodies is not sufficient to explain the far infrared emission. There must also be some extremely active star formation areas, of the sort which are also found in colliding ultra-luminous galaxy systems.

The discovery of the quasars at the start of the 1960's was a real sensation. Until then, no celestial bodies with such high spectral redshifts were known. Initially, there were disputes as to how the redshifts should be interpreted. The nature of the quasars was also discussed for a long time. Nowadays, the opinion prevails that these are extremely luminous cores of galaxies which are up to ten billion or more light years away. In a region which is probably not all that larger than our planetary system, these celestial bodies generate up to 10^{15} solar luminosities, making them as much as several tens of thousands of times brighter than whole galaxies. This means that they are visible at great distances.

The »central engine« is assumed to be a massive black hole which sucks up surrounding matter; this then heats up and emits the intense radiation. Quasars are considered to be the most luminous members of the larger group of active galactic cores. This group also comprises so-called starburst galaxies, in which large star formation regions contribute towards the total emission.

The classical Palomar-Green catalogue contains 114 quasars that were identified in the green wavelength range at the Palomar Observatory during the 1980's. Only about 20 % of these so-called PG-quasars could be detected in the infrared with the IRAS satellite (1983). ISO offered far higher sensitivity than IRAS. For this reason, together with colleagues from the Heidelberg State Observatory, the Max Planck Institute of Radio Astronomy, Bonn, and the Astronomical Institute of Bochum University, astronomers at the MPIA observed a random sample of 17 quasars in the wavelength range from 4.8 µm to 200 µm with ISOPHOT. In addition, there were observations at 1.3 mm by the German-FrenchInstitute of Millimetre Wave Radio Astronomy (IRAM). The random sample comprises a large redshift range from $z = 0.06$ to $z = 2.04$, i.e. distances of8×10^8 up to 77.7×10^9 light years (calculated for a Hubble constant $H_0 = 70$ km s^{-1}/Mpc and an acceleration parameter $q_0 = 0$).

Of the 17 quasars 14 could be detected with ISO. In view of the random choice of the sources, this detection rate of about 80 % is tremendously high. Only three sources remained below the detection limit, and these are located in regions of the sky with an especially bright Galactic foreground. In cirrus-free regions, detection of dust emission would probably have presented no problems with ISO. At a wavelength of 1.3 mm, ten quasars were measured with IRAM. For the first time, this provides extensive infrared data for a consistent random sample of optically selected quasars.

Black Holes and Star Forming Regions

The form of the spectral energy distribution makes it clear that the observed infrared radiation really does involve the thermal emission from dust, and not the synchrotron emission from electrons in magnetic fields which has also been discussed until now: the measured intensity rises from the optical up to the far infrared, reaching a maximum in the range from 50 to 100 µm (Fig. IV.42). Beyond 100 µm, the spectrum falls sharply to very low values as far as 1.3 mm. This underlines the importance of the new data, which have closed a data gap that existed until now, especially in the extreme far infrared. The radiation originates from thermally emitting dust whose temperature is in the range between 20 and 120 K. At shorter wavelengths, warmer components with temperatures of up to 1000 K can also be detected. This large range of dust temperatures supplies valuable clues about the possible distribution of the interstellar matter in the quasar.

On optical images from the ground, quasars appear as points, so that no spatial details can be seen. American researchers used the Hubble space telescope to observe some of the particularly close PG quasars, including the quasar PG 0052+251, which also appears in the Iso random sample with a redshift of $z = 0.155$. On this high-resolution image, it can be seen that the quasar is located in a spiral galaxy with a ring of bright nodes which are probably hot, young star forming regions (Fig. IV.43).

This already suggests that in at least some of the observed quasars, star formation plays a major role. This hypothesis is also supported by the new infrared observations: classical models actually indicate that the radiation generated in the central area may be able to heat up the nearby dust to high temperatures, but that it does not transport sufficient energy into the more remote cool areas. For example, a thick dust disc surrounding the central black hole would explain the emission in the near and mid infrared, but not the excess in the far infrared. If we wish to interpret this exclusively as heating due to a central source, we must either assume very special (and in some cases physically rather implausible) dust distributions, or else very different models need to be developed.

For example, if the active galactic core is surrounded by a very non-homogeneous, »clumpy« dust disc, high-energy X- and UV-radiation could find its way through the gaps into the cooler outer areas, where it could cause large dust masses to shine in the far infrared. However, the starburst hypothesis in particular (see below) is impressively elegant as an alternative explanation for the far infrared excess.

On closer analysis, interesting differences emerge in the form of the energy distributions. In rough terms, three groups can be formed (Fig. IV.42):

- Group 1: intensity rise from the near IR to the far IR according to a power law. This distribution could be created by dust which is warmed from a central course, and whose temperature decreases as the distance increases. The most probable explanation here is a disrupted lumpy disc, but additional starbursts in the outer regions may also be a possibility.
- Group 2: also a rise to the far IR, with increased emission in the middle IR. An energy distribution of this sort could be produced solely by warm dust in the surroundings of the central black hole.
- Group 3: intensity rise with two maxima, a small one in the middle IR and a dominant one in the far IR. The quasar shown in Fig. IV.43 is also included in this group.

The best explanation for the dominance of the far infrared maximum is that numerous star forming regions are also heating up dust in addition to the active galactic core. To check these assumptions further multi-wavelength studies are needed.

Fig. IV.42: Spectral energy distributions of the quasars in the infrared.

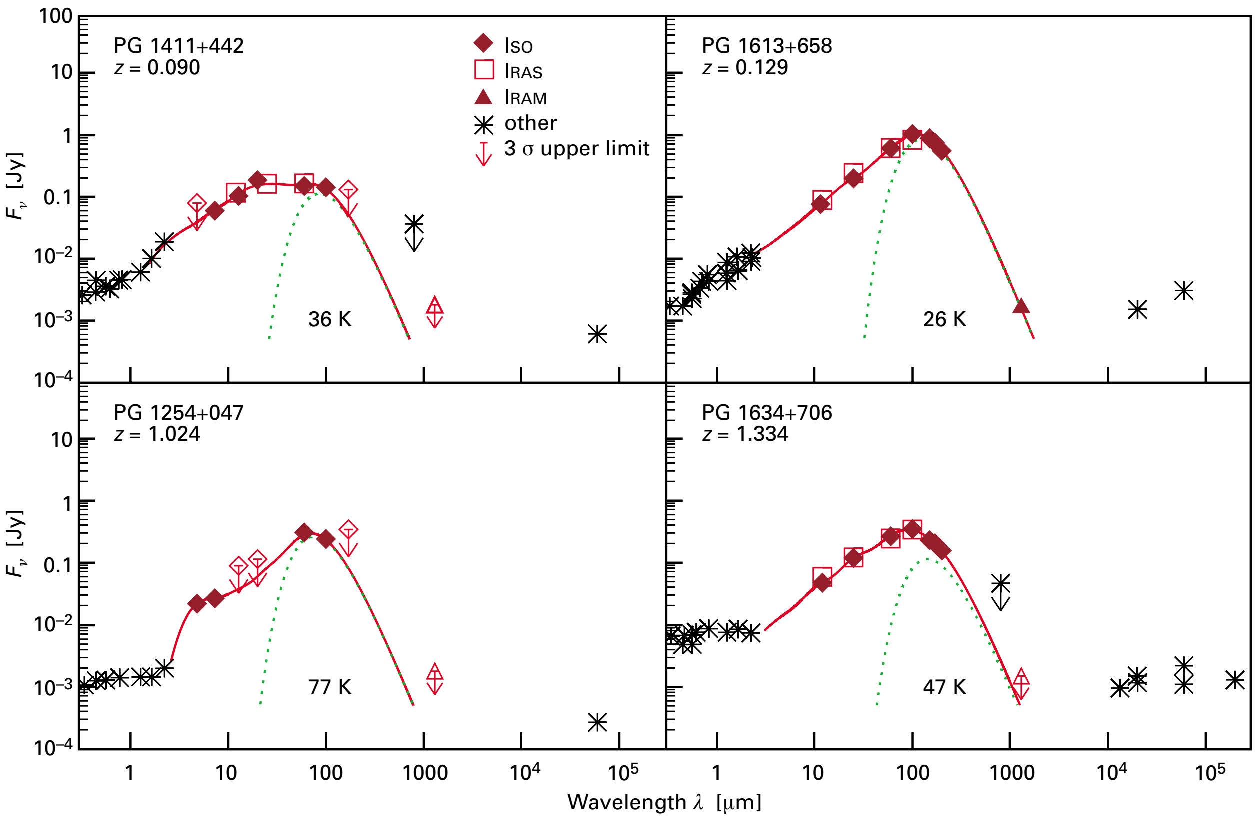

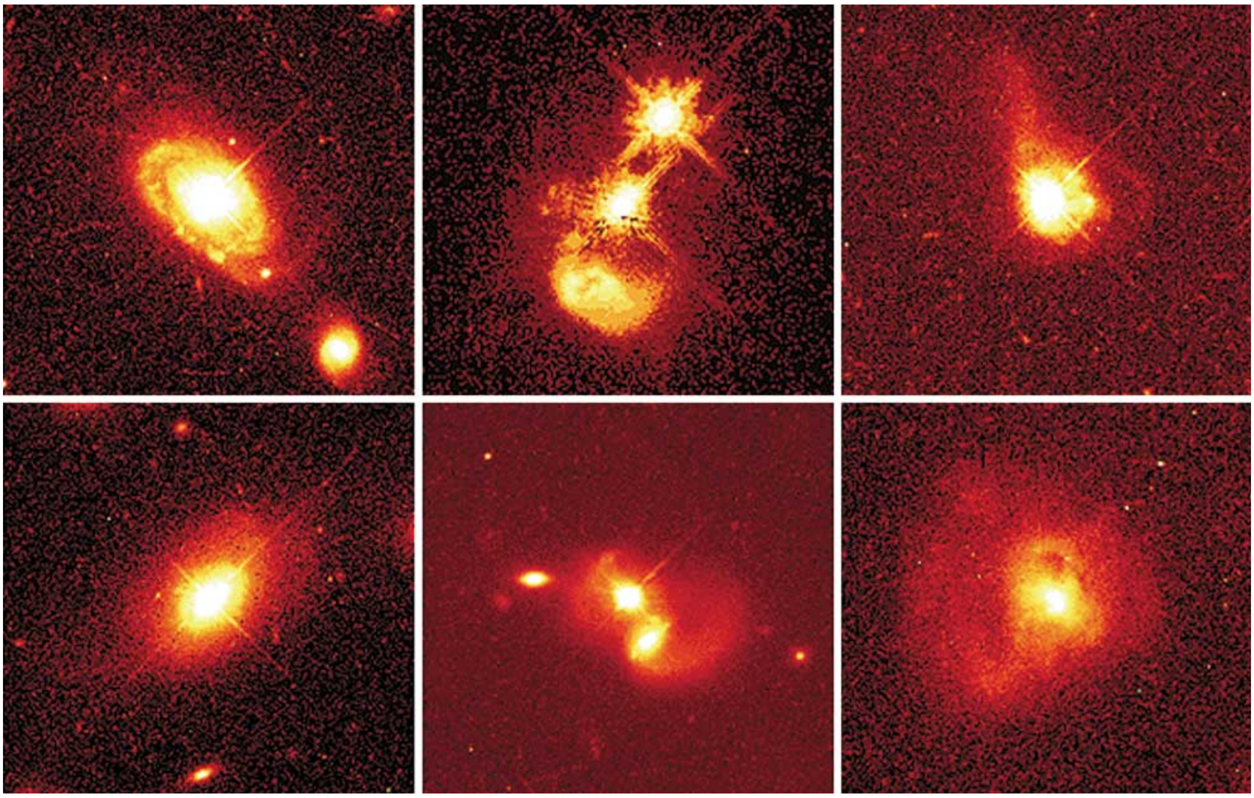

Fig. IV.43: The Hubble Space Telescope was used to observe some near quasars and the galaxies surrounding them, including PG 0052+251 which also appeared in the ISO study (top left).

Conclusive correlations

Observational data from other spectral ranges, such as the blue and the X-ray range, were already available for the selected quasars. In addition, all the redshifts (distances) are known, so that links can be sought between these parameters. In these cases, some unambiguous correlations emerged: for example, the infrared luminosities in the mid IR increase with those in the far IR. Likewise, the luminosities in the mid and far IR rise with those in the blue range (Figs. IV.44, 45 and 46).

The correlations suggest a common source or, even more interesting, an original connection between the two conceivable sources – the active galactic core and the star formation process. For example, intensive star formation is triggered during the collision of two galaxies – a process which has already been observed in the case of near galaxies, and one which leads to increased far infrared radiation. While stars fly past one another in a process of this sort, the interstellar matter collides. At the same time, it reduces its orbital velocity and hence its stabilising angular momentum as well. As a consequence, large quantities of it will spin

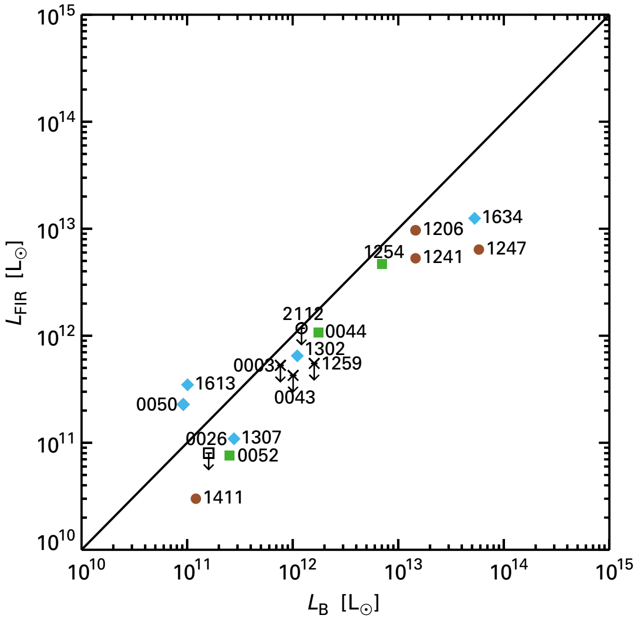

Fig. IV.44: The luminosity in the far infrared rises with that in the mid infrared.

off into the central region of the galaxy, where it will be especially effective at feeding the black hole. This increases the luminosity in blue light (especially due to the Lymanα hydrogen emission), and at the same time, the active galactic core heats up the surrounding dust even more so that it then shines in the mid infrared.

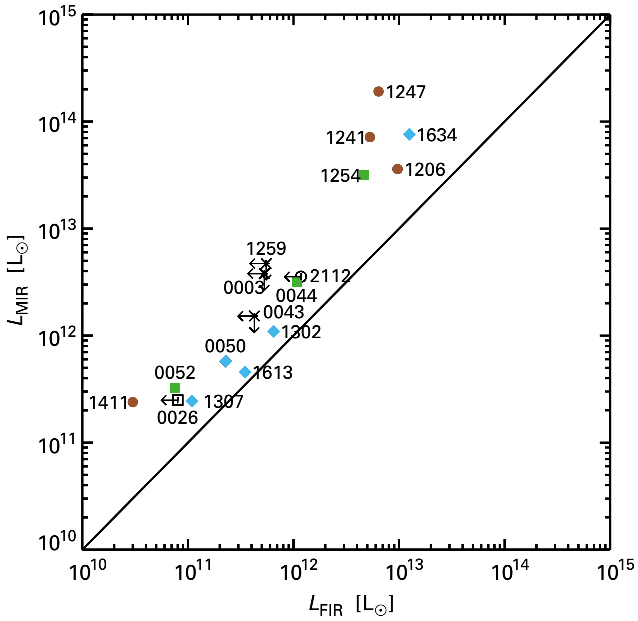

Abb. IV.45: Die Leuchtkraft im mittleren Infrarot steigt mit derjenigen im Blauen an.

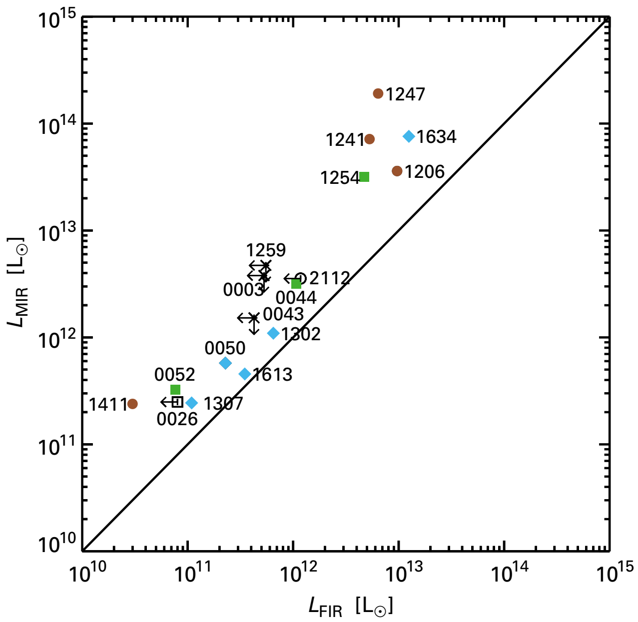

Fig. IV.46: The luminosity in the far infrared rises with that in the blue

Quasars and ultra-luminous infrared galaxies (ULIRGS)

The infrared energy output of the quasars, of 10^{11} to 10^{14} solar luminosities, is very high. The highest values far exceed the range of 10^{12} to 10^{13} solar luminosities for the ultra-luminous infrared galaxies. Interestingly, their IR luminosity is mainly attributed to intense star formation. Only a few so-called »warm« ULIRGS with relatively high intensity in the mid infrared contain a strong active core. Just a short while after they were discovered by IRAS, the hypothesis (still the subject of heated discussion today) was put forward that the warm ULIRGS are the progenitors of quasars in a very early stage of evolution. However, the new ISO data suggest a more simple conclusion: warm ULIRGS and quasars are one and the same thing. The difference is merely that the quasars have been identified on optical images, and the ULIRGS have been identified in the far infrared.

The values derived from the luminosities and temperatures for the dust masses of the quasars lie in the range of 10^6 to 10^9 solar masses. Values of this sort are typical of both dust-rich spiral galaxies and ULIRGS. Now, how does a great deal of dust fit in with the blue – and hardly extincted – appearance of the quasars in the optical? If the dust lies along the line of sight to the quasar, the optical light should be heavily reddened. A suitable geometry which suggests itself is that the dust is concentrated in a disc, and that we see the system from above, that is to say from the polar direction, or at a slight inclination.

Which properties would a quasar of this sort show us if the system turned its edge towards us? A simple estimate shows that a dust disc of 10^8 solar masses surrounding the central area is sufficient to shadow the core completely: in the optical, a pale and shimmering, heavily reddened object of this sort would scarcely be recognized as a luminous quasar. But in the far infrared, it probably shines isotropically and just as brightly as its siblings seen from the polar direction. Its apparent brightness in the mid infrared depends on the shadowing of the core region by the outer dust layers. However, it is conceivable that the mid infrared radiation is also attenuated. A quasar seen edge-on then appears to us like a cool ULIRG. At the moment, there are virtually no possibilities of proving or refuting the existence of an active core in a cool ULIRG beyond doubt – a hard nut for the researchers to crack!

IV.3 The Solar System

Did a Nearby Star Disturb the Formation of the Planets?

In 1992, American astronomers discovered a very faint object with a diameter of about 200 kilometres that is orbiting the Sun at a distance of 40 astronomical units (AU). It was the first known member of the so-called Kuiper belt beyond the orbits of Pluto and Neptune. Up to now, more than a hundred Kuiper objects have been discovered and there are probably a total of several tens of thousands of bodies with diameters in excess of a hundred kilometres in this area of the planetary system. The orbits of the Kuiper objects beyond 42 AU feature unusually high eccentricities and are heavily inclined against the ecliptic. The theory group of the Institute found a possible explanation for this phenomenon with the help of numerical simulations: a star at a distance of only 160 AU disturbed the celestial bodies in the outer protoplanetary disc. As a result of this, they adopted the heavily eccentric and inclined orbits which they have retained until now.

As long ago as 1951, the astronomer Gerard Kuiper had predicted that there must be a swarm of small bodies beyond the orbit of Pluto. His considerations started out

Fig. IV.47: The distribution of some small bodies in the solar system. (Graphic: Minor Planet Center)

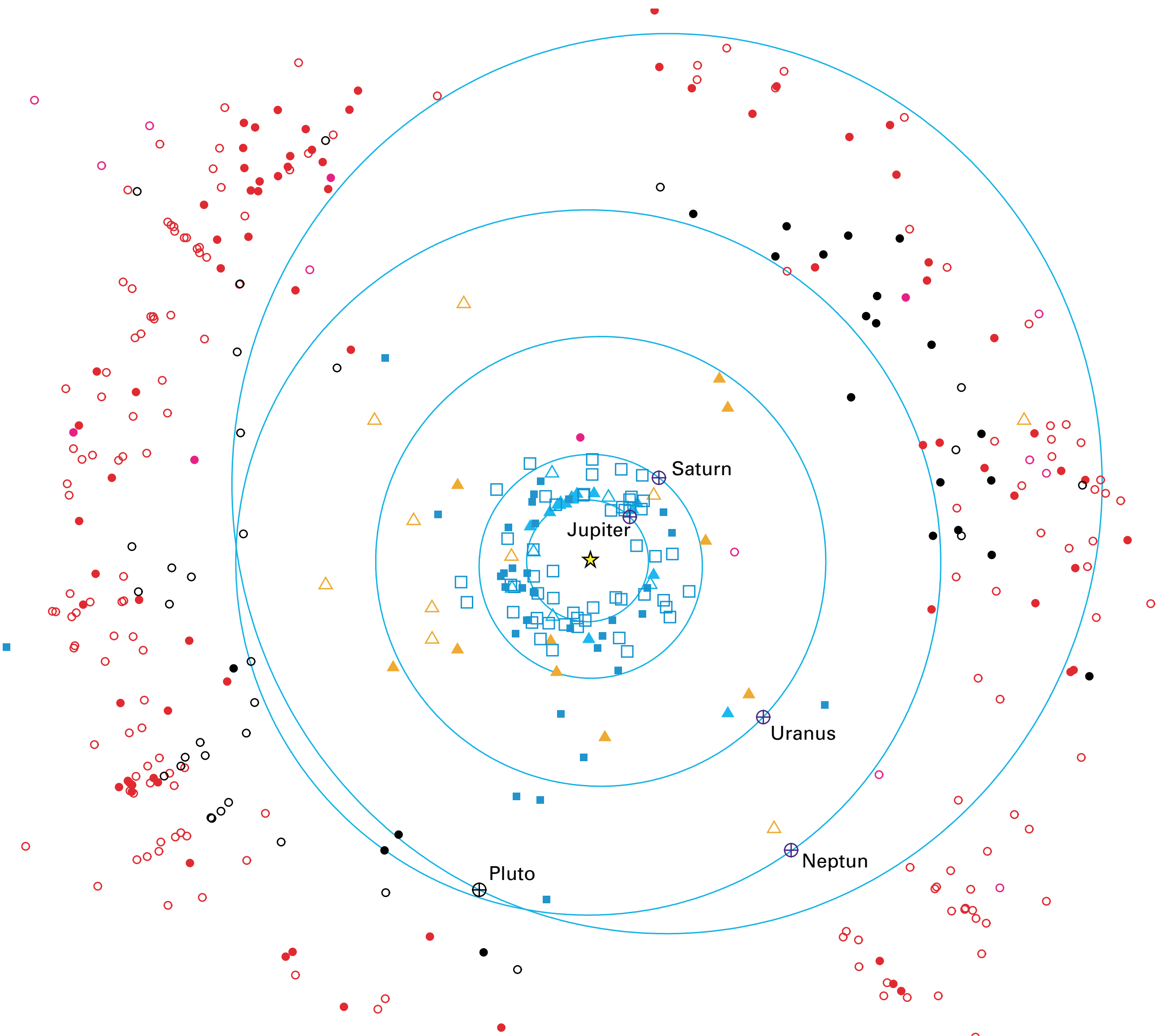

from the orbits of the comets. Long-period comets with periods of 130 years or more very probably originate from the Oort cloud. This is a spherical area which surrounds the Sun at a distance range of between 20,000 and 70,000 AU (Fig. IV.47). In this area, several hundred billion bodies are probably moving; due to gravitational disturbances, they can reach the inner solar system where they light up as comets.

However, orbit analyses suggest that short-period comets originate from a different location. They probably originate from a belt-shaped area which surrounds the Sun at a distance of about 30 to 500 AU. If a Kuiper object approaches the large planet Neptune, it can hurl the body into the inner solar system, where it appears as a comet when it is close to the Sun.

Three Groups of Kuiper Objects

In the meantime, sufficient Kuiper objects have become known for us to be able to differentiate them into three groups on the basis of their kinematics. Group 1 is located at a distance of 39.5 AU (Fig. IV.48). This population can be very easily explained by the fact that the orbital periods of the Kuiper objects here are in a resonance of 3:2 with the period of Neptune. In that past, this has caused bodies in the vicinity of this resonance orbit to be drawn into it due to the gravitational interaction with Neptune. Group 2 consists of the bodies of the so-called scattered disc (violet circles in Fig. IV.47). In the past, they once came so close to Neptune that its gravitation threw them onto extremely elliptical orbits with a pericentre close to Neptune's orbit.

Group 3 is formed by all Kuiper objects which are further than 42 AU from the Sun. Their orbits are heavily elliptical and in some cases they are inclined against the ecliptic. These characteristics cannot be explained by an interaction with Neptune. Instead, other mechanisms have been suggested which could in principle be responsible for the shapes of the orbits. For example, it has been speculated that in the outer areas of the solar system, planets of about the same size as the Earth may initially have existed and that these gravitationally scattered the surrounding population of Kuiper objects. Later on, these planets were then hurled out of the solar system. However, this hypothesis cannot be proven further.

Fig. IV.48: Eccentricities and orbit inclinations of the Kuiper objects known up to now.

Did a Nearby Star Shake up the Kuiper Population?

Together with colleagues from the University of Tokyo and Queen Mary and Westfield College, London, theoreticians at the MPIA pursued another hypothesis. Earlier work at the Institute had proven that most stars are formated in double or multiple systems. But about half of these systems disintegrate by the time the stars have reached the main sequence stage (see 1997 Annual Report, p. 49, and 1998 Annual Report, p. 47). For example, this may happen because two double star systems move past one another at close quarters. For this reason, we cannot rule out the possibility that the proto-Sun initially had a companion star, or that another star flew past the Sun at close quarters. If this happened at a time when the Kuiper objects had already formed, the star could have thrown some of them into heavily eccentric and inclined orbits on which they have been moving until now.

In order to test this hypothesis, it was assumed that a star of one solar mass is moving past the Sun on a parabolic orbit. The reaction of the Kuiper population, assumed to comprise 10,000 particles, was then observed. At the same time, the two decisive parameters were varied: the shortest distance of the star from the Sun (pericentre q) and the inclination of the orbital plane of the star against the ecliptic. In general, the interaction is

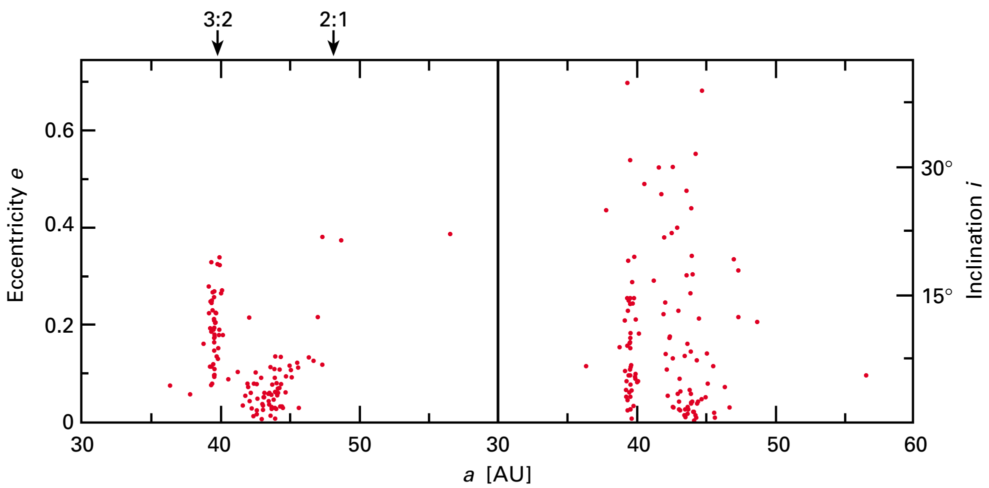

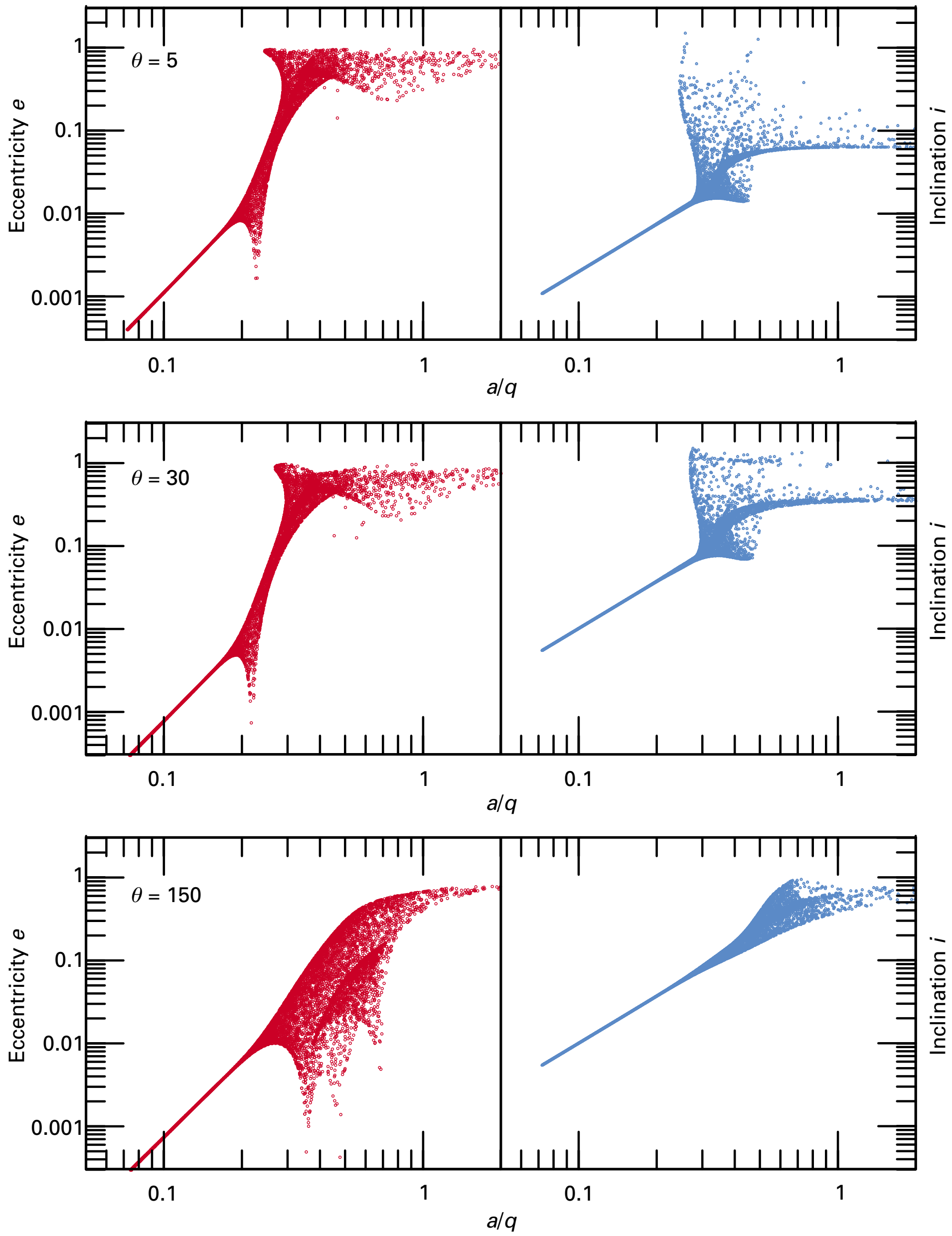

Fig. IV.49: Eccentricities and orbit inclinations of the objects in the Kuiper belt formed after a star has passed by. θ is the angle of inclination of the orbital plane of the star against the ecliptic, and a/q is the distance from the Sun in units of the pericentre q.

more intense for a more massive star, and for a smaller inclination angle and a minimal distance.

At the start of the simulations, the Kuiper particles were moving around the Sun on almost circular orbits in the ecliptic. After the close fly-by of the star, the eccentricities and orbital inclinations in the outer areas actually rose sharply as was hoped (Fig. IV.49). Fig. IV.50 shows how the orbits of the Kuiper objects change. The parameter selected here was the distance a/q normalized to the pericentre q. If the pericentre of the flyby is located at q = 100 AU, the eccentricities of the Kuiper orbits beyond 25 to 35 AU rise to more than 0.1. In such a process, many bodies are even hurled out of the solar system. To be precise, there are 75 % and 95 % at distances of a/q = 0.5 and 0.7 respectively (corresponding to 50 AU and 70 AU for a flyby at a minimum distance of 100 AU).

The best match between the theoretical and the observed values was obtained for an inclination angle of 30 degrees and a pericentre of 160 AU. If 500 particles are selected arbitrarily from this computing run in the range between 30 and 65 AU (Fig. IV.51), this provides a direct comparison with the observational data shown in Fig. IV.48. We can see the sharply rising eccentricities beyond about 42 AU, which are also observed.

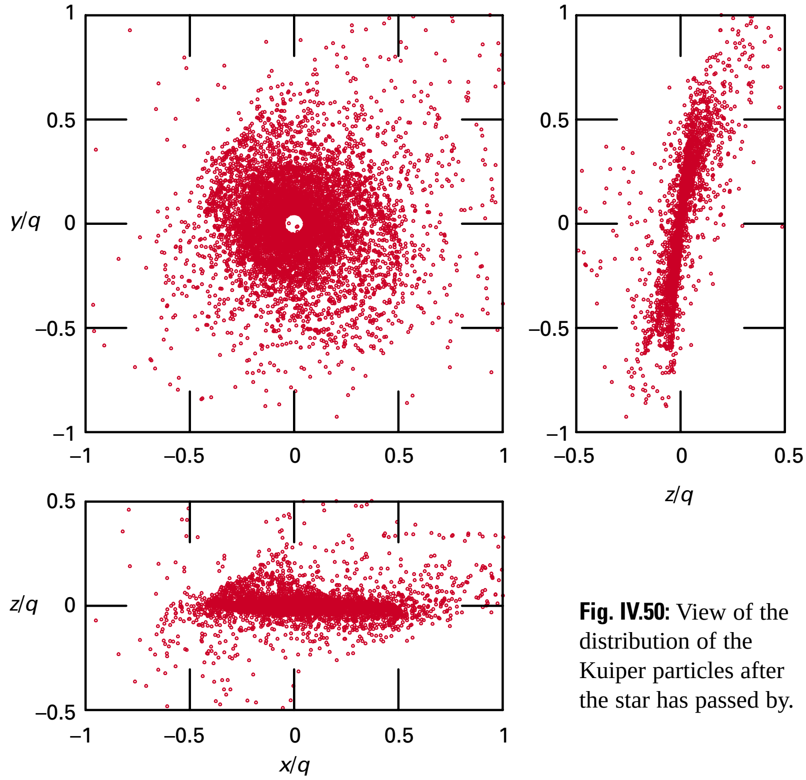

Fig. IV.50: View of the distribution of the Kuiper particles after the star has passed by.

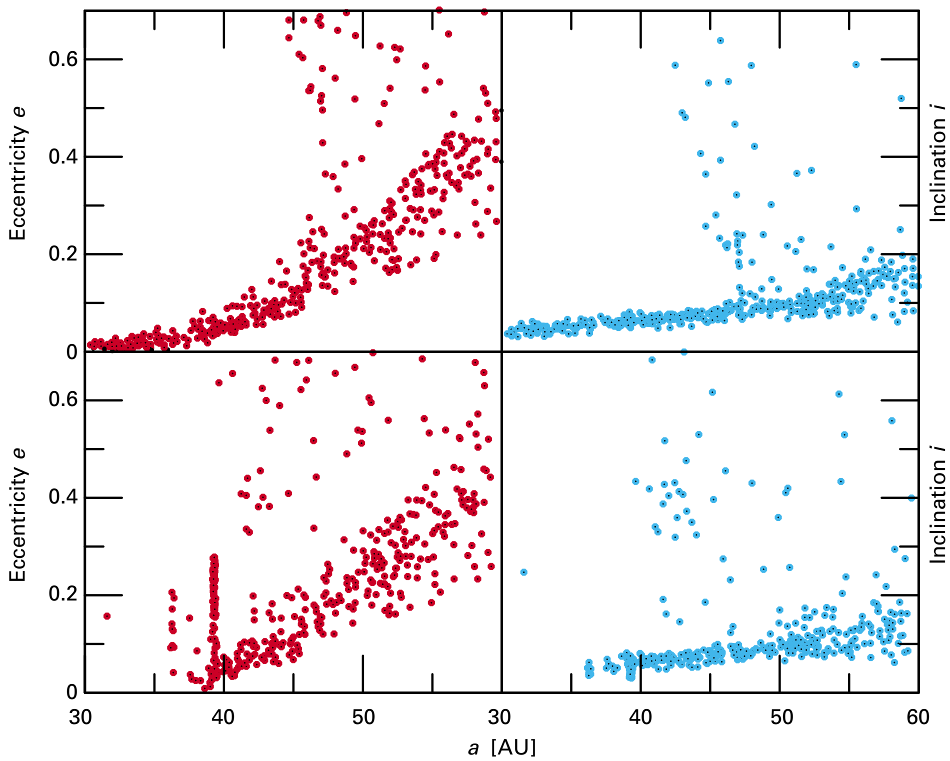

Fig. IV.51: Eccentricities and orbital inclinations of the Kuiper objects after a star has passed by at a distance of 160 AU, at an inclination angle θ of 30 degrees. Top: without the gravitational effect of Neptune; bottom: including this effect.

When the planet Neptune was also added into the simulation, the excess frequency of the bodies in the 3:2 resonance turned out to be about 39.5 AU (Fig. IV.51, below). Bodies within 30 AU which do not enter into this resonance can be thrown onto orbits with high inclination angles if a close flyby occurs. They form Group 2 of the »scattered disc«.

A concluding estimate shows that the Kuiper objects have remained on these orbits until today. A close passage by a star may therefore have left its »fingerprint« in the form of the Kuiper orbits. The simulated scenario can also be verified with the help of further observations. In fact, it predicts that the average eccentricities must rise sharply with increasing distance from the Sun. This is altogether contrary to the hypothesis that planets of the size of the earth disrupted the Kuiper objects. If this were the case, the eccentricities would reduce again as the distance from the Sun increased.

Staff

In Heidelberg

Directors: Appenzeller (temporary), Beckwith (on leave to STScI), Rix (since 1.1.).

Scientists: Ábrahám, Bailer-Jones, Beetz, Bianchi (since 1.11.), Birkle, Burkert, Dehnen (since 1.7.), Feldt (since 1.2.), Fried, Graser, Haas, Herbst, Hippelein, Huang (until 31.1.), Ibata (since 1.10.), Klaas, Kley (since 1.10.), Kümmel (since 1.2.), Leinert, Lemke, Lenzen, Ligori, MacLow (until 30.6.), Marien, Meisenheimer, Mundt, Neckel, Patsis (1.1.-30.9.), Radovich (until 14.9.), Röser, Schmid (1.4.-30.9.), Schmidtobreick (until 31.7.), Slyz, Staude, Stickel, Wilke (since 1.1.), R. Wolf, Zickgraf (1.2.-31.3.).

Ph.D. Students: Baumann, Eckardt (until 28.2.), Geyer (since 1.1.), Hartung (since 1.6.), Heitsch, Hetznecker, Hotzel, Jester, Kasper, Kranz, Lang (since 1.10.), Maier (since 1.10.), Naab, Phleps, Rudnik (24.5.-6.8.), Schuller, Seidel (until 30.4.), v. Kuhlmann, Weiss (since 1.6.), Woitas (until 31.8.).

Diploma Students: Helfert (since 1.2.) Jesseit (since 1.2.), Khochfar (since 1.4.), Krause, Wackermann (until 30.9.), Wetzstein (since 1.12.). Von der FH Mannheim: Lebong (15.3.-14.9.), Lehmitz (until 31.3.), Müller (since 1.9.), Müller-Zumstein (1.3.-31.8.), Steckel (until 28.2.), Thomas (until 28.2.).

Scientific Services: Bizenberger, Fabian (since 1.10.), Hiller, Khan (until 30.4.), Ortlieb (until 31.7.), Laun (since 1.8.), Mathar (since 1.2.), Quetz, Tusche (until 31.7.).

Computers, Data Processing: Briegel, Hippler, Rauh, Storz, Tremmel, Zimmermann.

Electronics: Becker, Ehret, Grimm, Grözinger, Klein, Lehmitz (1.9.-31.12.), Ridinger, Salm, Unser, Wagner, Werner, Westermann, Wrhel.

Fine Mechanics: Böhm, Geuer (since 1.3.), Heitz, Meister, Meixner, Morr, J. Pihale, Sauer.

Drawing Office: Baumeister (since 1.8.), Benesch, Franke, Münch, Rohloff.

Photo Shop: Anders-Özçan.

Graphic Artwork: Meißner-Dorn, Weckauf.

Administration, Secretariate: Behme, de Mooij (until 30.11.), Fink (until 31.10.), Flock, Gieser, Goldberger (since 1.4.), Hartmann, Heißler, Heukäufer, Janssen-Bennynck, Kellermann, Papousado, Rushworth, Schleich, Ullrich (1.7.-31.12.), Zähringer.

Technical Services: Behnke (since 1.12.), Gatz, O. Götz, Herz (since 1.8.), Klingmann (until 31.8), Lang, Nauss, Witzel, B., Witzel, F., Zergiebel.

Trainees: (Feinmechanik) Fabianatz, Greiner, Geuer (until 28.2.), Haffner, Jung, Lares (since 1.9.), Petri (since 1.9.), Wesp.

Free Collaborator: Dr. Bührke.

Scholarship Holders: Barrado-Navascués (DFG), Berkefeld (until 30.11.), Cretton (since 1.9.), Mori (until 31.7.), Fockenbrock (until 30.4.), Heraudeau, Kessel (DFG), Kroupa (since 1.11.), Maciejewski (until 8.11.), Nelson, Porro (until 14.10.), Robberto (until 30.4.), Thiering, Woitas (since 1.11.) Chr. Wolf (SFB), Xu (since 1.2.).

Guests: Courteau, Victoria/Canada (Aug), Cretton, Leiden (Feb/Mär), Guivarch, Marseille (Mai), Hensler, Kiel (Nov/Dez), Hozumi, Japan (Juni), Januzi, Tucson (Jul/Aug), McIntosh, Tucson (Jul/Aug), Sarzi, Padova (since Aug), Steinmetz, Tucson (Jul/Aug), O'Dell, Houston (Juli), Salucci, Triest (Okt), Shields, Athens/ USA (Juni/Juli), Toth, Budapest (Jul/Aug), Travaglio, Florenz (Feb/Nov), Yahagi, Tokyo (Jul/Aug), Zheng, Baltimore (Sept).

Due to regular meetings of the ISOPHOT Co-investigators associated to other Research Institutes and industrial Firms in Germany and from abroad, numerous guests were at the MPIA for short times, who are not mentioned here individually.

Co-operative Students: Matschina (15.9.-12.11.), Lösch (17.2.-26.3.), Mayer, Middelburg (17.2.-26.3.), Müller (1.5.-30.6.), Ochotta (2.8.-12.9.) Rettinghaus (9.8.-18.9.), Theuermeister (1.7.-30.9.).

Calar Alto/Almería

Local Directors: Gredel, Vives.

Astronomy, Night Assistants: Aceituno, Aguirre, Alises, Frahm, Hoyo, Marcos, Montoya, Pedraz (since 1.1.) Prada (since 1.2.), Quesada (on leave), Thiele.

Telescope Techniques: Capel, de Guindos, Garcia, Helmling, Henschke, L. Hernández, Raúl López, Morante, W. Müller, Nuñez, Parejo, Schachtebeck, Usero, Valverde, Wilhelmi.

Technical Services: A. Aguila, M. Aguila, Ariza, Barón, J. Braun (until 28.2.), Carreño, Dominguez, Gómez, Góngora, Manuel Hernandez, Klee, Rosario López, Marquez, Martinez, Puertas, F. Restoy, Romero, Sáez, Sanchez, Schulz, Tapias.

Administration, Secretariate: M. Hernández, M. J. Hernández, M. I. López, C. Restoy.

Working Groups and Scientific Collaborations

Instrumental Projects

ALFA
Stefan Hippler, M. Kasper, M. Feldt, Th. Berkefeld, T. Herbst, R.-R. Rohloff, K. Wagner, P. Bizenberger and all technical Departments of MPIA and Calar Alto Observatory, in collaboration with: MPI für extraterrestrische Physik, Garching, University of Massachusetts, Amherst, USA

CONICA
Rainer Lenzen, W. Benesch, P. Franke, M.A. Khan, N. Münch, N. Ortlieb, R.-R. Rohloff, C. Storz, A. Tusche, K. Wagner, in collaboration with: MPI für extraterrestrische Physik, Garching,

MIDI
Christoph Leinert, U. Graser, B. Grimm, T. Herbst, St. Hippler, R. Lenzen, R. Ligori, R. Mundt, N. Ortlieb, E. Pitz, I. Porro, M. Robberto, R.-R. Rohloff, N. Salm, K. Wagner in collaboration with: Univ. Amsterdam, Netherlands, Sterrewacht Leiden, Netherlands, Observatoire de Meudon, France, Observatoire de Nice, France Kiepenheuer-Institut, Freiburg, Thüringer Landessternwarte Tautenburg.

PACS for FIRST
Dietrich Lemke, O. Krause, U. Grözinger, S. Eckardt, U. Klaas, in collaboration with: MPI für extraterrestrische Physik, Garching, DLR, Berlin, Universität Kaiserslautern

LAICA
Josef Fried, W. Benesch, R.-R. Rohloff, Baumeister, B. Grimm, Unser, C. Marien, Zimmermann, Briegel

ISO
Dietrich Lemke, ISOPHOT-PI and the ISO-Group at the MPIA: P. Abraham, S. Bianchi, J. de Mooij, S. Eckhardt, U. Grözinger, M. Haas, P. Heraudeau, S. Hotzel, U. Klaas, T. Kranz, O. Krause,T. Müller, M. Radovich, A. Rushworth, L. Schmidtobreick, M. Stickel, C. Surace, L.V. Toth, K. Wilke.

UKIRT
Ralf-Rainer Rohloff, E. Pitz, in collaboration with: Astronomisches Rechen-Institut, Heidelberg, Royal Observatory, Edinburgh, Joint Astronomy Center, Hilo, Hawaii.

Research Programmes

CADIS and the Evolution of Galaxies
Josef Fried, B.v. Kuhlmann, K. Meisenheimer, H.-W. Rix, C. Wolf, H.H. Hippelein, M. Kümmel, S. Phleps, H.J. Röser, T. Thierring.

Astrophysics with Gravitational Lenses
Hans-Werner Rix, in collaboration with: Harvard Smithsonian Center for Astrophysics, Cambridge, USA, University of Arizona, Tucson, USA, Space Telescope Science Institute, Baltimore, USA,

Hydrocarbons – Puzzling Actors in Dust
Dietrich Lemke, Ch. Leinert, in collaboration with: University of Helsinki, Finland, ISO Science Operations Center, Villafranca, Spain, Universy of Paris, France, MPI für Radioastronomie, Bonn.

Dust around Young and Massive Stars
Peter Abraham, Ch. Leinert, S. Ligori, D. Lemke, in collaboration with: Astrophysikalisches Institut und Sternwarte Jena

Migrating Young Planets
Willy Kley, in collaboration with: Queen Mary & Westfield College, London, UK.

From Low Mass Stars to Brown Dwarfs
Christoph Leinert, Jens Woitas, Reinhard Mundt, C.A.L. Bailer-Jones, in collaboration with: Astronomisches Rechen-Institut, Heidelberg, Harvard Smithsonian Center for Astrophysics, Cambridge, USA, Lowell Observatory, Flagstaff, USA, Observatoire de Grenoble, France, University of California, Berkeley, USA.

A New Age Scale for Star Clusters
David Barrado y Navascues, in Zusammenarbeit mit: Harvard Smithsonian Center for Astrophysics, Cambridge, USA, Observatoire de Grenoble, Frankreich.

The Age of »Disk Stars« Wega, Fomalhaut and Beta Pictoris
David Barrado y Navascues, in collaboration with: Harvard Smithsonian Center for Astrophysics, Cambridge, USA, University of Georgia, Athens, USA, Harvard University, Cambridge, USA,

The Bar Structure in the Interior of the Milky Way
Walter Dehnen

CADIS supplies Knowledge of the Interior of the Milky Way
Stefanie Phleps, K. Meisenheimer, C. Wolf, in collaboration with: Astronomisches Rechen-Institut, Heidelberg.

ISO Serendipity Survey
Manfred Stickel, D. Lemke, U. Klaas, in collaboration with: Imperial College of Science, London, UK, ESO, Garching, Astrophysikalisches Institut, Potsdam, California Institute of Technology, Pasadena, USA, ISO-Data Center, Villafranca, Spain.

When Dwarf Galaxies Lose their Gas
Andreas Burkert, in collaboration with:University of Tokio, Japan.

How Spiral Galaxies Form Elliptical Galaxies by Merging
Thorsten Naab, A. Burkert, in collaboration with: Center for Astrophysics, Cambridge, USA.

Dust in Quasars
Martin Haas, S.A.H. Müller, K. Meisenheimer, U. Klaas, D. Lemke, in collaboration with: Universität Bochum, MPI für Radioastronomie, Bonn, Landessternwarte Heidelberg.

Did a Nearby Star Disturbed the Formation of our Planetary System?
Andreas Burkert, in collaboration with: Tokyo Institute of Technology, Tokio, Japan, Queen Mary and Westfield College, London, UK

Dark Matter Halos around Galaxies
Andreas Burkert in collaboration with: University of California, Berkeley, USA.

Stellar Densities in Elliptical Galaxies
Andreas Burkert in collaboration with: Shiga University, Shiga, Japan, Kyoto University, Kyoto, Japan.

Formation of CH^+ in interstellar Clouds
Roland Gredel

Dynamics of Circumstellar Disks
Andrew Nelson in collaboration with: Universität Bern, Schweiz, University of Arizona, Tucson, USA.

Observations of NGC 7582 with ISOPHOT
Mario Radovich, U. Klaas, in collaboration with: Instituto de Astrofisica, La Laguna, Spanien.

Collaboration with Industrial Firms

Calar Alto Observatory
DSD Dillinger Stahlbau GmbH, Saarlouis
Fa. Endevco, Heidelberg
PEP Modular Computers GmbH, Kaufbeuren
Carl Zeiss, Jena und Oberkochen

ALFA
AOA Inc., Cambridge, Massachusetts, USA
Cambridge Innovations, Farmingham, Massachusetts, USA
Microgate S.r.l., Bolzano, Italy,
MIT/Lincoln Laboratory, Lexington, Massachusetts, USA
University of Massachusetts, Amherst, Massachusetts, USA

Wide Field Imager
Omega, Vermont, USA

MIDI
Applied Software Technology
BFI Optilas, Dietzenbach
Bürklin, München
Cryophysics, Darmstadt
EBV-Elektronik, Leonberg;
Edwards Hochvakuum, Marburg
Faber Industrietechnik, Mannheim
Geier Metallhandel
Haefele, Schriesheim
Janos, Townshend, Vermont, USA
Kniel, Karlsruhe
Knürr, Mainhausen
Lesker, East Sussex, UK
Leybold Vakuum, Köln
Linos, Göttingen
LOT Oriel
MACCON, München
MAXIM, Planegg
Messer Griesheim, Krefeld
Physik Instrumente, Waldbronn
Raytheon, Goleta,CA, USA
Rutronic, Ispringen
Saskia, Ilmenau
Schroff, Straubenhardt
Spindler & Hoyer, Göttingen
Stegmann, Donaueschingen
SUN Online
Thorlabs, Grünberg
TRIAD Solutions, Moorpark, CA,USA
Witzenmann, Pforzheim
Würzburger Fotoversand, Würzburg;

CONICA
Barr, Westford, Massachusetts, USA
Carl Zeiss, Jena
Janos, Townshend, Vermont, USA
Linos Photonics, Göttingen
Leybold, Hanau
Möller, Wedel
Omega, Vermont, USA
Pörschke, Höchst
Präzisionsoptik, Gera
Queensgate, Barkshire, GB
Richardson Grating, Rochester, USA
Vitron, Jena

PACS
Alternate Computer, Linden
ANTEC,
AVNET, Braunschweig
Buerklin, Munich
California Fine Wire, Grover Beach, USA
ChemPur, Karlsruhe
Comtronic GmbH, Heiligkreuzsteinach
CSEM, Neuchatel, Swizerland
Cunz, Frankfurt
ELNA Transformatoren, Sandhausen
ESM Eberline, Erlangen
GSF Forschungszentrum, Unterschleissheim
Hewlett-Packard, Böblingen
Hoschar, Karlsruhe
HY-LINE Power Compon., Unterhaching
IMEC, Leuven, Belgien
Kayser-Threde. Munich
MagnaC, Wendlingen
Meilhaus Elektronik, PuchheimKarte
Messer-Griesheim, Ludwigshafen
Oxford Instruments, Wiesbaden
Polytec Gmbh, Waldbronn
Rutronik GmbH, Ispringen
Teldix, Heidelberg
Thyssen-Krupp, Bochum
Timet, Duesseldorf
Vacuumschmelze, Hanau
Zeiss, Oberkochen

Mirror for UKIRT
Kaufmann Präzisionsoptik, Crailsheim
Schott, Mainz
BNM, Jena
Carl Zeiss, Oberkochen
Praezisionsoptik, Gera
Physik Instrumente, Waldbronn

CCD Techniques

Dataman, Pliezhausen
EEV Ltd., GB
Haefele, Schriesheim.
Heraeus, Hanau
Lockheed Martin Fairchild Syst., USA
Micro-Optronic-Messtechnik, Langebrück
New Focus, Santa Clara, USA
Philips, Eindhoven, Niederlande
Roth, Karlsruhe
SITe Corp., Beaverton, Oregon, USA
Steward Observatory, Tucson, Arizona, USA
Tafelmeier, Rosenheim

Computers

AKRO, Unterschleißheim
Additive, Friedrichsdorf
Creaso, Gilching
Draco, Hamburg
Edo, Hockenheim
PROUT, Darmstadt
ProMedia, Oftersheim
Seicom, Ismaning
Sun, Langen
Transtec, Tübingen

Mechanics and Electronics

ABB (ehem. Hartmann + Braun), Alzenau
Almet-AMB, Mannheim
Amphenol-Tuchel Electronics, Heilbronn
APE Elektronik, Kuppenheim
Astro- und Feinwerktechnik, Berlin
AVIMO, Somerset, U.K.
Best Power Technology, Erlangen
Binder Magnete, Villingen-Schwenningen
Börsig, Neckarsulm
Bubenzer Bremsen, Kirchen-Wehrbach
Bürklin, München
Cadillac-Plastic, Viernheim
Carl Roth, Karlsruhe
Cherry Mikroschalter, Auerbach
Com Pro, Stuttgart
Compumess Electronik, Unterschleissheim
C&K Components, Neuried b. München
Comtronic GmbH, Heiligkreuzsteinach
Conrad Electronic, Hirschau
Cryophysics, Darmstadt
Dalektron, Dreieich
Dannewitz, Linsengericht
Dürkes & Obermayer, Heidelberg
Dyna Systems NCH, Mörfelden-Walldorf
EBJ, Ladenburg
EBV-Electronik, Leonberg
EC Motion, Mönchengladbach
Edsyn Europa, Kreuzwertheim
Eldon, Büttelborn
Elna Transformatoren, Sandhausen
elspec, Geretsried
ELV Electronik, Leer
ERNI, Adelberg
eurodis Enatechnik, Quickborn
EWF, Eppingen
Farnell Electronic Components, Deisenhofen
Farnell Electronic Services, Möglingen
FCT Electronic, München
Fischer Elektronik, Lüdenscheid
Franke, Aalen
FRIATEC, Mannheim
Fritz Faulhaber, Schönaich
Future Electronics Deutschland, Unterföhring
Gould Nicolet Meßtechnik, Dietzenbach
Helukabel, Hemmingen
Herz, Leister Geräte, Neuwied
Hewlett-Packard Direkt, Böblingen
Holz Electronik, Kirchheim
Hommel-Hercules Werkzeughandel, Viernheim
Horst Göbel, Ludwigshafen
Horst Pfau, Mannheim
HOT Electronic, Taufkirchen
HTF Elektro, Mannheim
Huber + Suhner, Taufkirchen
IBF Mikroelektronik, Oldenburg
Inkos, Reute/Breisgau
iSystem, Dachau
ITE, Sandhausen
Jacobi Eloxal, Altlussheim
Jarmyn, Limburg
Kniel, Karlsruhe
Knürr, München
Lambda Electronics, Achern
Lemo Electronik, München
LPKF CAD/CAM Systeme, Garbsen
Macrotron, München
Matsuo Electronics Europe, Eschborn
Matsushita Automation, Holzkirchen
Maxim Ges. f. elektronische integrierte Bausteine, Planegg
Menges electronic, Dortmund
Metrofunkkabel-Union, Berlin
Mitsubishi-Electric, Weiterstadt
MSC Vertriebs-GmbH, Stutensee
MTI, Baden-Baden
Nanotec, Finsing
Nickel Schalt- und Meßgeräte, Villingen-Schwenningen
Niebuhr Optoelectronik, Hamburg
Nies Electronic, Frankfurt
Nova Electronik, Pulheim
Otto Faber, Mannheim
Parametric Technology, Muenchen
Physik Instrumente, Waldbronn
pbe Electronic, Elmshorn
Phytec Meßtechnik, Mainz
Plastipol, Runkel
PSI Tronix, Tulare, California, USA

Püschel Electronik, Mannheim
R.E.D. Regional-Electronic-Distribution, Rodgau-Jügesheim
Radiall, Rödermark
Rau-Meßtechnik, Kelkheim
Reinhold Halbeck, Offenhausen
Retronic, Ronneburg
Riekert & Sprenger, Wertheim
Rittal-Werk, Herborn
Roland Häfele Leiterplattentechnik, Schriesheim
RS Components, Mörfelden-Walldorf
Rufenach Vertriebs-GmbH, Heidelberg
Rutronik, Ispringen
Sasco, Putzbrunn
Scantec, Planegg
Schaffner Elektronik, Karlsruhe
Schuricht, Fellbach-Schmiden
SCT Servo Control Technology, Taunusstein
SDRC, Neu-Isenburg
SE Spezial-Electronic, Bückeburg
Siemens IC-Center, Mannheim
Spindler & Hoyer, Göttingen
Spoerle Electronic, Dreieich
Synatron, Hallbergmoos
TMS Test- und Meßsysteme, Herxheim/Hayna
Tower Electronic Components, Schriesheim
TreNew Electronic, Pforzheim
TS-Optoelectronic, München
TWK-Elektronik, Karlsruhe
Vacuumschmelze, Hanau
Vero Electronics, Bremen
W. & W. Schenk, Maulbronn
Wikotec, Bramsche
Wilhelm Gassert, Schriesheim
WS CAD Electronic, Berk Kirchen

Teaching Activities

Winter Term1998/99:

I. Appenzeller: Interstellar Matter and Star Formation (Lecture)

A. Burkert: Formation and Evolution of Star Clusters (Lecture)

A. Burkert: Structure, Kinematics and Dynamics of Star Systems (Seminar)

Ch.Leinert, D. Lemke, R, Mundt, H.-J. Röser: Astronomy and Astrophysics III (Seminar)

The Astronomy Lecturers: Astronomical Colloquium.

Summer Term 1999:

J. Fried: Galaxies (Lecture)

I. Appenzeller: Relativistis Astrophysics (Lecture)

H.-J. Röser: Clusters of Galaxies (Lecture)

K. Meisenheimer: Extremely Redshifted Galaxies (Lecture)

Ch. Leinert, D. Lemke, R. Mundt: Astronomy and Astrophysics III (Seminar)

K. Meisenheimer: Stellar Dynamics (Seminar)

A. Burkert: Acceleration, Propagation and Radiation of Relativistic Particles in highly Redshifted Radio Galaxies (Seminar)

H.-W. Rix: Cosmology (Graduate Course, October 1999)

The Astronomy Lecturers: Astronomical Colloquium.

Public Lectures

S. Beckwith: Science with the NGST: 22. Januar, Space Telescope Science Institute, ADM Division, Baltimore; Space Science Update: 9. Februar, NASA Television Production on Protoplanetary Disks, Washington; Extrasolar Planetary Systems: 18. Februar, UVOIR Untergremium des Untersuchungskomitees Astronomy and Astrophysics, Baltimore; Wide Field Planetary Camera 3 IR: 22 Februar, Origins Unterkomitee, Cocoa Beach; From the Big-Bang to Life: 16 März, Kent Island Social Group, Kent Island; The Hubble Space Telescope: 15 April, Maryland Sciene Ceter Opening, Baltimore; Air, Space and the Search for Distant Planets: 20 April, American Geophysical Union, Annapolis; Astronomy from Space: 21 April, Boston Museum of Science, Boston; STScI and Goddard Space Flight Center: Opportunities for Science: 9. Juni, Goddard Space Flight Center, Greenbelt, USA

H. Elsässer: Neue Wege und Ziele der Astronomie: 19. Januar, Urania Berlin, 16. Februar, Witheit Olbers Ges. Bremen, 6. Dezember Univ. Hohenheim, Studium Generale; Aktuelle Fragen der extragalaktischen Forschung: 20 Januar, Wilhelm-Foerster-Sternwarte, Berlin; Entwicklung und Entstehung von Galaxien: 2. Februar, Physikalisches Kolloquium, Dresden; Bau und Entwicklung des Universums: 22. September, Wissenschaft im Rathaus, Dresden

J. Fried: Astologie – Wissenschaft oder Aberglaube? 15. Dezember 1999, Rüsselsheim

T. Herbst: New Eyes for the New Millenium: A Revolution in Large Telescope Design, Max-Planck-Institut für Astronomie, Heidelberg, (Lehrerkurs), Oktober 1999

S. Hippler und S. Rabien: Scharfe Bilder: Adaptive Optik mit dem Laser-Guide-Star. Radiosendung »Radius« des Bayrischen Rundfunks (Bayern 2), 8. November 1999

K. Meisenheimer: Die ersten Galaxien, Rüsselsheim, 17. September 1999

J. Staude: Formation of Stars and Planetary Systems, invited talks in Heidelberg, Heppenheim, Rüsselsheim, as well as five talks in schools in and near Dortmund.

Meetings and Invited Talks

The 13. Calar Alto Colloquium with more than 20 contribution was held at Königstuhl in March

Arcetri Astrophys. Observatorium, Florence, Italy, January: M. Haas (invited talk).

American Astronomical Society, Austin, USA, January: S. Beckwith (invited talk)

Astronomisches Kolloquium der Hamburger Sternwarte, January: Chr. Wolf (invited talk)

Kolloquium der University of Chicago, Januar: A. Burkert

Freitagskolloquium der Universitäts-Sternwarte, München, Februar: St. Phleps, (invited talk)

Optical Astronomers' Tea, Pasadena, USA, März: Chr. Wolf (talk)

VLT Opening Symposium, Antofagasta, Chile, März: R. Lenzen

Conference on Optical and Infrared Spectroscopy of Circumstellar Matter, Tautenburg, März: T. Herbst, R. Gredel (invited talks)

Colloquium at the University of Leiden, March: T. Herbst

Rencontres de Moriond – Building Galaxies: From the Primordial Universere to the Present, Les Arcs, France, March: H.-W. Rix (invited talk)

Conference on Imaging the Universe in Three Dimensions: Astrophysics with Advanced Multi-wavelength Imaging Devices, Walnut Creek, CA, USA, März: T. Herbst (Poster), Chr. Wolf (talk)

26th Saas Fee Advanced Course: Physics of Star Formation in Galaxies, Les Diablerets, Schweiz, März: J. Woitas

Meeting on Galaxy Dynamics, Venice, Italy, March: N. Cretton (invited talk)

Workshop on NGST Detectors, Baltimore, USA, April: S. Beckwith (talk)

Colloquium at the University of Tübingen, April: A. Burkert

New York University, New York, USA, April: S. Beckwith (talk)

Conference on Instrumentation at the Isaac Newton Group – The Next Decade, Sheffield, UK, April: R. Gredel (invited talk)

Physikalisches Kolloquium, University of Köln, April: D. Lemke (invited talk).

Astronomical Colloquium, University of Helsinki, Finland, April: D. Lemke (invited talk).

Symposium at Cornell University for the 60th birthday of Yervant Terzian, Ithaca, USA, May: S. Beckwith (talk)

Euroconference on Stellar Clusters and Associations: Convection, Rotation, and Dynamos, Palermo, Italy, May: D. Barrado y Navascués (talk and poster)

Institute for Astronomy, Cambridge, United Kingdom, May: A. Burkert

Workshop on ISO Polarization Observations,VILSPA, May: U. Klaas (talks).

Working on the Fringe – An International Conference on Optical and IR Interferometry from Ground and Space, Dana Point, USA, May: S. Ligori, S. Hippler, M. Kasper, I. Porro, M. Ollivier

Ringberg Conference on Satellite Galaxies, June: A. Burkert (invited talk)

Astronomisches Kolloquium, University of Basel, June: H.-W. Rix (invited talk)

Heidelberger Kolloquium des Physikalischen Instituts, Universität Heidelberg, Juni: H.-W. Rix (invited talk)

Conference on Gravitational Lensing: Recent Progress and Future Goals, Boston University, Boston, Juni: H.-W. Rix (talk)

Kolloquium am Max-Planck-Institut für Radioastronomie, Bonn, Juni: K. Meisenheimer (invited talk)

Gordon Konference on the Origins of the Solar System, USA, Junei: Nelson (invited talk and poster)

American Astronomical Society Meeting, Chicago, USA, Juni: D. Barrado y Navascués (poster)

Conference on Star Formation, Nagoya, Japan, Juni: A. Nelson and S. Ligori (poster)

Conference on Early Stages of Globular Clusters, Liège, Belgium, July: A. Burkert (invited talk)

IAP Conference on Dynamics of Galaxies, Paris, July: A. Burkert

Clustering at High Redshift, Marseille, June/July: H.-J. Röser

Joint Astronomical Center Hilo, Hawaii, July: M. Haas (talk)

University of Honolulu, Juli: M. Haas (invited talk)

SPIE Conference on Infrared Spaceborne Remote Sensing VII, Denver, USA, July: D. Lemke (invited talk)

Canterbury Conference on Wavefront Sensing and its Applications, Canterbury, UK, July: M. Kasper, S. Hippler, Th. Berkefeld, M. Feldt (talks)

AIP, Potsdam, July: M. Haas (invited talk)

UCSC Summer Workshop Structures of dark matter halos, Santa Cruz, CA., USA, August: A. Burkert (invited talk)

IAU Symposium 197, Astrochemistry: From Molecular Clouds to Planetary Systems, Sogwipo, S. Korea, August: R. Gredel (poster)

Ringberg Symposium Galaxies in the Young Universe II, August: H.-J. Röser (SOC), Chr. Wolf (talk), B. v. Kuhlmann, K. Meisenheimer (SOC, talk), St. Phleps, H. Hetznecker, H. Hippelein (SOC), H.-W. Rix (talk)

Black Hole Workshop, Munich, September: H.-W. Rix (talk)

Astronomische Gesellschaft, Meeting in Göttingen (September): ISO Splinter meeting on Galaxies in the

Infrared: D. Lemke (organisation); U. Klaas, L. Schmidtobreick (invited talks); M. Geyer, B. v. Kuhlmann, M. Haas, S. Hotzel (poster); M. Kümmel, H. Hetznecker

International School of Space Science: High Resolution Observations in Astronomy, L'Aquila, Italy, September: S. Ligori

Conference on Modern Theories of Large Scale Structure, Porto, September: H. Hetznecker (poster)

Plasma Turbulence and Energetic Particles in Astrophysics, Krakow, Poland September: F. Heitsch

Workshop on Galactic Disks 99, organized by MPIA and Research Center for Astronomy and Applied Mathematics of the Academy of Athens, Heidelberg, October: H.-W. Rix (SOC, talk), Panos Patsis (talk), A. Burkert (talk), W. Dehnen (talk), P. Héraudeau (poster), R. Jesseit, T. Kranz (poster), S. Khochfar, T. Naab (poster), K. Wilke (poster)

R. Gredel was visiting scholar at Nagoya City University in Nagoya, Japan in october (talks in Nagoya University and Nobeyama Millimetre Observatory)

Milky Way Magnetic Field Mapping Mission (M4), Workshop, Boston, USA, October: U. Klaas (talk).

Meeting in Honour of the 65th Birthday of Prof. Martinet, Genève, Swizerland, October: N. Cretton

The Second Annual Meeting of the European Star and Planet Formation Network, Puerto de La Cruz, Teneriffa, Spanien, October: F. Heitsch, O. Kessel-Deynet, A. Burkert (talk),

The 11th Cambridge Workshop on Cool Stars, Stellar Systems and the Sun, Teneriffa, Spanien, Oktober: C. Bailer-Jones, R. Mundt, D. Barrado y Navascués (talk and poster)

Division of Planetary Sciences of the American Astronomical Society annual meeting, Padua, Italy, October: P. Ábrahám (poster)

Colloquium at the Institute for Astronomy, Cambridge, United Kingdom, November: A. Burkert

33. ESLAB Symposium: Star Formation from the Small to the Large Scale, ESTEC, Noordwijk, Netherlands, November: F. Heitsch; P. Ábrahám, S. Hotzel (poster).

Centre Européen Astronomique, Saclay, November: M. Haas (invited talk).

Darwin and Astronomy, Stockholm, November: T. Herbst (SOC, talk)

XI. Canary Islands Winter School of Astrophysics Galaxies at High Redshift, November: B. v. Kuhlmann (poster)

Ringberg-Symposium ISO surveys of a dusty universe, November: D. Lemke (SOC), U. Klaas, M. Stickel, K. Wilke (LOC); M. Stickel (invited talk); M. Haas, S. Hotzel (Poster).

Universität Padua, Dezember: M. Haas (invited talk).

Dynamic Models of Early-Type Galaxies, Straßburg, Dezember: N. Cretton (invited seminar)

Service in Committees

R. Gredel: Member of Time Allocation Committee for Calar Alto

T. Herbst: Member of the Scientific Advisory Group for the Darwin Projekt of ESA, of the VLTI MIDI-Team, of the LBT Near IR Spectroscopy Working Group; he organized the Meeting LBT Interferometry and Adaptive Optics partecipated to the meeting of the Science Advisory Committee of the LBT Corporation .

Ch. Leinert: Member of Nomination Commission of the University of Jena for the C3 Chair for Astrophysics.

D. Lemke: Member of the Experts Panel Astrophysics of the Bundesministerium für Bildung und Forschung and of the ISO Science Team of the European Space Agency.

K. Meisenheimer: Member of the ESO Working Group on Surveys

R. Mundt: Member of the Time Allocation Committee

H.-W. Rix was responsible for the Organization of the German-American Frontiers of Science Meeting, which was held in Sommer 2000 by the Humboldt Foundation and the National Academy of Science; he was member of the VLTI-Steering Committee, of the Sloan Digital Sky Survey (SDSS) Council and of the Esa Astronomy Working Group.

H.-W. Rix and A. Burkert were members of the Committee in charge of the Memorandum on Astronomy of the Rat Deutscher Sternwarten.

Publications

Ábrahám, P., Ch. Leinert and D. Lemke: Interplanetary Dust as Seen in the Zodiacal Light with ISO. In: Solid Interstellar Matter: The ISO Revolution, Les Houches No.11, (Eds.) L. D'Hendecourt, C. Joblin, A. Jones. EDP Sciences, Springer, Berlin 1999. 3.

Ábrahám, P., Ch. Leinert, J. Acosta-Pulido and D. Lemke: The Mid-infrared Spectrum of the Zodiacal Light Observed with ISO-PHOT. Bulletin of the American Astronomical Society 31 (1999) 1591.

Ábrahám, P., A. Burkert, Ch. Leinert, D. Lemke and Th. Henning: Far-Infrared mapping of Herbig Ae/Be stars with ISO. In: Proceedings of conference »The Universe as seen by ISO«, Paris, (Eds.) P. Cox, M. F. Kessel. ESA-SP-427, ESA Publ. Div., Noordwijk 1999, 265–268.

Ábrahám, P., Ch. Leinert, J. Acosta-Pulido, L. Schmidtobreick and D. Lemke: Zodiacal light observations with ISOPHOT. In: Proccedings of conference »The Universe as seen by ISO«, Paris, (Eds.) P. Cox, M. F. Kessel. ESA-SP-427, ESA Publ. Div., Noordwijk 1999, 145–148.

Ábrahám, P., Ch. Leinert, A. Burkert, D. Lemke and Th. Henning: Search for cool circumstellar matter in the Ursae Majoris Group with ISO. In: Proccedings of conference »The Universe as seen by ISO« Paris, (Eds.) P. Cox, M. F. Kessel. ESA-SP-427, ESA Publ. Div., Noordwijk 1999, 261–264.

Acosta-Pulido, J. A., U. Klaas and R. J. Laureijs: The Starburst Galaxy NGC\,6090: An ISO view. In: Proceedings of conference »The Universe as seen by ISO«, Paris, (Eds.) P. Cox, M. F. Kessel. ESA-SP-427, ESA Publ. Div., Noordwijk 1999, 849–852.

Appenzeller, I.: The Demise of Spherical and Stationary Winds. In: Variable and Non-spherical Stellar Winds in Luminous Hot Stars, (Eds.) B. Wolf, O. Stahl, A. W. Fullerton. IAU Colloquium 169, Springer, Berlin 1999, 416–422.

Baade, D., K. Meisenheimer, O. Iwert, J. Alonso, Th. Augusteijn, J. Beletic, H. Bellemann, W. Benesch, A. Böhm, H. Böhnhardt, J. Brewer, S. Deiries, B. Delabre, R. Donaldson, Ch. Dupuy, P. Franke, R. Gerdes, A. Giliotte, B. Grimm, N. Haddad, G. Hess, G. Ihle, R. Klein, R. Lenzen, J.-L. Lizon, D. Mancini, N. Münch, A. Pizarro, P. Prado, G. Rahmer, J, Reyes, F. Richardson, E. Robledo, F. Sanchez, A. Silber, P. Sinclair, R. Wackermann, S. Zaggia: The Wide Field Imager at the 2.2m MPG/ESO Telescope: First Views with a 67-Million-Facette Eye. The Messenger 95, 15–17 (1999).

Bailer-Jones, C. A. L. and R. Mundt: A Search for Variability in Brown Dwarfs and L Dwarfs. Astronomy and Astrophysics 348, 800–804 (1999).

Bailer-Jones, C. A. L., H. K. D. H. Bhadeshia and D. J. C. MacKay: Gaussian Process Modelling of Austenite Formation in Steel. Materials Science and Technology 15, 287–294 (1999).

Barnstedt, J., N. Kappelmann, I. Appenzeller, A. Fromm, M. Gölz, M. Grewing, W. Gringel, C. Haas, W. Hopfensitz, G. Krämer, J. Krautter, A. Lindenberger, H. Mandel and H. Widmann: The ORFEUS II Echelle Spectrometer: Instrument Description, Performance and Data Reduction. Astronomy and Astrophysics Supplement Series 134, 561–567 (1999).

Barrado y Navascués, D.: Litium and Binarity. In: The 10th Cambridge Workshop on Cool Stars, Stellar Systems and the Sun, (Eds.) R. Donahue, J. Bookbinder. Conference Series 154, Astronomical Society of the Pacific, San Francisco 1998, 894–903.

Barrado y Navascués, D.: The Age of Beta Pic Type Stars: Vega, Fomalhaut, Beta Pic and HR 4796. Astrophysics and Space Sciences 263, 235–238 (1999).

Barrado y Navascués, D., J. R. Stauffer and J. Bouvier: Brown Dwarfs and Very Low Mass Stars: Towards a New Age Scale for Young Open Clusters. Astrophysics and Space Science 263, 239–242 (1999).

Barrado y Navascués, D., J. R. Stauffer and B. Patten: The Lithium-Depletion Boundary and the Age of the Young Open Cluster IC 2391. The Astrophysical Journal 522, L53–L56 (1999).

Barrado y Navascués, D., J. R. Stauffer, J. Bouvier and E. L. Martin: The Mass Function at the End of the Main Sequence: The M 35 Open Cluster. Astrophysics and Space Science 263, 303–306 (1999).

Barrado y Navascués, D., J. R. Stauffer, I. Song and J.-P. Caillault: The Age of Beta Pictoris. The Astrophysical Journal 520, L123–L126 (1999).

Barth, A. J. H.-W. Rix, L. C. Ho, A. V. Filippenko and W. L. W. Sargent: Ionized Gas Kinematics and the Central Mass of NGC 3245. American Astronomical Society Meeting 195 1999) 115.11.

Bastian, U., W. Dehnen and E. Schilbach: A »DIVA«for Observational Stellar Dynamics. In: Schielicke, R. E. (Ed.). Astronomische Gesellschaft Abstract Series 15 (1999), 31.

Bennert, N., I. König, W. Hovest, M. Nielbock, T. Jürges, K. Rösler, M. Pohlen, C. Tappert, R. Vnscheidt, J. Sanner, D. Münstermann, D. Reymann, A. Hovest and L. Schmidtobreick: Astrometry of Several Comets. In: Schielicke, R. E. (Ed.), Astronomische Gesellschaft Abstract Series 15 (1999), 94.

Bechtold, J., K. Enniko, T. P. Greene, J. H. Burge, M. J. Rieke, G. H. Rieke, H.-W. Rix, E. T. Young, M. P. Lesser, R. Sarlot, J. R. Angel, D. W. McCarthy, L. Lesyna, K. Triebes and J. E. Gunn: The University of Arizona/Lockheed Martin Conceptual Study of the NGST Science Instrument Module. American Astronomical Society Meeting 194 (1999), 91.14.

Beckwith, S. V. W.: Circumstellar Disks. In: The Origin of Stars and Planetary Systems, (Eds.) C. J. Lada, N. D. Kylafis. NATO Science Series 540, Kluwer, Dordrecht 1999, 579.

Berkefeld, T.: Possibilities and Performance of Multi-Conjugate Adaptive Optics. Bulletin of the American Astronomical Society 31 (1999), 837.

Bodenheimer, P., H. Yorke and A. Burkert: Formation of Disks and Binaries. In: Proceedings of the International Conference on Numerical Astrophysics, Tokyo 1998. (Eds.) Shoken M. Miyama, Kohji Tomisaka, Tomoyuki Hanawa. Kluwer, Boston 1999, 123.

Böhnhardt, H., N. Rainer, K. Birkle and G. Schwehm: The Nuclei of Comets 26P/Grigg-Skjellerup and 73P/ Schwassmann-Wachmann 3. Astronomy and Astrophysics 341, 912–917 (1999).

Böhnhardt, H., K. Birkle, A. Fiedler, L. Jorda, S. Peschke, H. Rauer, R. Schulz, G. Schwehm, N. Thomas, G. Tozzi and R. West: Dust Morphology of Comet Hale-Bopp (C/1995 01): I. Pre-Perihelion Coma Structures in 1996. Earth, Moon and Planets 78, 179–187 (1999).

Burkert, A.: The Formation of Brown Dwarfs by Fragmentation. In: Schielicke, R. E. (Ed.). Astronomische Gesellschaft Abstract Series 15 (1999), 18.

Burkert, A., J. Silk: On The Structure and Nature of Dark Matter Halos. In: Dark Matter in Astro and Particle Physics, (Eds.) H. V.

Klapdor-Kleingrothaus, L. Baudis. Institute of Physics Publishing, Bristol 1999, 375–386.

Butler, D. J., R. I. Davies, H. Fews, W. K. Hackenberg, S. Rabien, Th. Ott, A. Eckart and M. Kasper: Calar Alto ALFA and the Sodium Laser Guide Star in Astronomy. In: Adaptive Optics Systems and Technologiy, (Eds.) R. K. Tyson, R. Q. Fugate. Proceedings of the SPIE 3762, SPIE Bellingham 1999, 184–193.

Castro-Tirado, A. J., J. Gorosabel, E. Costa, M. Feroci, L. Piro, F. Frontera, D. dal Fiume, L. Nicastro, E. Palazzi, J. Greiner, K. Birkle, R. Fockenbrock, E. Thommes, Chr. Wolf, C. Bartolini, A. Guarnieri, N. Masetti, A. Picciono, M. Mignoli, J. Heidt, T. Seitz, H. Pedersen, S. Guziy, A. Shlyapnikov, L. Metcalfe, R. Laureijis, B. Altieri, M. Kessler, L. Hanlon, B. McBreen, N. Smith, J. Studt, N. Benítez, E. Martínez-González, H. Kristen, A. Broeils, M. Wold, M. Lacy, and M. V. Alonso: Optical/IR Follow-Up Obsevations of GRBS Detected by BEPPOSAX,. In: Gamma-Ray Bursts: 4th Huntsville Symposium, (Eds.) Ch. A. Meegan R. D. Preece, Th. M. Koshut. Woosbury New York: Conference Proceedings 428, AIP, San Francisco 1998, 489.

Castro-Tirado, A. J., M. Zapatero-Osorio, N. Caom, M. C. Luz, J. Hjorth, H. Pedersen, M. I. Andersen, J. Gorosabel, C. Bartolini, A. Piccioni, F. Frontera, N. Masetti,E. Palazzi, E. Pian, J. Greiner, R. Hudec, R. Sagar, A. K. Pandey, V. Mohan, R. K. S. Yadav, N. Nilakshi, G. Bjornsson, P. Jakobsson, I. Burud, F. Courbin, Gaetano, A. Piersimoni, J. Aceituno, L. M. Montoya, S. Pedraz, R. Gredel, Ch. F. Claver ,T. A. Rector, J. E. Rhoads, F. Walter, J. Ott, H. Hippelein, V. Sanchez-Bejar, C. Gutierrez, A. Oscoz, J. Zhu, J. Chen, H. Zhang, J. Wei, A. Zhou, S. Guziy, A. Shlyapnikov, J. Heise, E. Costa, M. Feroci and L. Piro: Decay of the GRB 990123 Optical Afterglow: Implications for the Fireball Model. Science 283, 2069–2073 (1999).

Castro-Tirado, A. J., M. R. Zapatero-Osorio, J. Gorosabel, J. Greiner, J. Heidt, D. Herranz, S. N. Kemp, E. Martínez-González, A. Oscoz, V. Ortega, H.-J. Röser, Chr. Wolf, H. Pedersen, A. O. Jaunsen, H. Korhonen, I. Ilyin, R. Duemmler, M. I. Andersen, J. Hjorth, A. A. Henden, F. J. Vrba, J. Fried, F. Frontera and L. Nicastro: The Optical/IR Counterpart of the 1998 July 3 Gamma-Ray Burst and Its Evolution. The Astrophysical Journal 511, L85–L88 (1999).

Ciliegi, P., R. G. McMahon, G. Miley, C. Gruppioni, M. Rowan-Robinson, C. Cesarsky, L. Danese, A. Franceschini, R. Genzel, A. Lawrence, D. Lemke, S. Oliver, J.-L. Puget and B. Rocca-Volmerange: A Deep VLA Survey at 20 cm of the ISO ELAIS Survey Regions. Monthly Notices of the Royal Astronomical Society 302, 222–244 (1999).

Cinzano, O., H.-W. Rix, M. Sarzi, E. Corsini, W. Zeilinger and F. Bertola: The Kinematics and Origin of the Ionized Gas in NGC 4036. Monthly Notices of the Royal Astronomical Society 307, 433–448 (1999).

Courteau, S. and H.-W. Rix: Maximal Disks and the Tully-Fisher Relation. The Astrophysical Journal 513, 561–571 (1999).

Cox, D. P., R. L. Shelton W. Maciejewski, R. K. Smith, T. Plewa, A. Pawl and M. Rózyczka: Modeling W 44 as a Supernovae Remnant in a Density Gradient with a Partially Formed Dense Shell and Thermal Conduction in the Hot Interior. I. The Analytical Model. The Astrophysical Journal 524, 179–191 (1999).

Cretton, N. and F. van den Bosch: Evidence for a Massive Black Hole in the S0 Galaxy NGC 4342. The Astrophysical Journal 514, 704–724 (1999).

Cretton, N. P. T. de Zeeuuw, R. P. van der Marel and H.-W. Rix: Axisymmetric Three-Integral Models for Galaxies. The Astrophysical Journal Supplement 124, 383–401 (1999).

Davies, R. I., W. Hackenberg, T. Ott, A. Eckart, S. Rabien, S. Anders, S. Hippler, M. Kasper, P. Kalas, A. Quirrenbach and A. Glindemann: The Science Potential of ALFA: Adaptive Optics with Natural and Laser Guide Stars. Astronomy and Astrophysics, Supplement Series 138, 345–353 (1999).

Dehnen, W.: The Pattern Speed of the Galactic Bar. The Astrophysical Journal 524, L35–L38, 1999.

Dehnen, W.: Simple Distribution Functions for Stellar Disks. The Astronomical Journal 118, 1201–1208, 1999.

Dehnen, W.: Approximating Stellar Orbits: Improving on Epicycle Theory. The Astronomical Journal 118, 1190–1200, 1999.

Dehnen, W.: The Distribution of Nearby Stars in Velocity Space. In: Galaxy Dynamics, (Eds.) D. R. Merritt, M. Valluri, J. A. Sellwood. Conference Series 182, Astronomical Society of the Pacific, San Francisco 1999, 297–301.

Dietrich, M., I. Appenzeller, S. J. Wagner, W. Gässler, R. Häfner, H.-J. Hess, W. Hummel, B. Muschielok, H. Niclas, G. Rupprecht, W. Seifert, O. Stahl, T. Szeifert and K. Tarantik: Spectroscopic Study of High Redshift Quasars. Astronomy and Astrophysics 352, L1–L4 (1999).

Moorwood, S. Oliver, W. T. Reach, M. Rowan-Robinson and M. Stickel: FIRBACK far infrared survey with ISO: Data reduction, analysis and first results. In: Proceedings of conference »The Universe as seen by ISO«, Paris, (Eds.) P. Cox, M. F. Kessel. ESA-SP-427, ESA Publ. Div., Noordwijk 1999, 1031–1036.

Eckart, A., R. I. Davies, W. Hackenberg, T. Ott, S. Rabien, S. Hippler, M. Kasper, P. Kalas, K. Wagner and R.-R. Rohloff: Status of the ALFA Project. Astronomische Gesellschaft Abstract Series 14 (1998), 69.

Falco, E., C. Impey, C. Kochanek, J. Lehár, B. McLeod, H.-W. Rix, C. Keeton, J. Muñoz and C. Peng: Dust and Extinction Curves in Galaxies with $z > 0$: The Interstellar Medium of Gravitational Lenses. The Astrophysical Journal 523, 617–632 (1999).

Garcia-Berro, E., S. Torres, J. Isern and A, Burkert: Monte Carlo Simulations of the Disc White Dwarf Population. Monthly Notices of the Royal Astronomical Society 302, 173–188 (1999).

Geyer, M. P. and A. Burkert: Gas Expulsion from Young Globular Clusters. In: Schielicke, R. E. (Ed.). Astronomische Gesellschaft Abstract Series 15 (1999), 117.

Gorosabel, J., A. J. Castro-Tirado, H. Pedersen, D. Thompson, M. Guerrero, A. Oscoz, N. Sabalisck, E. Villaver and N. Lund: Optical and Near-infrared Observations of the GRB 970615 Error Box. Astronomy and Astrophysics Supplement Series 138, 455–456 (1999).

Gredel, R.: Interstellar C_2 Absorption Lines Towars CH^+ Forming Regions. Astronomy and Astrophysics 351, 657–668, 1999.

Gredel, R.: Interstellar CH^+ – An Outstanding Enigma. In: Millimeter-Wave Astronomy: Molecular Chemistry and Physics in Space, Proceedings of the 1996 INAOE Summer School of Millimeter-Wave Astronomy, Mexico 1996, (Eds.) W.F. Wall, A. Carramiñana, L. Carrasco. Kluwer, Dordrecht 1999, 369–378.

Gredel, R.: Chemical Signatures of Turbulence. In: Optical and Infrared Spectroscopy od Interstellar Matter, (Eds.) E. Guenther, B. Stecklum S., S. Klose. Conference Series 108, Astronomical Society of the Pacific, San Francisco 1999, 187–196.

Gredel, R.: Interstellar C_2 and CN Absorption Lines Towards CH^+ Forming Regions. In: IAU Symposium 197, Abstract Book, 1999, 151–152.

Gredel, R., S. Tiné, S. Lepp and A. Dalgarno: The Excitation of Molecular Hydrogen in XDRs. In: Millimeter-Wave Astronomy: Molecular Chemistry and Physics in Space, Proceedings of the 1996 INAOE Summer School of Millimeter-Wave Astronomy, Mexico 1996, (Eds.) W.F. Wall, A. Carramiñana, L. Carrasco. Kluwer, Dordrecht 1999, 247–256.

Grosbol, P. and P. Patsis: Three-Armed Galaxy NGC 7137. In: Galaxy Dynamics, (Eds.) D. R. Merritt, M. Valluri, J. A. Sellwood. Conference Series 182, Astronomical Society of the Pacific, San Francisco 1999, 217–218.

Grün, E., S. B. Peschke, M. Stickel, T. G. Müller, H. Krüger, H. Böhnhardt, T. Y. Brooke, H. Campins, J. Crovisier, M. S. hanner,, I. Heinrichsen, H. U. Keller, R. Knacke, P. Lamy, Ch. Leinert, D. Lemke, C. M. Lisse, M. Muller, D. J. Osip, M. Solc, M. Sykes, V. Vanysek, J. Zarnecki: ISOPHOT Observations of Comet Hale-Bopp: Initial Data reduction. In: Proceedings of conference »The Universe as seen by ISO«, Paris, (Eds.) P. Cox, M. F. Kessel. ESA-SP-427, ESA Publ. Div., Noordwijk 1999, 181–184.

Gruppioni, C., P. Ciliegi, M. Rowan-Robinson, L. Cram, A. Hopkins, C. Ceasarsky, L. Danese, A. Franceschini, R. Genzel, A. Lawrence, D. Lemke, R. G. McMahon, G. Miley, S. Oliver, J.L. Puget and B. Rocca-Volmerange: A 1.4-GHz Survey of the Southern European Large-Area ISO Survey Region. Monthly Notices of the Royal Astronomical Society 305, 297–308 (1999).

Gürtler, J., K. Schreyer, Th. Henning, W. Pfau and D. Lemke: Infrared Bands Towards Young Stars in Chamaeleon. Astronomy and Astrophysics 346, 205–210 (1999).

Haas, M., D. Lemke, M. Stickel, H. Hippelein, M. Kunkel, U. Herbstmeier and K. Mattila: Cold Dust in the Andromeda Galaxy mapped by ISO. In: Proccedings of conference »The Universe as seen by ISO«, Paris, (Eds.) P. Cox, M. F. Kessel. ESA-SP-427, ESA Publ. Div., Noordwijk 1999, 885–886.

Haas, M. R. Chini, K. Meisenheimer, M. Stickel, D. Lemke, U. Klaas, E. Kreysa and S. Müller: On the far infrared emission of quasars. In: Proceedings of conference »The Universe as seen by ISO«, Paris, (Eds.) P. Cox, M. F. Kessel. ESA-SP-427, ESA Publ. Div., Noordwijk 1999, 887–888.

Haas, M., S. A. H. Müller, R. Chini, K. Meisenheimer, U. Klaas, D. Lemke, E. Kreysa and M. Camenzind: Dust in PG Quasars. In: Schielicke, R. E. (Ed.): Astronomische Gesellschaft Abstract Series 15 (1999), P96.

Heidt, J., K. Nilsson, J. Fried, L. Takalo and A. Sillanpää: 1ES 1741+196: a BL Lacertae Object in a Triplet of Interacting Galaxies? Astronomy and Astrophysics 348, 113–116 (1999).

Heidt, J., K. Nilsson, I. Appenzeller, K. Jäger,W. Seifert, T. Szeifert, W. Gässler, R. Häfner, W. Hummel, B. Muschielok, H. Nicklas and O. Stahl: Observations of the Host Galaxies of the BL Lacertae Objects H0414+009 and OJ 287 with FORS 1 at VLT-UT1. Astronomy and Astrophysics 352, L11–L16 (1999).

Heinrichsen, I., H. J. Walker, U. Klaas, R. J. Sylvester and D. Lemke: An Infrared Image of the Dust Disc around β Pic. Monthly Notices of the Royal Astronomical Society, 304, 589–594 (1999).

Heitsch, F.: Effects of Magnetized Turbulence on the Structure and Dynamical Evolution of the Molecular Clouds. In: Schielicke, R. E. (Ed.), Astronomische Gesellschaft Abstract Series 15 (1999), 70.

Heitsch, F. and T. Richtler: The Metal-Rich Globular Clusters of the Milky Way. Astronomy and Astrophysics 347, 455–472 (1999).

Heitsch, F., M.-M. MacLow and R. Klessen: Hydro and MHD Turbulent Support Against Gravitational Collapse. In: Schielicke, R. E. (Ed.). Astronomische Gesellschaft Abstract Series 15 (1999), 140.

Heitsch, F., M.-M. MacLow and R. Klessen: Effects of Magnetized Turbulence on the Structure and Dynamical Evolution of Molecular Clouds. In: Plasma Turbulence and Energetic Particles in Astrophysics, Proceedings of the International Conference, (Eds.) M. Ostrowski, R. Schlickeiser. Uniwersytet Jagiellonski, Kraków 1999, 103–106.

Henning, Th. and W. Kley: Planetenentstehung in Akkretions-scheiben. Physikalische Blätter 55, 47–50 (1999).

Héraudeau, Ph., F. Simien, G. Maubon and Ph. Prugniel: Stellar Kinematic Data for the Central Region of Spiral Galaxies. II. Astronomy and Astrophysics Supplement 136, 506–514 (1999).

Héraudeau, Ph., C. Surace, D. Lemke, S. Oliver, M. Rowan-Robinson and the ELAIS consortium: The European Large-Area ISO Survey: Near-Infrared follow-up observations of the southern fields. In: Proceedings of conference »The Universe as seen by ISO«, Paris, (Eds.) P. Cox, M. F. Kessel. ESA-SP-427, ESA Publ. Div., Noordwijk 1999, 1041–1044.

Herbst, T., D. Thompson, R. Fockenbrock, H.-W. Rix and S. V. W. Beckwith: Constraints on the Space Density of Methane and the Substellar Mass Function from a Deep Near-Infrared Survey. The Astrophysical Journal 526, L17–L20 (1999).

Hippel, T. von and C. Bailer-Jones: Applying Parallel Network Techniques To SETI. Bioastronomy 99: A New Era in Bioastronomy. 6th Bioastronomy Meeting – Kohala Coast Hawaii – August 2–6, 129 (1999).

Hotzel, S., D. Lemke, M. Stickel and L. V. Tóth: Cold Cloud Cores in Chamaeleon. In: Schielicke, R. E. (Ed.), Astronomische Gesellschaft Abstract Series 15 (1999), 97.

Hotzel, S., D. Lemke, L. V. Tóth, M. Stickel, O. Krause, U. Klaas, S. Bogun, M. F. Kessler, R. J. Laurejis, M. Burgdorf, C. A. Beichmann, M. Rowan-Robinson, A. Efstathiou, G. Richter and M. Braun: Cold Spots in the Camaeleon Dark Clouds. In: Proceedings of conference »The Universe as seen by ISO«, Paris, (Eds.) P. Cox, M. F. Kessel. ESA-SP-427, ESA Publ. Div., Noordwijk 1999, 675–678.

Howarden, T. G., N. P. Rees, T. C. Chuter, A. C. Chrysostomou, Ch. P. Cavedoni, R.-R. Rohloff, E. Pitz, D. G. Pettie, R. J. Bennett and E. Atad-Ettedgui: Postupgrade Performance of the 3.8m United Kingdom Telescope (UKIRT). In: Advanced Telescope Design, Fabrication and Control, (Ed.) William Roybal. Proceedings of the SPIE 3785, SPIE Bellingham 1999, 82–93

Hozumi, S., A. Burkert and T. Fujiwara: The Origin and Formation of Cuspy Density Profiles Through Violent Relaxation of Stellar Systems. In: Proceedings of the International Conference on Numerical Astrophysics, Tokyo 1998. (Eds.) Shoken M. Miyama, Kohji Tomisaka, Tomoyuki Han awa. Kluwer, Boston 1999, 63.

Hujeirat, A., P. Myers, M. Camenzind and A. Burkert: Collapse of Weakly Ionized Rotating Turbulent Cloud Cores. In: Schielicke, R. E. (Ed.), Astronomische Gesellschaft Abstract Series 15 (1999), 16.

Hummel, W., T. Szeifert, W. Gässler, B. Muschielok, W. Seifert, I. Appenzeller and G. Rupprecht: A Spectroscopic Study of Be Stars in the SMC Cluster NGC 330. Astronomy and Astrophysics 352, L31–35 (1999).

Ibata, R., B. Richter, R. L. Gilliland and D. Scott: Faint Moving Objects in the Hubble Deep Field: Components of the Dark Halo? The Astrophysical Journal 524, L95–97 (1999).

Ibata, R., H. B. Richter, G. G. Fahlmann, M. Bolte, H. E. Bond, J. E. Hesser, C. Pryor and P. B. Stetson: Hubble Space Telescope Photometry of the Globular Cluster M 4. The Astrophysical Journal Supplement 120, 265–275 (1999).

Ida, S. J. Larwood and A. Burkert: Evidence for Early Stellar Encounters in the Orbital Distribution of Edgeworth-Kuiper Belt Objects. American Astronomical Society, DPS Meeting 31 (1999), 10.95.

Jäger, K. J. Heidt, I. Appenzeller, R. Bender and K. J. Fricke: The FORS Deep Field (FDF) Selection and First Impressions. In: Schielicke, R. E. (Ed.), Astronomische Gesellschaft Abstract Series 15 (1999), 43.

Jäger, K., K. J. Fricke, I. Appenzeller, W. Seifert, T. Szeifert, W. Gässler, R. Häfner, W. Hummel, B. Muschielok, H. Niclas and O. Stahl: Imaging and Spectroscopy with FORS1 in the Field of Q 0307-0015. Astronomy and Astrophysics 352, L17–21 (1999).

Khochfar, S. and A. Burkert: Estimating Merger Probabilities of Dark Matter Halos by Use of Merger Trees. In: Schielicke, R. E. (Ed.), Astronomische Gesellschaft Abstract Series 15 (1999), 141.

Kim, S. Y., M.-M. MacLow and Y.-H. Chu: Evolution of Hypernovae Remnants in the Interstellar Medium. American Astronomical Society Meeting 194 (1999), 72.04.

Klaas, U., M. Haas and B. Schulz: Ultra-Luminous Infrared Galaxies: Far Infrared Spectral Energy Distributions. Procceedings of conference »The Universe as seen by ISO«, Paris. (Eds.) P. Cox, M. F.

Kessel. ESA-SP-427, ESA Publ. Div., Noordwijk 1999, 901–904.

Klaas, U., R. J. Laureijs and J. Clavel: FIR Polarization of the Quasar 3C 279. The Astrophysical Journal 512, 157–161 (1999).

Klaas, U., R. J. Laureijs, T. G. Müller, E. Kreysa and W. Krätschmer: Data reduction, Calibration and Performance of the ISOPHOT Polarization Modes. In: Proceedings of the Workshop on ISO Polarization Observations, Villafranca, (Eds.) R. J. Laureijs, R. Siebenmorgen. ESA-SP-435, ESA Publ. Div., Noordwijk 1999, 19–22.

Klaas, U., M. Haas, S. A. H. Müller, I. M. Coulson, M. Albrecht and B. Schulz: The 10-1000 µm Spectral Energy Distributions of Ultra-Luminous IR-Galaxies. In: Schielicke, R. E.(Ed.), Astronomische Gesellschaft Abstract Series 15 (1999), 52.

Klaas, U., T. G. Müller, R. J. Laureijs, J. Clavel, J. S. V. Lagerros, R. J. Tuffs, A. Moneti, E. Kreysaand W. Krätschner: Polarization Measurements with ISOPHOT: Performance and First Results. In: Proceedings of the Conference: »The Universe as seen by ISO«, Paris, (Eds.) P. Cox, M. F. Kessel. ESA-SP-427, ESA Publ. Div. Noordwijk 1999, 77–80.

Klahr, H. H., T. Henning and W. Kley: On the Azmimuthal Structure of Thermal Convection in Circumstellar Disks. The Astrophysical Journal 514, 325–343 (1999).

Kley, W.: Mass Flow and Accretion through Gaps in Accretion Disks. Monthly Notices of the Royal Astronomical Society 303, 969–710 (1999).

Kley, W. and Lin D. N. C.: Evolution of FU Ori Outbursts in Protostellar Disks. The Astrophysical Journal 518, 833–847 (1999).

Kley, W. and G. Schäfer: Relativistic Dust Disks and the Wilson-Mathews Approach. Physical Review 60 27501 (1999).

Kochanek, C., E. Falco, C. Impey, J. Lehar, B. McLeod and H.-W. Rix: Results from the CASTLES Survey of Gravitational Lenses. In: After the Dark Ages: When Galaxies were Young (the Universe at $2 < z < 5$). 9th Annual October Astrophysics Conference in Maryland, (Eds.) S. Holt, E. Smith. AIP, San Francisco 1999, 163.

Kraft, S., O. Frenzel, L. Hermans, R. Katterloher, D. Rosenthal, U. Grözinger and J. Beeman: Modular 25×16 pixel stressed array for PACS aboard FIRST. In: Infrared Spaceborne Remote Sensing VII, (Eds.) M. Strojnik et al. Proceedings of the SPIE 3759, SPIE, Denver 1999, 214–220.

Krautter, J., F.-J. Zickgraf, I. Appenzeller, I. Thiering, W. Voges, C. Chavarria, R. Kneer, R. Mujica, M. W. Pakull, A. Serrano and B. Ziegler: Identification of a Complete Sample of Northern ROSAT All-Sky Survey X-Ray Sources. IV. Statistical Analysis. Astronomy and Astrophysics 350, 743–752 (1999).

Krusch, E. R. Chini and M. Haas: ISO Reveals Frosty Cold Protostellar Cores. In: Schielicke, R. E. (Ed.), Astronomische Gesellschaft Abstract Series 15 (1999), 97.

Kuhlmann, B. von and J. Fried: Luminousity Function of Field Galaxies Between $z = 0.2$ and 1. In: Schielicke, R. E. (Ed.), Astronomische Gesellschaft Abstract Series 15 (1999), 42.

Lagerros, J. S. V., T. G. Müller, U. Klaas and A. Erikson: ISOPHOT Polarization Measurements of the Asteroids (6) Hebe and (9) Metis at 25 µm. Icarus 142, 454–463 (1999).

Langer, N., G. García-Segura and M.-M. MacLow: Giant Outbursts of Luminous Blue Variables and the Formation of the Homunculus Nebula around Eta Carinae. The Astrophysical Journal 520, L49–L53, (1999).

Laureijs, R. J. and U. Klaas: Processing Steps and Signal Analysis of ISOPHOT Polarization Observations at 170 micron. In: Proceedings of the Workshop on ISO Polarization Observations,Villafranca, (Eds.) R. J. Laureijs, R. Siebenmorgen. ESA-SP-435, ESA Publ. Div., Noordwijk 1999, 27–30.

Lehtinen, K., D. Lemke and K. Mattila: ISOPHOT far-infrared observations of the dark cloud DC 303.8-14.2. In: Proceedings of the conference »The Universe as seen by ISO«, Paris, (Eds.) P. Cox, M. F. Kessel. ESA-SP-427, ESA Publ. Div., Noordwijk 1999, 695–698.

Leinert, Ch. and Th. Encrenaz: ISO Observations of Solar System Objects. In: Highlights of Astronomy 11. XXIIIrd General Assembly of the IAU, 1997, (Ed.) J. Andersen. Kluwer, Dordrecht 1998, 1151.

Leinert, Ch. and K. Mattila: Natural Optical Sky Background. In: Highlights of Astronomy 11. XXIIIrd General Assembly of the IAU, 1997, (Ed.) J. Andersen. Kluwer, Dordrecht 1998, 208.

Lemke, D.: Observations with ISOPHOT. In: Highlights of Astronomy 11. XXIIIrd General Assembly of the IAU, 1997, (Ed.) J. Andersen. Kluwer, Dordrecht 1998, 1116.

Lemke, D.: Foreword. In: Highlights of Astronomy 11. XXIIIrd General Assembly of the IAU, 1997, (Ed.) J. Andersen. Kluwer, Dordrecht 1998, 1105.

Lemke, D.: SPS II: Highlights in the ISO Mission. In: Highlights of Astronomy 11. XXIIIrd General Assembly of the IAU, 1997, (Ed.) J. Andersen. Kluwer, Dordrecht 1998, 1101.

Lemke, D.: Infrared Astronomy with the ISO Satellite. Cryogenics 39, 125–133 (1999).

Lemke, D.: Infrared Astronomy with the ISO Satellite.: In: Proceedings of the Workshop »Space Cryogenics«, ESTEC, Noordwijk, The Netherlands 1998. WPP-157 1999, ISSN 1022-6656, 7–29.

Lemke, D.: Staub, Ruß, Wasser und Eis – ISO erkundet den kalten Kosmos. Sterne und Weltraum 38, 754–760 (1999).

Lemke, D.: Is small beautifull? Sterne und Weltraum 38, 827 (1999).

Lemke, D.: Tiefer Blick ins kalte Universum. Innovationen 7, 12–17 (1999).

Lemke, D. and U. Klaas: ISOPHOT – Performance, results and outlook. In: Proceedings of the conference »The Universe as seen by ISO« Paris, (Eds.) P. Cox, M. F. Kessel. ESA-SP-427, ESA Publ. Div., Noordwijk 1999, 51–60.

Lemke, D., U. Grözinger, O. Krause, R. Rohloff and R. Habeerland: Focal Plane Chopper for the PACS instruments aboard the Far Infrared Space Telescope FIRST. In: Infrared Spaceborne remote Sending VII, (Eds.) M. Strojnik et al. Proceedings of the SPIE 3759, SPIE, Denver 1999, 205–213.

Ligori, S., M. Robberto and T. Herbst: Mid-IR Images of W51. In: Star Formation, (Ed.) T. Nakamoto, Nobeyama Radio Observatory, Nagoya 1999, 377–378.

Maciejewski, W. and D. P. Cox: Supernova Remnants in a Stratified Medium: Explicit, Analytical Approximations for Adiabatic Expansion and Radiative Cooling. The Astrophysical Journal 511, 792–797 (1999).

Maciejewski, W. and L. S. Sparke: Bars within Bars in Galaxies. In: Galaxy Dynamics, (Eds.) D. Merritt, M. Valluri, J. Sellwood. Conference Series 182, Astronomical Society of the Pacific, San Francisco 1999, 245–248.

MacLow, M.-M.: The Interaction of the Disk with the Halo. In: New Perspectives on the Interstellar Medium, (Eds.) A.R. Taylor, T. Landecker. G. Joncas. Conference Series 168, Astronomical Society of the Pacific, San Francisco 1999, 303–314.

MacLow, M.-M.: Wolf-Rayet abd LBV Nebulae as the Result of Variable and Non-Spherical Stellar Winds. In: Variable and Non-Spherical Stellar Winds in Luminous Hot Stars, (Eds.) B. Wolf, O. Stahl, A. W. Fullerton. IAU Colloquium 169, Springer, Heidelberg 1999, 391–399.

MacLow, M.-M.: The Energy Dissipation Rate of Supersonic, Magnetohydrodynamic Turbulence in Molecular Clouds, The Astrophysical Journal 524, 169–178 (1999).

MacLow, M.-M.: Blast Waves and Shells in the Turbulent ISM. American Astronomical Society Meeting 194 (1999), 64.08.

MacLow, M.-M. and A. Ferrara: Starburst-Driven Mass Loss from Dwarf Galaxies: Efficiency and Metal Ejection. The Astrophysical Journal 513, 142–155 (1999).

MacLow, M.-M., F. Heitsch and R. Klessen: Hydrodynamical and MHD Turbulent Support Against Gravitational Collapse. American Astronomical Society Meeting 194 (1999), 69.10.

Mandel, H., I. Appenzeller, W. Seifert, W. Xu, T. Herbst, R. Lenzen, M. Thatte, F. Eisenhauer, R. Lemke, D. Bomans, T. Luks, P. Weiser and C. Spörl: LUCIFER – a NIR Spectrograph and Imager for the LBT. In: Schielicke, R. E. (Ed.), Astronomische Gesellschaft Abstract Series 15 (1999), 144.

Mattila, K., K. Lehtinen and D. Lemke: Detection of Widely Distributed UIR Band Emission in the Disk of NGC 891. Astronomy and Astrophysics 342, 643–654 (1999).

Mattila, K., K. Lehtinen and D. Lemke: Mid-Infrared Spectrophotometry of the Diffuse Disk Emission of NGC891 and its Twilling Galaxy the Milky Way. In: Schielicke, R. E. (Ed.), Astronomische Gesellschaft Abstract Series 15 (1999), 2.

McIntosh, D. H., H.-W. Rix and N. Caldwell: Searching for Young S0 Galaxies in Abell 2052. American Astronomical Society Meeting 195 (1999), 10.10.

McIntosh, D. H., H.-W. Rix, M. Riecke and C. B. Foltz: Redshifted and Blueshifted Broad Lines in Luminous Quasars. The Astrophysical Journal 517, L73–L76 (1999).

McIntosh, D., M. Rieke, H.-W. Rix, C. Foltz and R. Weymann: A Statistical Study of Rest-Frame Optical Emission Properties in Luminous Quasars at $2.0 < z < 2.5$. The Astrophysical Journal 514, 40–67 (1999).

Meisenheimer, K.: High-Frequency Observations and Spectrum of the Jets in M 87. In: The Radio Galaxy Messier 87, Lecture Notes in Physics 530, (Eds.) Röser, H.-J., K. Meisenheimer. Springer, Heidelberg 1999, 188–210.

Möllenhoff, C., I. Appenzeller, W. Gässler, R. Häfner, J. Heidt, W. Hummel, B. Muschielok, H. Niclas, G. Rupprecht, W. Seifert, O. Stahl and T. Szeifert: Morphological Structure and Colors of NGC 1232 and NGC 1288. Astronomy and Astrophysics 352, L5–L10 (1999).

Mori, M. and A. Burkert: Ram Pressure Stripping of Dwarf Galaxies in a Cluster of Galaxies. Astronomische Nachrichten 320, 302 (1999).

Müller, T. G., J. S. V. Lagerros and U. Klaas: Polarization

Measurements of Asteroids at 25 µm with ISOPHOT. In: Proceedings of the Workshop on ISO Polarization Observations, Villafranca, (Eds.) R. J. Laureijs, R. Siebenmorgen. ESA-SP-435, ESA Publ. Div., Noordwijk 1999, 31–36.

Müller, S. A. H., M. Haas, R. Chini, K. Meisenheimer, U. Klaas, D.

Lemke, E. Kreysa and M. Camenzind: Dust in PG Quasars. In: Schielicke, R. E. (Ed.), Astronomische Gesellschaft Abstract Series 15 (1999), 51.

Munoz, J. A., E. E. Falco, C. S. Kochanek, J. Lehar, B. A. McLeod, C. D. Impey, H.-W. Rix and C. Y. Peng: The CASTLES Project. Astrophysics and Space Science, 263, 51–54, 1999.

Muschielok, B., R. Kruditzki, I. Appenzeller, F. Bresolin, K. Butler, W. Gässler, R. Häfner, H. J. Hess,, W. Hummel, D. J. Lennon, K.-H. Mantel, W. Meisl, W. Seifert, S. J. Smartt, T. Szeifert and T Tarantik: VLT FORS Spectra of Blue Supergiants in the Local Group

Galaxy NGC 6822. Astronomy and Astrophysics 352, L40–44 (1999).

Naab, Th. and A. Burkert: Formation of Elliptical and SO Galaxies by Close Encounters. In: Galaxy Dynamics, (Eds.) D. R. Merritt, M. Valluri, J. A. Sellwood. Conference Series 182, Astronomical Society of the Pacific, San Francisco 1999, 477–480.

Naab, Th. and A. Burkert: Formation of Elliptical Galaxies in the Merger Scenario. In: Schielicke, R. E. (Ed.), Astronomische Gesellschaft Abstract Series 15 (1999), 136.

Naab, Th., A. Burkert and L. Hernquist: On the Formation of Boxy and Disky Elliptical Galaxies. The Astrophysical Journal 523, L133–L136 (1999).

Naito, T., T. Yoshida, M. Mori and T. Tanimori: Radio to TeV Gamma-ray Emission from SN 1006 and Shock Acceleration around its Rim. Astronomische Nachrichten 320, 205–206 (1999).

Neistein, E., D. Maoz, W.-W. Rix and J. Tonry: A Tully-Fisher Relation for S0 Galaxies. The Astronomical Journal 117, 2666–2675 (1999).

Nelson, A. and W. Benz: Towards Understanding Jovian Planet Migration. In: Proceedings of a conference on Star Formation, (Ed.) T. Nakamoto. Nobeyama Radio Observatory, Nagoya 1999, 251–252.

Nieten, Ch., R. Beck, E. Berkhuijsen and M. Haas: Cold Dust in the Southwest of M 31. In: Schielicke, R. E. (Ed.), Astronomische Gesellschaft Abstract Series 15 (1999), 52.

Olling, R. P. and W. Dehnen: Oortís Constants Measured from the Tycho/ACT Catalogues. Bulletin of the American Astronomical Society Meeting 31, (1999), 1379.

Ossenkopf, V., F. Bensch, M.-M. MacLow and J. Stutzki: Molecular Cloud Structure Analysis by Direct Simulation. In: The Physics and Chemistry of the Interstellar Medium, Proccedings of the 3rd Cologne-Zermatt Symposium 1998, (Eds.) V. Ossenkopf, J. Stutzki, G. Winnewisser, GCA-Verlag Herdecke 1999, 216.

Ott, J., F. Walter, U. Klein and E. Brinks: Investigating the Low Mass End of Dwarf Galaxies: The Low Surface Brightness Galaxy Holmberg I. In: Schielicke, R.E. (Ed.), Astronomische Gesellschaft Abstract Series 15, G06 (1999).

Patsis, P. A. and D. E. Kaufmann: Resonances and the Morphology of Spirals in N-body Simulations. Astronomy and Astrophysics 352, 469–478 (1999).

Patsis, P. A. and D. E. Kaufmann: Signature and Density Wave Resonances in N-body Simulations of Spiral Galaxies. In: Proceedings of the International Conference on Numerical Astrophysics, Tokyo 1998. (Eds.) Shoken M. Miyama, Kohji Tomisaka, Tomoyuki Hanawa., Kluwer Boston 1999, 65.

Peletier, R. F., M. Balcells, R. L. Davies, Y. Andredakis, A. Vazdekis, A. Burkert and F. Prada: Galactic Bulges from Hubble Space Telescope NICMOS Observations: Ages and Dust. Monthly Notices of the Royal Astronomical Society 310, 703–716 (1999).

Peng, C. Y., C. D. Impey, E E. Falco, C. S. Kochanek, J. Lehár, B. A. McLeod, H.-W. Rix, C. R. Keeton and J. A. Muñoz: The Quasar Pair Q 1634 + 267 A, B and the Binary QSO vs. Dark Lens Hypotheses. The Astrophysical Journal 524, 572–581 (1999).

Peschke, S. B., M. Stickel, I. Heinrichsen, CM. Lisse, E. Grün and D. J. Osip: First Maps of Comet Hale-Bopp in the Far-Infrared, in Relation to Radial Profiles at other Wavelengths. In: Proceedings of the Conference »The Universe as seen by ISO«, Paris, (Eds.) P. Cox, M. F. Kessel. ESA-SP-427, ESA Publ. Div., Noordwijk 1999, 185–188.

Pittichová, J., Z. Sekanina, K. Birkle, H. Böhnhardt, D. Engels and P. Keller: An Early Investigation of the Striated Tail of Comet Hale-Bopp (C/1995 O1). Earth, Moon and Planets 78, 329–338 (1999).

Philipp, S., R. Zylka, P. Mezger, W. Duschl, T. Herbst and R. Tuffs: The NuclearBulge. I K Band Observations of the Central 30 pc. Astronomy and Astrophysics 348, 768–782 (1999).

Radovich, M., U. Klaas, D. Lemke and J. Acosta-Pulido: The 10-200 µm Spectral Energy Distribution of the Prototype Narrow-Line

X-Ray Galaxy NGC 7582*. Astronomy and Astrophysics 348, 705–710 (1999).

Rafanelli, P., V. Afanasiev, K. Birkle, P. Boehm, T. Boller, S. Dodonov, M. Radovich, G. Richter, M. Salvato and J. Vennik: MKN 298: an AGN hidden by Starbursts. Memorie della Societá Astronomica Italiana. 70, 81–84 (1999).

Richards, P. J., L. B. G. Knee, S. C.Russell and M. Haas: FIR Mapping of Bok Globules CB202, CB220 and CB236 (L1166) with ISOPHOT. In: Proceedings of the conference »The Universe as seen by ISO«, Paris, (Eds.) P. Cox, M. F. Kessel. ESA-SP-427, ESA Publ. Div., Noordwijk 1999, 513–516.

Richichi, A, R. Köhler, J. Woitas and Ch. Leinert: Discovery of a Close Companion to the Young Star/Object Haro 6-37. Astronomy and Astrophysics 346, 501–504 (1999).

Rix, H.-W.:The Past and the Future Fate of the Universe and the Formation of Structure in it. Proceedings of the National Academy of Sciences, USA, 96, 8334–8335, 1999.

Rix, H.-W., C. M. Carollo and K. Freeman: Large Stellar Disks in Small Elliptical Galaxies. The Astrophysical Journal 513, L25–L28 (1999).

Robberto, M., S. V. W. Beckwith and T. Herbst: Circumstellar Disks in Orion: First Results from a Mid IR Survey. In: Star Formation 1999, Proceedings of Star Formation. (Ed.) T. Nakamoto. Nobeyama Radio Observatory, Nagoya 1999, 231–233.

Robberto, M., M. R. Meyer, A. Natta and S. V. W. Beckwith: ISOPHOT Observations of Circumstellar Disks around Young Stellar Objects. Proceedings of Conference »The Universe as seen by ISO«, Paris, (Eds.) P. Cox, M. F. Kessel. ESA-SP-427, ESA Publ. Div., Noordwijk 1999. 195–202.

Roberts, E. R., J. R. Jeffries, D. E. Backman, D. Barrado y Navascués, K. E. Haisch and J. J. Dalton: Open Cluster Lower Main Sequences at 15 to 35 Myr. Bulletin of the American Astronomical Society 31, (1999) 1442.

Roche, N., St. A. Eales, H. Hippelein and Ch. J. Willott: The Angular Correlation Function of K~19.5 Galaxies and the Detection of a Cluster at z = 0.775. Monthly Notices of the Royal Astronomical Society 306, 538 (1999).

Rohloff, R.-R., E. Pitz, T. Hawarden, N. Rees, E. Ard-Ettedgui, H. W. Kaufmann and L. D. Schmadel: Lightweighted Secondary Mirror from the United Kingdom Infrared Telescope. In: Advanced Telescope Design, Fabrication and Control, (Ed.) William Roybal. Proceedings of the SPIE 3785, SPIE Bellingham 1999, 152–159.

Röser, H.-J. and K. Meisenheimer (Eds.): The Radio Galaxy Messier 87, Lecture Notes in Physics 530. Springer, Heidelberg 1999, 342.

Rowan-Robinson, M., S. Oliver, A. Efstathiou, C. Gruppioni, S. Serjeant, C. Cesarsky, L. Danese, A. Franceschini, R. Genzel, A. Lawrence, D. Lemke, R. McMahon, G.Miley, I. Perez-Fournon, J. L. Puget, B. Rocca-Volmerange, P. Ciliegi, P. Héraudeau, C. Surace, F. La Franca and the ELAIS consortium: The European Large Area ISO Survey: ELAIS. In: Proceedings of the conference »The Universe as seen by ISO«, Paris, (Eds.) P. Cox, M. F. Kessel. ESA-SP-427, ESA Publ. Div., Noordwijk 1999, 1011–1016.

Runacres, M. C., R. Blomme, K. Vyverman, M. Cohen, C. Leitherer, S. P. Owocki and M. Haas: ISOPHOT Observations of Wolf-Rayet Winds. In: Wolf-Rayet Phenomena in Massive Stars and Starburst Galaxies. Proceedings of the 193rd Symposium of the International Astronomical Union, (Eds.) K. van der Hucht, G. Koenigsberger, Ph. Eenens. Astronomical Society of the Pacific, San Francisco 1999, 96.

Sandquist, E. L., R. Taam and A. Burkert: Formation and Mechanisms for Helium White Dwarfs in Binaries. American Astronomical Society Meeting 194 (1999), 75.04.

Schmid, H.M., J. Krautter, I. Appenzeller and H. Mandel: FUV ORFEUS Spectroscopy of the Slowly Evolving Symbiotic Nova RR Tel. In: Unsolved Problems in Stellar Evolution: Poster Papers from the Space Telescope Science Institute Symposium, (Ed.) M. Livio. Baltimore 1999, 77.

Schmid, H. M., J. Krautter, I. Appenzeller, J. Barnstedt, T. Dumm, A. Fromm, M. Gölz, M. Grewing, W. Gringel, C. Haas, W. Hopfensitz, N. Kappelmann, G. Krämer, A. Lindenberger, H. Mandel, U. Mürset, H. Schild, W. Schmutz and H. Widmann: ORFEUS Spectroscopy of the O VI Lines in Symbiotic Stars and the Raman Scattering Process. Astronomy and Astrophysics 348, 950–971 (1999).

Schmidtobreick, L., M. Haas and D. Lemke: About the Nature of the FIR Dust Knots in M 31. In: Schielicke, R. E. (Ed.), Astronomische Gesellschaft Abstract Series 15 (1999) 49.

Scholz, R.-D., M. Irwin, A. Schweitzer and R. Ibata: APMPM JO237-5928: a New Nearby Active M 5 Dwarf Detected in a High Proper Motion Survey of the Southern Sky. Astronomy and Astrophysics 345, L55–L57 (1999).

Scholz, R.-D., M. McCaughrean, H. Zinnecker, M. Irwin, A. Schweitzer, J. Stauffer and R. Ibata: Brown Dwarfs Among Newly Detected High-Proper Motion Stars? In: Schielecke, R. E. (Ed.), Astronomische Gesellschaft Abstract Series 15 (1999), P15S.

Schulz, B., S. Huth, U. Kinkel, D. Lemke, J.A. Acosta Pulido, M. Braun, H. O. Castañeda, L. Cornwall, C. Gabriel, I. Heinrichsen, U. Herbstmeier, U. Klaas, R. J. Laurejis and T. G. Müller. ISOPHOT – Photometric Calibration of Point Sources. In. Proceedings of conference »The Universe as seen by ISO«, Paris, (Eds.) P. Cox, M. F. Kessel. ESA-SP-427, ESA Publ. Div., Noordwijk 1999, 89–94.

Shelton, R. L.,D. P. Cox, W. Maciejewski, R. K. Smith, T. Plewa, A. Pawl and M. Rózyczka: Modelling W44 as a Supernova Remnant in a Density Gradient with a Partially Formed Dense Shell and Thermal Conduction in the Hot Interior. II. The Hydrodynamic Models. The Astrophysical Journal 524, 192–212 (1999)

Slyz, A. and K. H. Prendergast: Time-Independent Gravitational Fields in the BGK Scheme for Hydrodynamics. Astronomy and Astrophysics Supplement Series, 139, 199–217 (1999).

Song, I., J.-P. Caillaut, D. Barrado y Navascués and J. R. Stauffer: Ages of Vega-like Stars. Bulletin of the American Astronomical Society Meeting 31 (1999), 1409.

Stauffer, J. R., D. Barrado y Navascués, J. Bouvier, H. L. Morrison, P. Harding, K. L. Luhman, T. Stanke, M. McCaughrean, D. M. Terndrup, L. Allen and P. Assouad: Keck Spectra of Brown Dwarf Candidates and a Precise Determination of the Lithium Depletion Boundary in the α Persei Open Cluster. The Astrophysical Journal 527, 219–229 (1999).

Stecklum, B., M. Feldt, Th. Henning and W. Pfau: Infrared Observations of Young Massive Stars. In: Wolf-Rayet Phenomena in Massive Stars and Starburst Galaxies. Proceedings of the 193 rd Symposium of the International Astronomical Union, (Eds.) K. van der Hucht, G. Koenigsberger, Ph. Eenens. Astronomical Society of the Pacific, San Francisco 1999, 497.

Stickel, M., D. Lemke, L. V. Tóth, S. Hotzel, U. Klaas, S. Bogun, M. F. Kessler, R. Laurejis, M. Burgdorf, C. A. Beichman, M. Rowan-Robinson, A. Efstathiou, G. Richter and M. Braun: The ISO Serendipity Far-Infrared Sky Survey – a status report. In: Proceedings of the conference »The Universe as seen by ISO«, Paris, (Eds.) P. Cox, M. F. Kessel. ESA-SP-427, ESA Publ. Div., Noordwijk 1999, 839–844.

Surace, C., P. Héraudeau, D. Lemke, S. Oliver, M. Rowan-Robinson and the ELAIS consortium: The European Large-Area ISO Survey: ISOPHOT results using the MPIA pipeline. In: Proceedings of the conference »The Universe as seen by ISO«, Paris, (Eds.) P. Cox, M. F. Kessel. ESA-SP-427, ESA Publ. Div., Noordwijk 1999, 1059–1062.

Temporin, S., P. Rafanelli, G. Richter, J. Vennik, S. Ciroi and K. Birkle: The Seyfert-2 Galaxy To1 1238-364 and its Companion ESO 381-G009: Long-Slit Spectroscopy and IRAS Data Analysis. Memorie della Societá Astronomica Italiana 70, 87–88 (1999).

Thompson, D., S.V.W. Beckwith, R. Fockenbrock, J. Fried, H. Hippelein, J.-S. Huang, B. von Kuhlmann, Ch. Leinert, K. Meisenheimer, S. Phleps, H.-J. Röser, E. Thommes and Chr. Wolf: The Surface Density of Extremely Red Objects. The Astrophysical Journal 523, 100–106 (1999).

Tóth, L. V., D. Lemke, O. Krause, S. Hotzel, M. Stickel, U. Klaas, S. Bogun, M. F. Kessler, R. J. Laurejis, M. Burgdorf,C. A. Beichman, M. Rowan-Robinson, A. Efstathiou, G. Richter and M. Braun: Interstellar Clouds as seen in the ISO Serendipidity Survey. In. Proceedings of the conference »The Universe as seen by ISO«, Paris, (Eds.) P. Cox, M. F. Kessel. ESA-SP-427, ESA Publ. Div., Noordwijk 1999, 771–774.

Travaglio, C., D. Galli, R. Gallino, M. Busso, F. Ferrini and O. Straniero: Galactic Chemical Evolution of Heavy Elements: From Barium to Europium. The Astrophysical Journal 521, 691–702 (1999).

Travaglio, C., R. Gallino, S. Amari, E. Zinner, S. Woosle and R. S. Lewis: Low-Density Graphite Grains and Mixing in Type II Supernovae. The Astrophysical Journal 510, 325–354 (1999).

Vives, T.: Cuando empieza el tercer milenio? Tribuna de Astronomía y Universo No. 5, 22–28 (1999).

Walker, H. J., I. Heinrichsen, U. Klaas and R. J. Sylvester: Infrared Mapping of the Dust around Main Sequence Stars. In: Proceedings of Conference »The Universe as seen by ISO«, Paris, (Eds.) P. Cox, M. F. Kessel. ESA-SP-427, ESA Publ. Div., Noordwijk 1999, 425–428.

Wilke, K.: Mass Distribution and Kinematics of the Barred Galaxies NGC 3992 and NGC 7479. In: Schielicke, R. E. (Ed.), Astronomische Gesellschaft Abstract Series 15 (1999) 38.

Wilke, K., C. Möllenhoff and M. Matthias: Mass Distribution and Kinematics of the Barred Galaxy NGC 2336. Astronomy and Astrophysics 344, 787–806 (1999).

Wolf. Chr.: Multicolor Classification in CADIS and the Search for Quasars. The Publications of the Astronomical Society of the Pacific 111, 1048 (1999).

Wolf, Chr., K. Meisenheimer, H.-J. Röser, S. V. W. Beckwith, R. Fockenbrock, H. Hippelein, B. von Kuhlmann, S. Phleps and E. Thommes: Did Most High-Redshift Quasars Escape Detection? Astronomy and Astrophysics 343, 399–406 (1999).

Yahagi, H., M. Mori and Y. Yoshii: The Forest Method as a New Parallel Tree Method with the Sectional Voronoi Tesselation. The Astrophysical Journal Supplement 124, 1–9 (1999).

Yoshikoshi, T., S. A. Dazeley, S. Gunji, S. Hara, T. Hara, J. Holder, J. Jimbo, A. Kawachi, T. Kifune, H. Kubo, J. Kushida, S. Le Bohec, Y. Matsubara, Y. Mizumoto, M. Mori, M. Moriya, H. Muraishi, Y. Muraki, T. Naito, K. Nishijima, J. R. Patterson, M. D. Roberts, G. P. Rowell, K. Sakurazawa, R. Susukita, T. Tamura, T. Tanimori, S. Yanagita, T. Yoshida and A Yuki: Present Status of the 7-10 m Telescope CANGAROO II. Astroparticle Physics 11, 267–269 (1999).

Zickgraf, F.-J., J. M. Alcalá, J. Krautter, M. F. Sterzik, I. Appenzeller, S. Frink and E. Covino: The Late-Type Stellar Component in the ROSAT All-Sky Survey at High Galactic Latitude. In: Schielicke, R. E. (Ed.), Astronomische Gesellschaft Abstract Series 15 (1999), L02Z.

Diploma Thesis

Wackermann, R.: Test und Inbetriebnahme der Weitfeldkamera am 2.2-m-MPG/ESO-Teleskop. Heidelberg 1999

Doctorate Thesis

Eckardt, St.: The Effect of Cosmic Rays on Infrared Detectors on Satellites. Specification of a Camera for FIRST. Heidelberg 1999.

Kessel-Deynet, O.: Smoothed Particle Hydrodynamics including Ionizing Radiation and its Application to the Dynamics of Cloud Cores in the Radiation Field of Massive Stars. Universität Heidelberg 1999.

Wolf, Chr.: Multicolor Classification in CADIS and the Search for Quasars. Heidelberg 1999.

Woitas, J.: Properties of the Components of Young Double Stars. Heidelberg 1999.

Heidelberg – City map

The Max Planck Society

The Max Planck Society for the Promotion of Sciences was founded in 1948. In succession to the Kaiser Wilhelm Society, which was founded in 1911, the Max Planck Society operates at present 78 Institutes and other facilities dedicated to basic and applied research. With an annual budget of around 2.3 billion DM in the year 2000, the Max Planck Society has about 11000 employees, of which one quarter are scientists. In addition, annually about 6900 junior and visiting scientists are working at the Institutes of the Max Planck Society.

The goal of the Max Planck Society is to promote centers of excellence at the forefront of the international scientific research. To this end, the Institutes of the Society are equipped with adequate tools and put into the hands of outstanding scientists, who have a high degree of autonomy in their scientific work.

Max-Planck-Gesellschaft zur Förderung der Wissenschaften
Public Relations Office
Hofgartenstr. 8
D-80539 München

Tel.: 0049-89-2108-1275 or -1277
Fax: 0049-89-2108-1207
Internet: http://www.mpg.de

MAX-PLANCK-GESELLSCHAFT